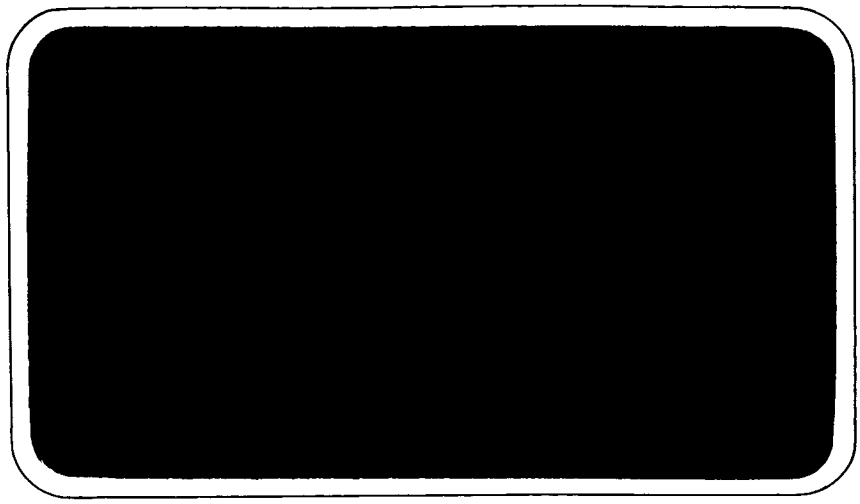

Westinghouse

ELECTRIC CORPORATION

1750A

VOLUME I
SUMMARY

Compilation Report
for
ADVANCED SPACEBORNE DETECTION, TRACKING, AND NAVIGATION SYSTEMS STUDY AND ANALYSIS

NAS 8 - 11205

July 1964

Prepared for

GEORGE C. MARSHALL SPACE FLIGHT CENTER
Huntsville, Alabama

By

WESTINGHOUSE DEFENSE AND SPACE CENTER
Aerospace Division
Baltimore, Maryland

ABSTRACT

19858

This set of five volumes has been compiled by the Aerospace Division of the Westinghouse Defense and Space Center, Baltimore from studies performed under contract NAS r-121 by Cornell Aeronautical Laboratory, Inc., under contract NAS w-469 by the Raytheon Company, and under contract NAS w-460 by the Aerospace Division of Westinghouse, and involves analytical data relative to the development of spaceborne detection, tracking, guidance, and navigational systems for use in manned or unmanned vehicles. The studies were conducted using paragraphs 3.4.3.1 and 3.4.3.2 of Mil-D-8684A (Aer) as a guide.

This Volume I is a summary volume; Volume II presents the Problem Definition, Volume III presents the Analytical Solution for the lunar mission. Volume IV contains both the Problem Definition, Analytical Solution, and Appendices for Earth Orbital Rendezvous. Volume V, the Analytical Supplement, contains the appendices to Volume III.

This volume, Volume I, contains the principal assumptions, results, and recommendations of the overall study.

AUTHOR ↑

TABLE OF CONTENTS

TABLE OF CONTENTS (Continued)

TABLE OF CONTENTS (Continued)

LIST OF ILLUSTRATIONS

LIST OF ILLUSTRATIONS (Continued)

LIST OF TABLES

LIST OF TABLES (Continued)

SUMMARY

This Volume I (Summary) is one of five volumes which, together, constitute the "Advanced Spaceborne Detection, Tracking, Navigation, and Guidance Systems Compilation Report" compiled for the Marshall Space Flight Center by the Aerospace Division of the Westinghouse Defense and Space Center, Baltimore, under Contract NAS8-11205. This report is compiled from the results of three parallel studies conducted independently by the Cornell Aeronautical Laboratory, Inc., Buffalo, N. Y., the Missile and Space Division of Raytheon Company, Bedford, Mass., and the Aerospace Division of Westinghouse Defense and Space Center, Baltimore, Md. These studies were performed primarily to determine sensor requirements for advanced space missions for the immediate post-Apollo time period and were conducted along guidelines furnished by Mil-D-8684A (Aer), paragraphs 3.4.3.1 and 3.4.3.2

This volume, Volume I, contains the principal assumptions, results, and recommendations of the overall study and is a summary of the study compilation as contained in the remaining four volumes.

Volume II contains the problem definition for the study and, in particular, for the lunar mission and shows the development of specific analytical models from the original contract requirements.

Volume III contains the analytical solution for the lunar mission. Specific guidance system models are analyzed and navigation sensor requirements are developed for five major phases of the manned lunar mission. Many of the results are also applicable to the unmanned lunar mission.

Volume IV contains those areas of the study applicable to earth orbital rendezvous and contains its own problem definition, in the main, and its own analytical solution and appendices.

Volume V contains the appendices to Volume III. These appendices constitute an analytic supplement and contain, in Appendix A, a general discussion of mathematical techniques used, and in the succeeding appendices, detailed mathematical techniques as applied in turn to each of the phases of the lunar mission.

Each volume contains its own bibliographical references. In addition, an overall compilation report bibliography is given at the end of this volume.

In Section 1 of this volume a brief summary of the study method is given and the purpose and contents of the Part I, Problem Definition, and Part II, Analytical Solution studies is discussed.

In Section 2, Midcourse Guidance, the problem statement and principal assumptions are given, principal results are shown in terms of the effects of various errors, and conclusions are drawn in subsections 2.10 through 2.15.

Section 3 summarizes the Lunar Parking and Descent Orbits studies. The principal assumptions are stated in subsections 3.1 through 3.3, results are given in subsection 3.4, and conclusions and recommendations are given in section 3.5.

In section 4.0 a complete summary of the Lunar Landing phase is given. The overall study as it applied to the Landing Phase is summarized in subsection 4.1. The principal assumptions are given in subsections 4.2, 4.3.1.1, and 4.3.1.2 for a linear predictive guidance model, and in subsections 4.3.2.1 and 4.3.2.2 for a proportional navigation guidance model. Results are given in subsection 4.3.1.3 for the linear predictive study and in 4.3.2.3 for the proportional navigation study. Overall conclusions for the Lunar Landing phase study are given in subsection 4.3.2.4.

Section 5 summarizes the Lunar Ascent Phase, and Section 6 summarizes the Lunar Rendezvous Phase.

The earth orbital rendezvous study, contained in Volume IV, is summarized in this volume in Section 7. The rendezvous mission is separated for analysis into four phases: injection, midcourse, active rendezvous, and docking. Injection is examined with respect to allowable injection accuracies; midcourse, a passive phase, is examined with respect to navigation sensor errors; and docking is not examined. To study active rendezvous, three different guidance models are employed: a continuous variable level thrust system using modified proportional navigation; an on-off constant thrust level system, automatically controlled; and an on-off constant thrust level system, pilot controlled. Assumptions for all phases and systems are given in subsections 7.1 through 7.3. Results and conclusions are given for all systems in subsections 7.4.1 through 7.4.4. A conclusions summary is given in subsection 7.5.

All statistical quantities are rms (1σ) unless otherwise stated in these volumes.

1. INTRODUCTION

A general objective approach to the determination of system requirements and specifications is used in conducting this study. Rather than assume that certain types of equipment might operate together in a proposed configuration, and then determine by analysis whether it would operate satisfactorily under certain conditions, this study first defines the basic problems with respect to the goals to be realized, to the constraints imposed by physical laws and natural phenomena, and to the possible mathematical solutions to the problems. This type of study, which has been used for several years in the design of complex weapons control systems for the Navy, develops basic specifications on the system and its subsequent mechanization. The study methods, refined with experience, were eventually defined by the Navy in a Military Specification MIL-D-8684A, paragraph 3.4.3, Engineering Report. Excerpts of this portion of the MIL Spec are given below:

3.4.3.1 Problem Definition (Part I)

a. Complete listing of all fixed inputs: tactical, environmental, logistic.

b. Complete definition of problem requirements.

3.4.3.2 Analytical Solution (Part II)

a. Analytical operation on the problem requirements of Part I.

b. Optimum solution of the problem, complete system description.

3.4.3.3 Mechanization Report (Part III)

3.4.3.4 Verification Report (Part IV)

The problem definition identifies the goals that a system must meet, the physical laws and constraints, and the methods which may be used for analysis. The analytical solution concerns a somewhat ideal, nominal solution, as well as parametric studies of variations about nominal values. It is important, however, that specific types of equipment are not considered in this phase of the study. The mechanization study considers possible devices - old, new, or to be created - which will make the analytical solution feasible. These studies result in a prototype design. Finally,

the verification studies consist of a series of experimental tests on a prototype of the mechanized system, or its subsystems, to illustrate that the actual system meets the specifications derived and specified in Part II of the study. The effects of differences between the actual and theoretical systems are also evaluated.

Systems studies, organized in this way, often indicate such things as basic system problems which must be solved independently of the type of mechanization used, and new research and development projects on subsystems and devices which would provide significant increases in system performances.

The study to be described herein is based on Parts I and II only; Parts III and IV were not initiated. The Part I study began with visits to various NASA centers to learn what had been done in this area of study and what information and analytical techniques were available to avoid duplication of other efforts. Based on information obtained and literature surveyed, areas were established for a general determination of sensor accuracy requirements. With the help of NASA, an order of mission priority was established as follows:

1. Manned Lunar Mission
2. Earth Space Station Rendezvous
3. Unmanned Lunar Mission
4. Interplanetary Mission

The manned lunar mission, with results in some cases applicable to the unmanned lunar mission, and earth space station rendezvous were selected for a detailed phase-by-phase analysis. The remaining portions of the Part I study include definition of constraints such as injection errors, possible figures of merit for study evaluation, study limitation to navigation sensor requirements, and choice of trajectories; selection of variable quantities such as observables, sensor error ranges, nominal trajectories, and initial and terminal conditions; and selection of general methods of analysis for the Part II study.

The Part II study, or Analytical Solution, based on the Part I Problem Definition evolves specific mathematical guidance system models and uses these for analysis of sensor error using a variety of mathematical techniques. The principal assumptions, results and recommendations of the overall Part II study are presented in succeeding sections of this volume.

2. MIDCOURSE GUIDANCE

2.1 PROBLEM STATEMENT AND GEOMETRY

Sensor requirements were determined for onboard navigation of spacecraft on lunar trajectories where midcourse is defined as that period between boost from an earth orbit and injection into lunar orbit, as shown in figure 2-1. This figure shows a typical trajectory requiring a 63.9-hour flight to achieve a periselenum of 133 km. The observation data, which consist of measurements of the space angle between some star and either the earth or moon, are also illustrated in the figure. These data are processed onboard the spacecraft to determine commands for the midcourse corrections. These impulsive velocity midcourse corrections are applied several times to reduce the indicated miss distance at periselenum.

2.2 MINIMUM VARIANCE EQUATIONS AND COMPUTER PROGRAM

In determining the sensor requirements it was assumed that the minimum variance procedure* was used to weight the observed data in order to obtain an updated trajectory estimate. The three fundamental equations of this recursive process are shown in table 2-1. The orbital estimate of state after each measurement consists of the predicted state, $\hat{\underline{X}}_{k-1}$ plus some increment, $K\left[y - H\phi \hat{\underline{X}}_{k-1} \right]$, which depends on the actual measurement, y, and the predicted measurement, $H\phi\hat{\underline{X}}_{k-1}$. The weighting factor K, varies inversely with Q, the assumed instrument variance; consequently less weight is put on each measurement if there is little confidence in the instrument accuracy.

The computer program used in this study consisted of statistical analyses of space flights on which system parameters and trajectories were varied. The inputs (variables) and outputs of this program are:

* A recursive method of estimating the state of a dynamic process, developed by Kalman (Ref. 2-1) and first applied to space navigation by Smith and Schmidt (Ref. 2-2).

Inputs	Outputs
Nominal trajectory	r = rms position deviation from nominal
Number, timing, and type of observations and corrections	v = rms velocity deviation from nominal
Initial errors	$\tilde{r}$ = rms position estimation error
Measurement errors	$\tilde{v}$ = rms position estimation error
Landmark errors	$\bar{\Sigma}\Delta v$ = total of rms velocity corrections
Velocity correction errors	

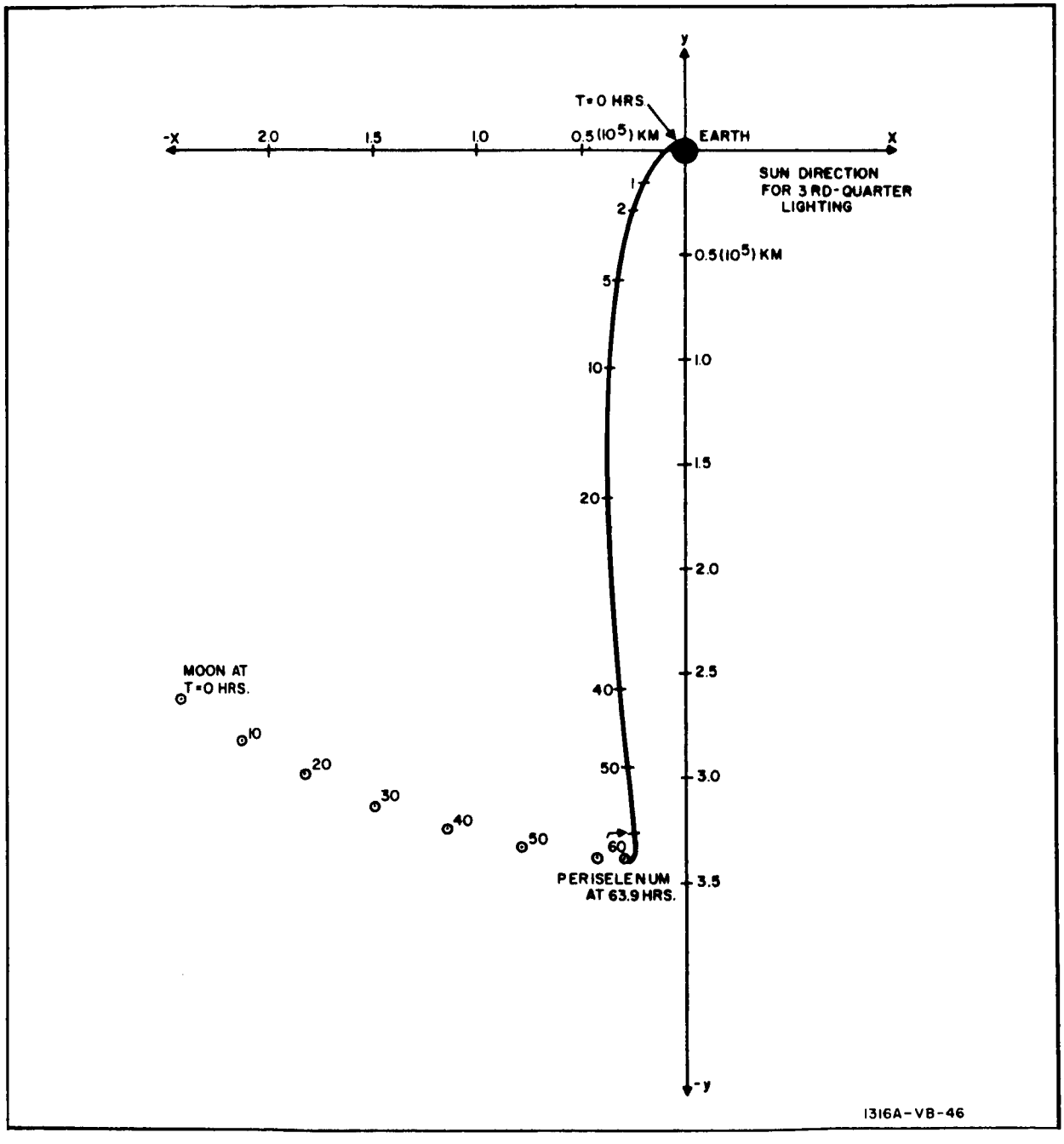

Figure 2-1. Geometry of Midcourse Guidance

TABLE 2-1

MINIMUM VARIANCE EQUATIONS FOR NAVIGATION

I) Estimation Equation:

$$\hat{\underline{x}} = \phi \hat{\underline{x}}_{k-1} + \underline{K} (y - H\phi \hat{\underline{x}}_{k-1})$$

- $\hat{\underline{x}}$: Estimate based on k measurements
- ϕ: Transition matrix from t_{k-1} to t_k
- $\underline{K}$: Weighting vector
- y: Measurement
- $\hat{\underline{x}}_{k-1}$: Estimate based on k-1 measurements

II) Weighting Vector:

$$\underline{K} = PH^T \left\{ HPH^T + Q \right\}^{-1}$$

- Q: Measurement noise

III) Covariance Matrix of Errors in Estimate:

$$P_{k+1} = \phi_{k+1} \left[P - \underline{K}HP \right] \phi^T_{k+1}$$

Est. Deviation Vector:

$$\underline{x} = \left[\hat{\delta X} \; \hat{\delta Y} \; \hat{\delta Z} \; \hat{\dot{\delta X}} \; \hat{\dot{\delta Y}} \; \hat{\dot{\delta Z}} \right]^T$$

Measurement Geometry Row Matrix:

$$H = \left[\frac{\partial \rho}{\partial X} \; \frac{\partial \rho}{\partial Y} \; \frac{\partial \rho}{\partial Z} \; 0 \; 0 \; 0 \right]$$

Covariance Matrix of Injection Errors:

$$P_o = E \left\{ \underline{x}_o \; \underline{x}_o \right\}^T$$

NOTE: All quantities are time-varying except Q, but are evaluated at t_k unless otherwise noted.

2.3 GENERAL DISCUSSION OF GUIDANCE SCHEDULING RESULTS

To generate sensor requirements, some analysis of the guidance scheduling problem was necessary. Figure 2-2 illustrates some of the important principles of navigation by use of measured angles between celestial bodies. These principles are as follows:

a. The efficiency of an angle measurement in reducing the absolute position uncertainty is inversely proportional to range. This is shown in figure 2-2a where $\frac{\partial \varsigma}{\partial X}\Big|_{X_2} > \frac{\partial \varsigma}{\partial X}\Big|_{X_1}$ and the reduction in uncertainties in the X direction is proportional to $\frac{\partial \varsigma}{\partial X}$. From this, it is evident that midcourse navigation at distances on the order of 100,000 km requires much tighter accuracy than orbital navigation requirements.

b. Figure 2-2b shows that uncertainties are reduced most in a plane perpendicular to the sightline of the planet involved in the measurement. Thus, $\frac{\partial \varsigma}{\partial X} > \frac{\partial \varsigma}{\partial X'}$ shows that the uncertainties in the X direction are reduced more than those in the X' direction. Also $\frac{\partial \varsigma}{\partial Y} = 0$, showing that there is no reduction in uncertainties along the sightline to the planet. This is significant in lunar midcourse, since the sightline to the moon rotates very little during the flight and it is very difficult to remove errors in this range direction by angle measurements.

c. Figure 2-2c shows that since $\frac{\partial \varsigma_1}{X} = \frac{\partial \varsigma_2}{X}$, any star sightline in the plane (of the figure) would be equally efficient in reducing in-plane uncertainties. Since uncertainties are greatest in the trajectory plane,

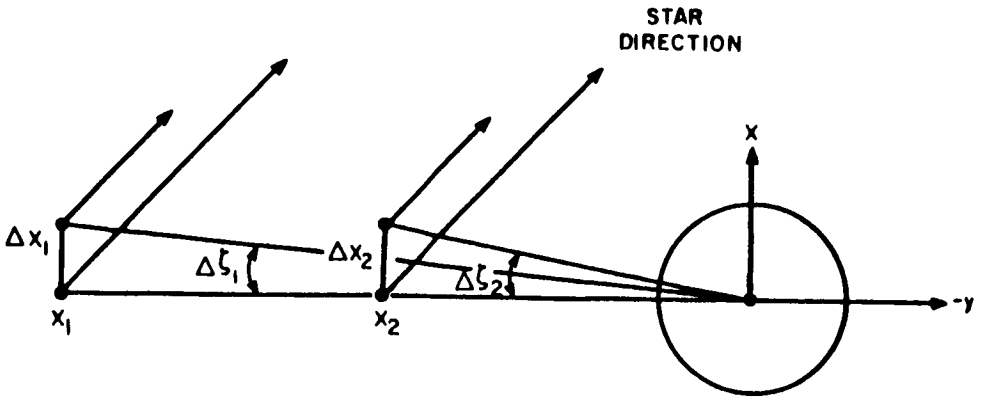

a. EFFECT OF RANGE ON MEASUREMENTS.

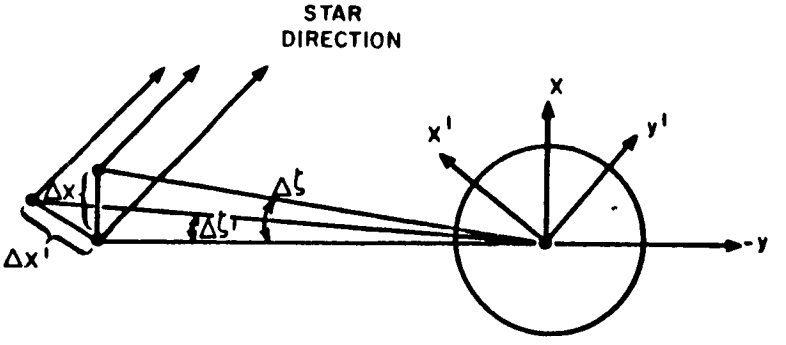

b. EFFECT OF MEASUREMENTS ON DIFFERENT COORDINATES.

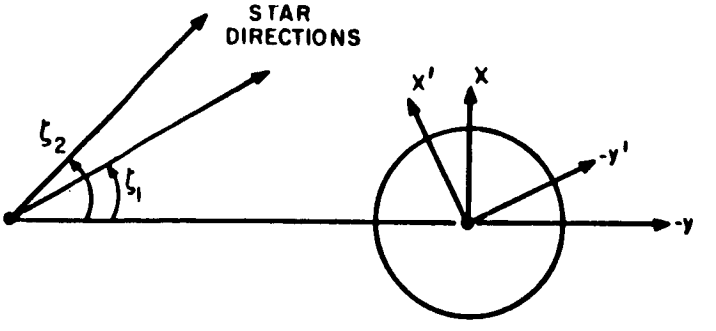

c. EFFECT OF ROTATING STAR SIGHTLINE IN MEASUREMENT PLANE.

1674A-VB-7

Figure 2-2. Principles of Optical Measurement Selections

any star in the trajectory plane could be used for most of the measurements with nearly equivalent results. Thus, since complicated star schedules and optimizations are not required for sensible guidance, the primary constraints on choice of stars for guidance will be visibility and recognizability.

With regard to timing of velocity corrections, it is clear that making corrections later in the flight reduces the miss distance at the cost of fuel. However, it was found that the final velocity correction could be made only 2 hours before periselenum without greatly increasing the magnitude of this correction.

2.4 SUMMARY OF SCHEDULING RUNS AND NOMINAL SCHEDULE

Preliminary computer runs were made to generate a typical guidance schedule to be used as a standard throughout the study. These runs indicated that scheduling is not critical as the "optimum" seems rather broad, and that reasonable results could be obtained with three velocity corrections, and that a total of about 45 measurements is near-optimum with a sensor of 10 arc-second accuracy.

As a result of these computer runs, standard schedules were adopted for the 72-hour and 63.9-hour trajectories. The schedule for the 72.2-hour trajectory, illustrated in figure 2-3 was considered the standard for parametic variations made in the study. Note that most of the measurements are made near the planets where the range is short and the sightline rotates rapidly. The velocity corrections are made at 11, 34, and 70 hours. This schedule is not exactly optimum, as it was later shown, but was considered standard for purposes of this study.

Figure 2-4 shows a time history of the reduction in expected position uncertainty on a 72-hour lunar flight using the standard schedule shown in figure 2-3 and standard system parameters defined in table 2-2. The impulsive drop at each pip represents the reduction in position uncertainty obtained by that measurement. Note that after periods when a particular measurement has not been made for some time, this measurement will sharply reduce uncertainties. Note also the sharp reduction in uncertainty in the vicinity of the moon due to the short range and rotating sightline.

Subsections 2.3 and 2.4 deal with some general problems of midcourse navigation by optical angle measurements. In subsection 2.5 some specific numerical results on system requirements are generated by showing the results obtained by varying the system parameters around the standard values listed in table 2-2.

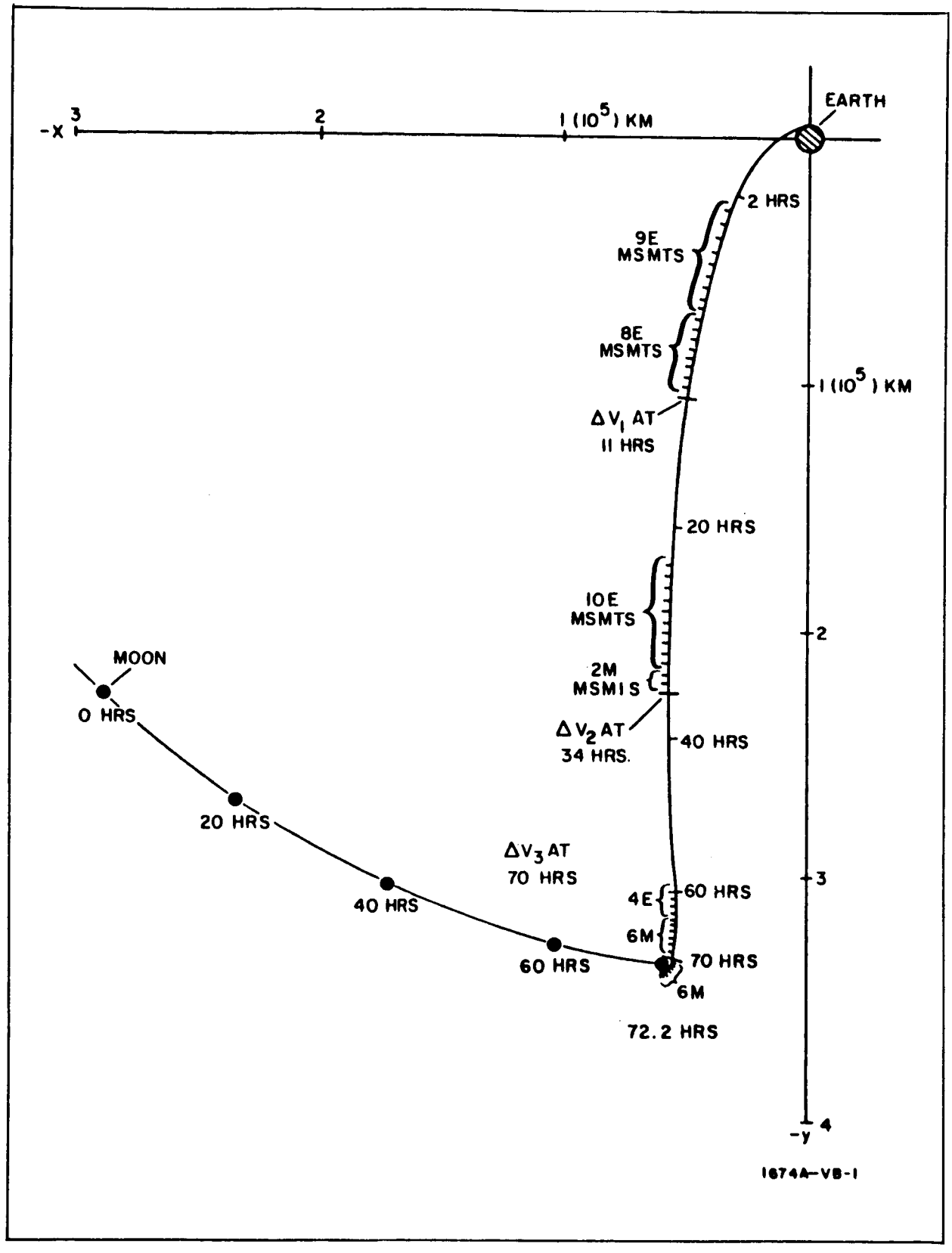

Figure 2-3. Standard Midcourse Guidance Schedule Used in Study

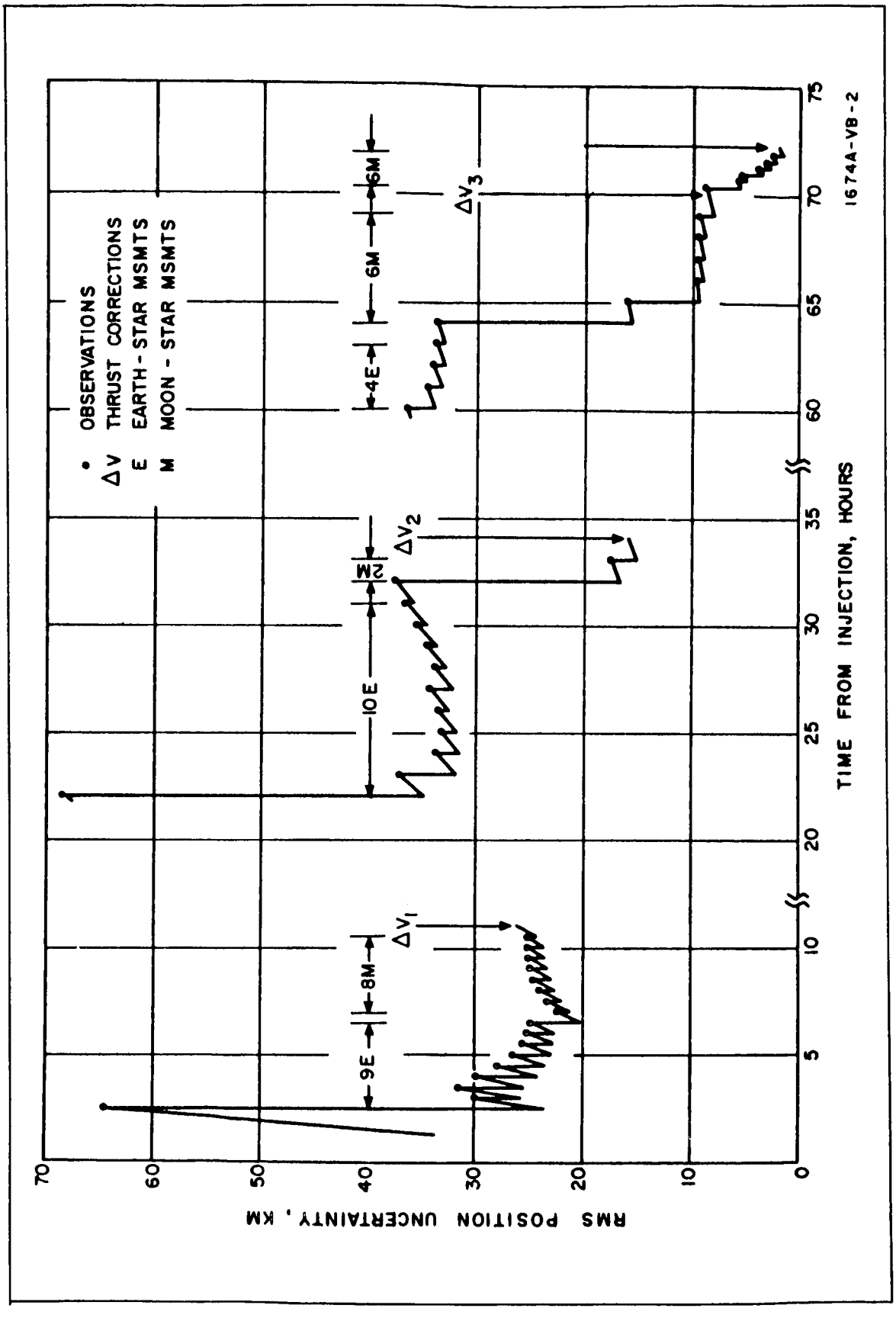

Figure 2-4. Time History of Reduction in Position Uncertainty

TABLE 2-2

LIST OF STANDARD SYSTEM PARAMETERS
USED AS REFERENCES FOR COMPARISON

Number of measurements:	45
Number of corrections:	3
Accuracy of optical instrument:	σ = 10 arc-seconds,rms.
Accuracy of correction errors:	
Percentage magnitude	σ_k = 1%, rms.
Pointing error	$\sigma\gamma$ = .05 degs., rms.
cutoff errors	σ_ϵ = .1 m/s, rms.
Initial error:	
Position	r_o = 2.76 km, rms.
Velocity	v_o = 4.24 m/s, rms.
Reference (landmark) errors:	
Earth	k_1 = 1.6 km, rms.
Moon	k_2 = 0.8 km, rms.

2.5 EFFECT OF SENSOR ACCURACY ON GUIDANCE SYSTEM PERFORMANCE

Figure 2-5 shows how variation of σ, the instrument accuracy, affects the terminal guidance parameters which are r and v, the rms position and velocity miss, $\Sigma\Delta v$, the total rms correction velocity and $\tilde{r}$ and $\tilde{v}$, the rms position and velocity estimation errors at the nominal periselenum of the 63.9 and 72.2-hour trajectories. The miss distance and fuel costs increase sharply with increasing instrument error. However, the estimation errors, $\tilde{r}$ and $\tilde{v}$, are not nearly so critical because these errors are primarily determined by the last few measurements before periselenum, which are made at short ranges. At these ranges, rms sensor errors on the order of 10 arc-seconds are insignificant compared to timing and landmark uncertainties. These results suggest that a somewhat poorer (than 10-arc-secs) sensor could be used if the additional cost and complexity of making a large correction near periselenum could be tolerated.

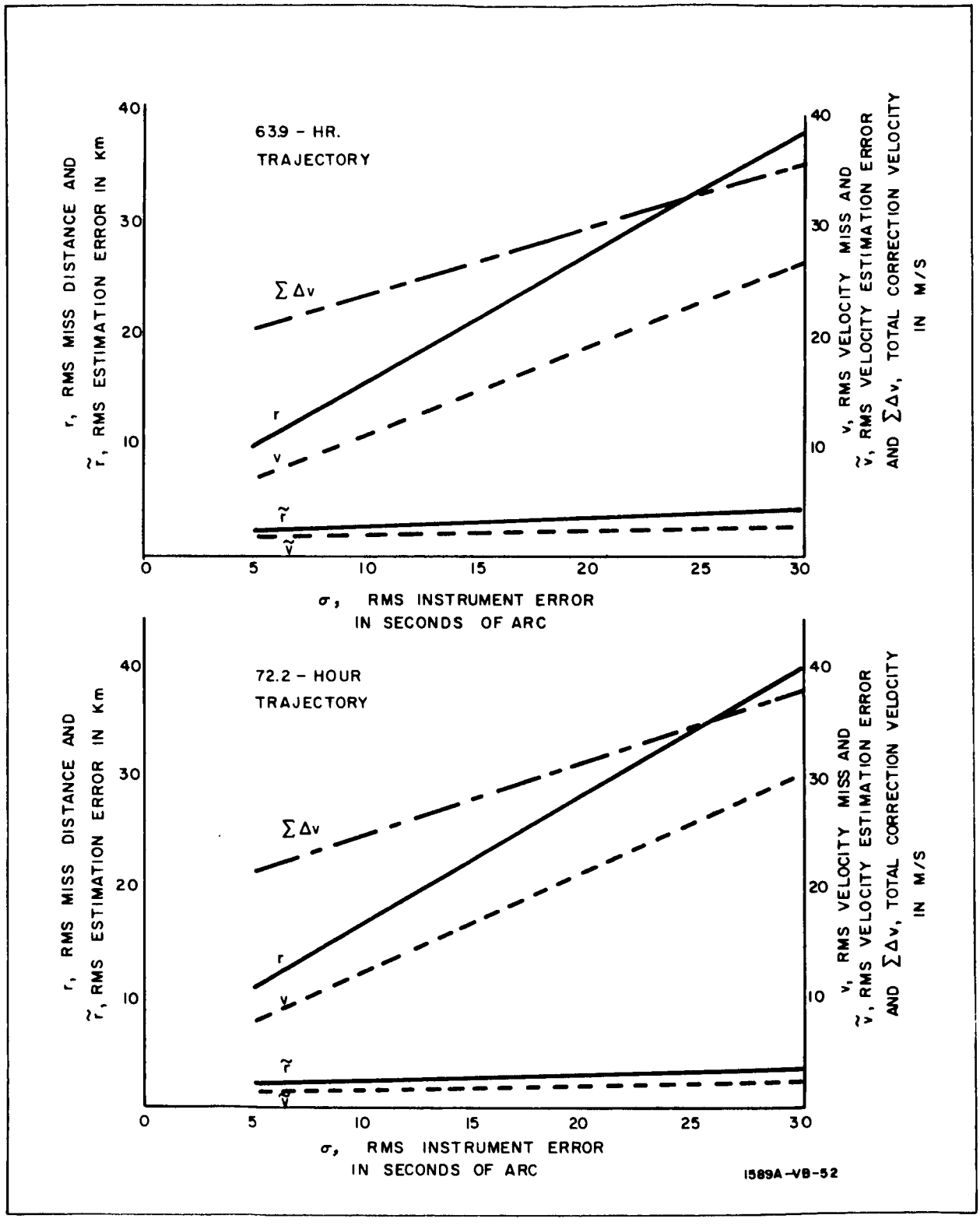

Figure 2-5. Effect of Sensor Accuracy on Guidance System Performance (Periselenum Results)

It is important to note that r, the rms miss distance shown on figure 2-5, is the total miss for a fixed-time-of-arrival guidance system. Since most of this miss is in a downrange direction, the altitude and cross range misses are only about 0.2r and 0.1r. Errors in timing the measurements were not considered in the computer program because analysis indicated that measurement timing errors no greater than 1 second during most of the flight and 0.1 second on the last few measurements would have negligible effect.

2.6 EFFECT OF CORRECTION ACCURACY ON GUIDANCE SYSTEM PERFORMANCE

Although instrument errors sharply affected guidance system performance, the same is not true for velocity correction errors like the standard rms values assumed in this study, which are 1 percent in magnitude, 0.5 degree in pointing, and 0.1 m/sec in cutoff accuracy. Figure 2-6, shows that even tripling all of these errors does not greatly degrade system performance because the primary source of error on each velocity correction, is the trajectory estimation uncertainty rather than the error in making the correction. This would not necessarily be true if ground tracking were used, due to the finer trajectory estimate that is possible.

2.7 INITIAL ERRORS

The translunar injection (from earth) errors assumed in the standard case were 2.76 km in position and 4.25 m/sec in velocity. Doubling these initial errors nearly doubled the correction velocity required, but had little effect on deviations or estimation errors at periselenum, indicating that initial conditions have little effect on the trajectory estimation (see table 2-3).

TABLE 2-3

EFFECT OF INJECTION ERRORS ON TERMINAL CONDITIONS

	r (km)	v (m/sec)	$\tilde{r}$ (km)	$\tilde{v}$ (m/sec)	$\Sigma\Delta$ v (m/sec)
Standard Errors*	16.8	12.1	2.38	1.50	24.3
Doubled Errors*	18.0	13.2	2.42	1.52	40.9

* - All quantities are rms values

2.8 LANDMARK AND HORIZON UNCERTAINTIES

The rms uncertainties in defining the horizons of the earth and moon were assumed to be 1.6 km and 0.8 km respectively. Doubling these

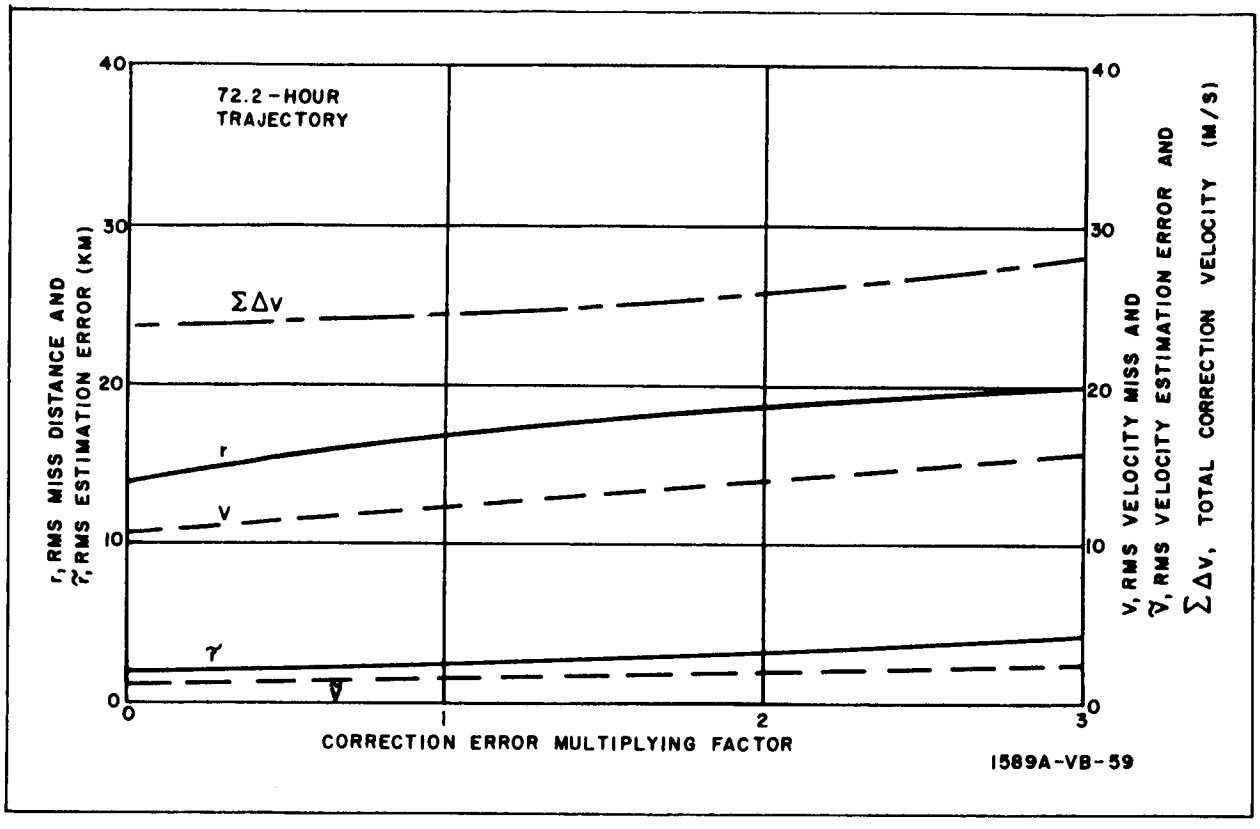

Figure 2-6. Effect of Correction Accuracy on Guidance System Performance

errors had little effect on miss or fuel requirements (r, v, or $\Sigma\Delta v$) but did significantly increase estimation errors ($\tilde{r}$ and $\tilde{v}$) as shown in table 2.4.

TABLE 2-4

EFFECT OF LANDMARK AND HORIZON UNCERTAINTIES ON TERMINAL CONDITIONS

	r (km)	v (km)	$\tilde{r}$ (km)	$\tilde{v}$ (km)	$\Sigma\Delta v$ (m/sec)
Standard Errors*	16.8	12.1	2.38	1.50	24.4
Doubled Errors*	18.7	13.0	3.68	2.23	24.7

* - All quantities are rms values.

2.9 SYSTEMATIC ERRORS

Only random errors were considered in the computer program. However, results of other studies (e.g., Ref. 2-3) indicated that:

a. The most important astrodynamic error is the uncertainty in μ_m, the moon's gravitational constant, which will have a measurable effect. However, this uncertainty may be reduced by the tracking of lunar probes before any manned lunar missions are attempted.

b. Bias errors of a certain magnitude will have an effect similar to random errors of the same magnitude.

c. Systematic errors may be reduced in the same way that random errors are, but at the expense of computing complexity.

2.10 EFFECT OF TRAJECTORY VARIATIONS

It was found that variations in trajectory parameters such as mission time, plane orientation, and periselenum attitude had some effect on guidance system performance, but not enough to make guidance system requirements a function of these parameters.

2.11 COMPARISON OF SINGLE AND DOUBLE-ANGLE MEASUREMENTS

Results discussed in previous subsections assumed that each measurement consists of the angle between some star sightline and a planet landmark or horizon. Another method is to measure the altitude and elevation of a planet in some inertial coordinate system defined by two stars. This

actually results in two angles being measured on each observation. The results obtained with this type of observation are compared with single-angle observation in table 2-5. It can be seen that the double-angle scheme, despite having twice as much data, gives only small improvements in system performance because most of these extra angle measurements provide information about uncertainties perpendicular to the trajectory plane and are of little value.

TABLE 2-5

COMPARISON OF SINGLE-AND DOUBLE-ANGLE MEASUREMENTS*

Nr.	Description	r (km)	v (km)	$\tilde{r}$ (km)	$\tilde{v}$ (m/sec)	$\Sigma\Delta v$ (m/sec)
6	Single Angle- 45** σ = 10 sec	16.81	12.2	2.38	1.50	24.37
53	Double Angle- 45** σ = 10 sec	15.38	10.34	2.05	1.26	22.81
54	Double Angle- 30** σ = 10 sec	19.68	12.69	*	*	24.00
55	Double Angle- 20** σ = 10 sec	21.81	14.13	*	*	25.24
140	Double Angle- 45** σ = 20 sec	26.20	17.82	2.51	1.55	28.14

* - All quantities are rms values.
** - Measurements

2.12 REDUCTION OF MISS DISTANCE BY ADDING RANGE MEASUREMENTS

It was mentioned in subsection 2.3 that optical angle measurements are inefficient during the part of the flight just before the third correction (at 70 hours) due to the lack of rotation of the sightline to the moon during this period. The effect of adding range measurements to the optical guidance in this period was investigated and the results are shown in figure 2-7. The curve shows miss distance as a function of rms error in five range measurements which are made at 69 hours from injection, with the miss without ranging (16.8 km) shown for comparison. Note that 10-km ranging accuracy at this time (16,000 km distance) results in a halving of the miss distance. Assuming an optical measurement device, the disc-measuring accuracy required at this range is 10 arc-seconds.

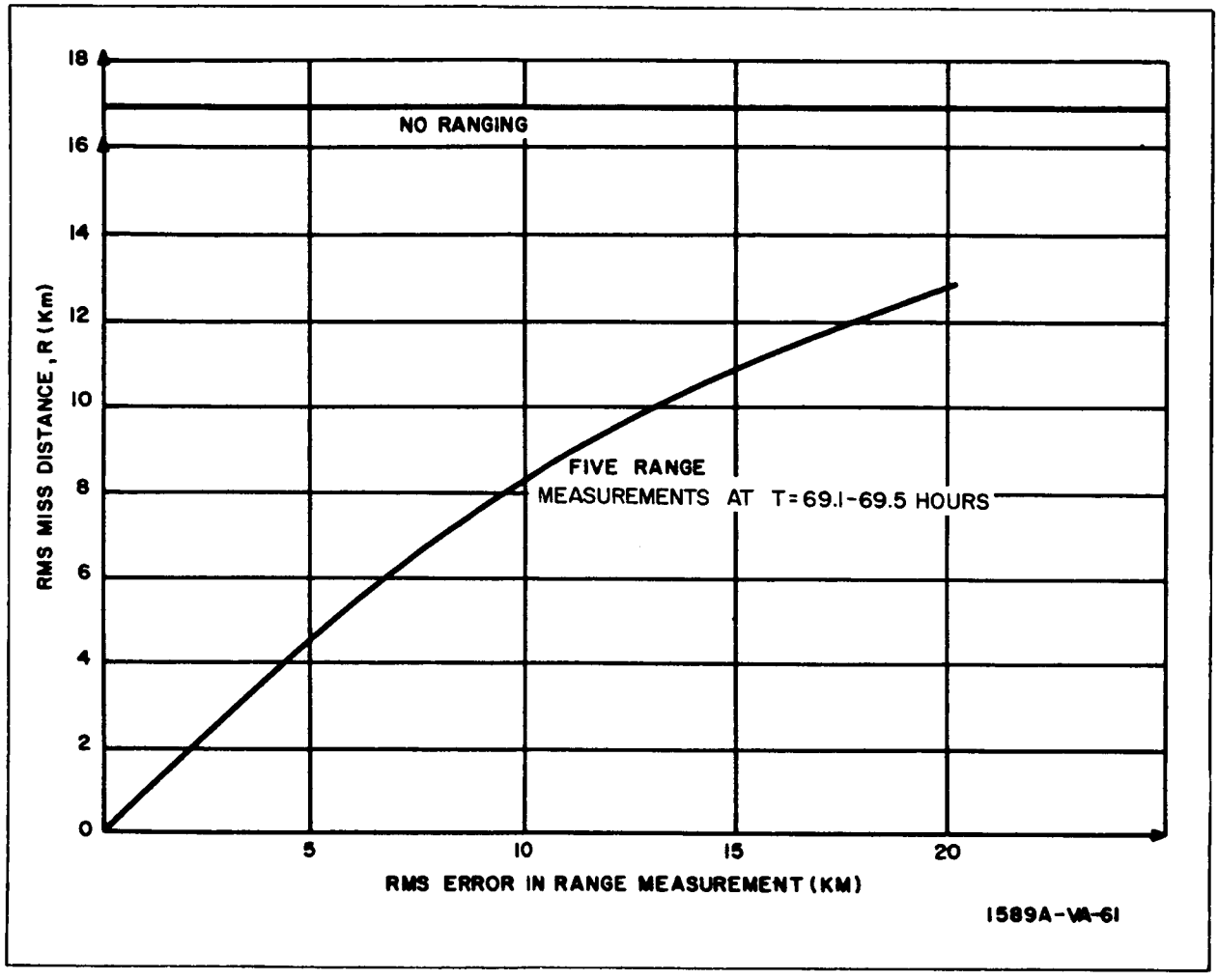

Figure 2-7. Reduction of Periselenum Miss Distance by Adding Five Range Measurements to the Standard Schedule

2.13 POWER AND DISH-SIZE REQUIREMENTS FOR MICROWAVE RANGING OFF LUNAR SURFACE

Since the desirability of ranging in midcourse is clear, consideration was given to the possibility of microwave ranging off the lunar surface, but the requirements are severe. Power and dish-size requirements for microwave ranging off the moon are given in figure 2-8 for a simple pulsed system.

2.14 COMPARISON OF GROUND TRACKING METHODS AND ONBOARD METHODS FOR MIDCOURSE NAVIGATION

A comparison of earth-based methods and the onboard methods analyzed in this study for midcourse navigation was not attempted. However, results of such a comparison in a recent, excellent reference (Ref. 2-4) indicate that:

a. Tracking methods are considerably superior for trajectory determination due to the greater accuracy of the individual measurements and the higher data rate.

b. Overall system performance is not greatly improved by using earth-based tracking since the guidance system is limited by the velocity correction accuracy.

2.15 SUMMARY OF RESULTS

A summary of requirements for the type of systems considered is given below, including an indication of the importance of each item listed:

a. Instrument Accuracy - 10 arc-sec rms, significant penalty (miss and fuel) for increasing.

b. Timing - one sec (in time), rms, 0.1 sec (in time) during terminal phase of lunar approach. Primarily affects estimation errors.

c. Corrections - magnitude 1 percent, pointing = 0.5 degree, cutoff = 0.1 m/sec; (all rms) not critical.

d. Injection - r_o = 2.76 km, v_o = 4.24 m/sec were rms values used. Doubling these values increases correction fuel requirements due to larger first correction, but makes little difference to terminal guidance accuracy.

e. Trajectory - choice of nominal trajectory evidently has little effect on requirements.

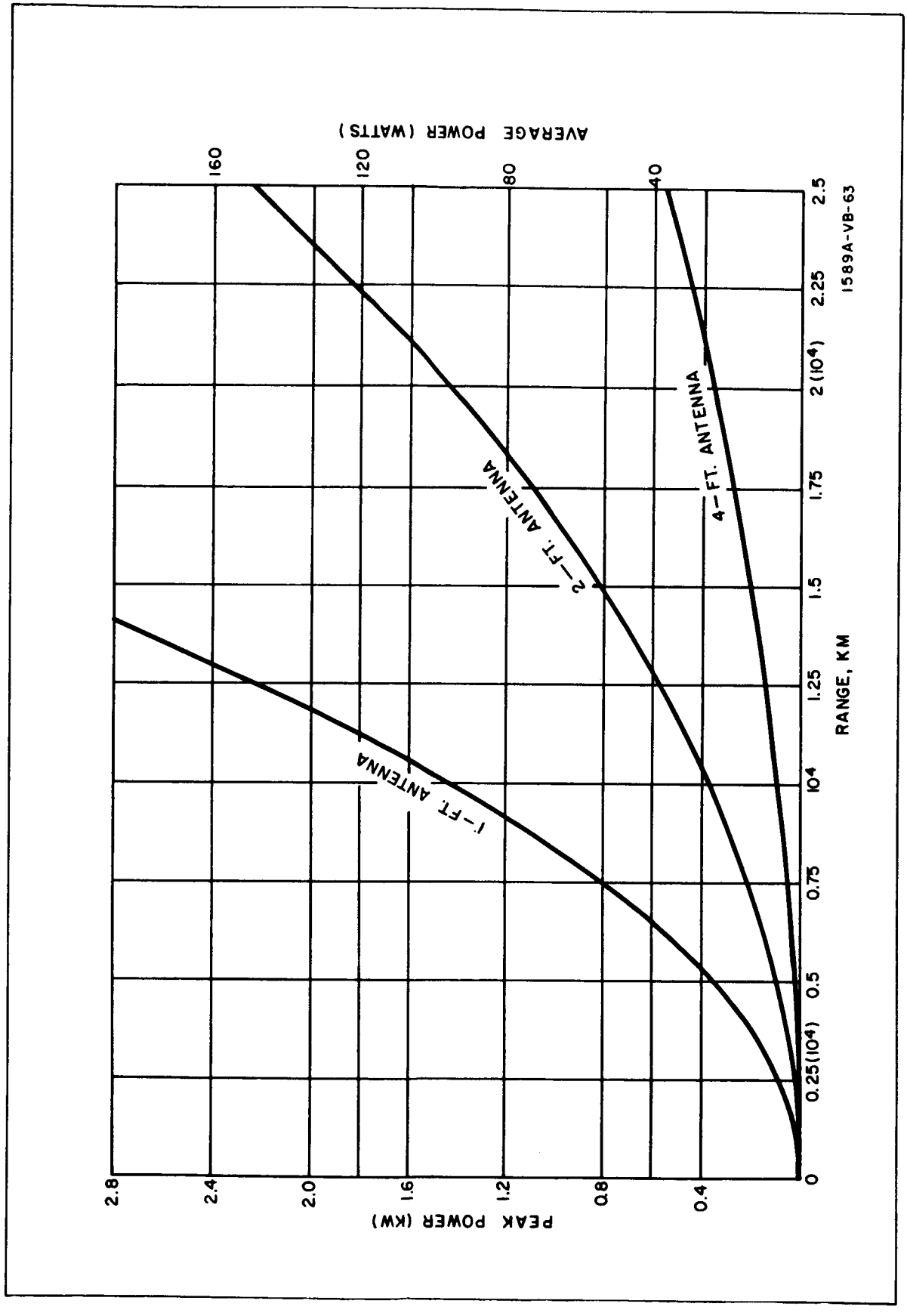

Figure 2-8. Power and Dish Size Requirement for Ranging Off Lunar Surface

f. Stars - choice of stars for guidance was shown to have little effect on system performance.

g. Horizon-Landmark - location of reference points on the moon assumed known to 0.8 km, and earth to 1.6 km. Doubling these errors affected miss distances only slightly, but increased estimation errors significantly.

h. Use of Double-Angle Measurement - scheme gave little improvement over single-angle measurements and would not be recommended if it is more complex than measuring one angle.

i. Range - accurate to 10 km at 16,000 km (typical) and is desirable. Requires 10 arc-sec measurement of planet disc.

3. LUNAR PARKING AND DESCENT ORBITS

This section describes the simulation of a self-contained onboard navigation system which utilizes Kalman's (Ref. 3-1) minimum variance estimation scheme in a vehicle orbiting the moon. By accounting for a number of practical navigation problems, this simulation has made it possible to draw important conclusions about the system requirements and performance.

The application of recursive minimum variance filter theory to celestial navigation was pioneered by Dr. Stanley F. Schmidt and his associates (Ref. 3-2, 3-3) and by Dr. R.H. Battin (Ref. 3-4). Following these and other related theoretical studies (Ref. 3-5, 3-6), some of the underlying simplifications common to early investigations were examined in more detail by Smith and McGee (Ref. 3-7) and by Gunckel (Ref. 3-8). This analysis continues the investigation of the idealizations present in earlier publications in a study which is directed toward the determination of sensor requirements in the orbiting phase of a lunar mission.

3.1 VEHICLE FLIGHT PATH

The nominal lunar trajectory consists of a circular parking orbit, and, for the landing vehicle, an elliptical descent arc of 90 degrees eccentric anomaly (see figure 3-1). The landing vehicle begins its descent during the second revolution in the circular orbit. Requirements for guidance accuracy during this phase are defined by the allowable 3-σ errors at initiation of the landing phase; i.e., 5 kilometers and 2.5 kilometers tangential and vertical error respectively (see Ref. 3-9). Deviations of the actual trajectory from the nominal are to be compensated by correcting the thrust to be applied at initiation of the parking orbit and the descent arc. The thrust vector corrections are to be computed from navigation data accumulated by an on board monitoring system.

3.2 NAVIGATION AND GUIDANCE SCHEME

At the termination of a translunar midcourse trajectory the vehicle, using fixed-time-of-arrival (FTOA) endpoint guidance, is injected into a parking orbit nominally defined as in figure 3-1. At regular intervals along the parking orbit, prescribed navigation measurements are taken and incorporated into recursive minimum variance equations to obtain an updated trajectory estimate. This operation continues until, after the last measurement, the

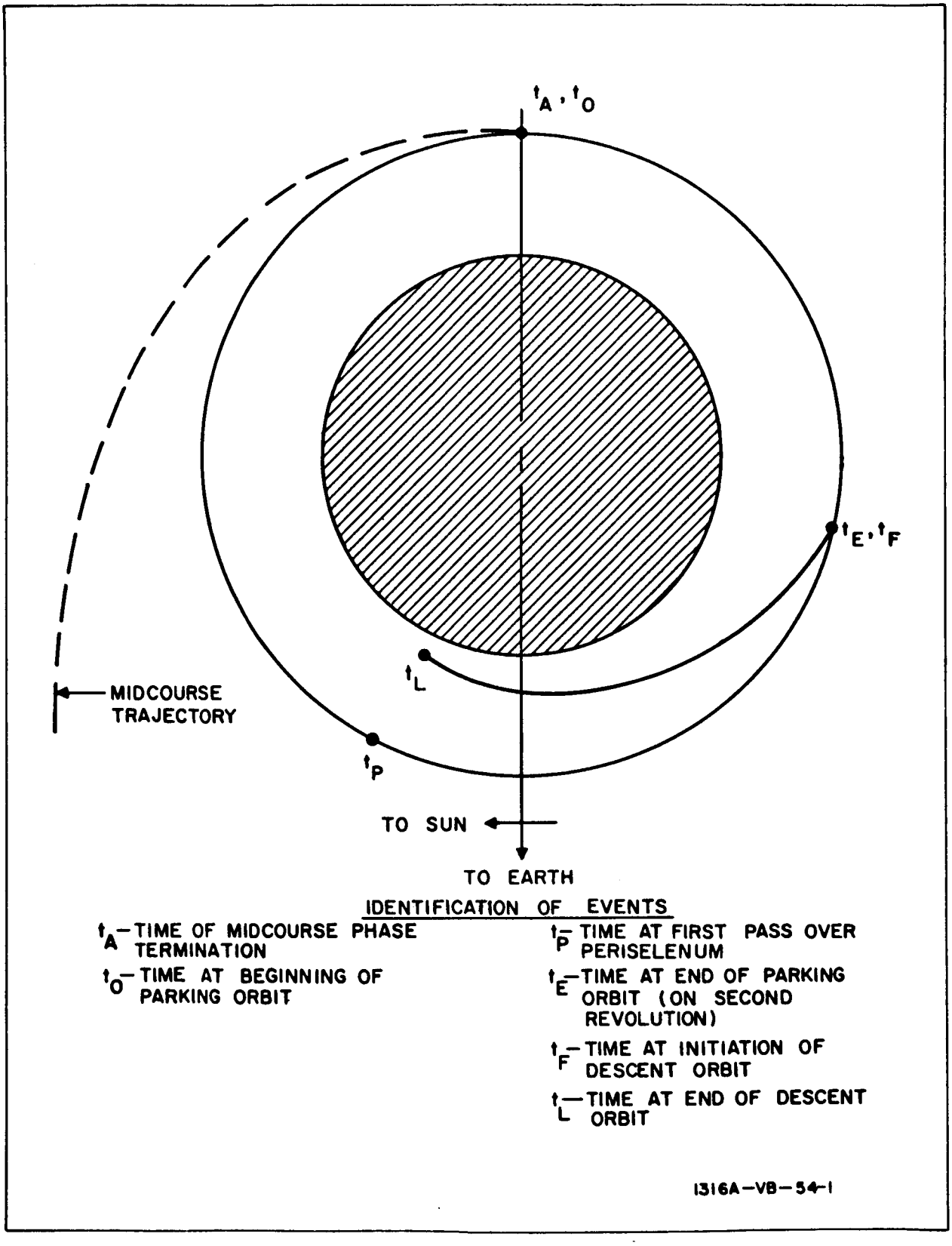

Figure 3-1 Plan View of Lunar Flight Path

estimated orbit and the desired future position are utilized to compute a guidance command. At the proper time, the vehicle is injected (again, using FTOA endpoint guidance) into an elliptical descent arc which is aimed toward a preselected periselenum for landing initiation.

The primary observables selected as navigation aids are angles between known stars (taken from Ref. 3-10) and the instantaneous local vertical, as illustrated in figure 3-2. These observables are chosen in accordance with considerations of accessibility, narrow field of view, low power, versatility, and minimum auxiliary data requirements for processing the measured readings. Two stars near the plane of the orbit are chosen, and a third star, near the pole of the orbit, is used whenever the vehicle local vertical is near the sightline connecting the star to the center of the moon. The utility of altitude measurements is also investigated.

3.3 ANALYSIS AND SIMULATION

The approach taken for simulation of the orbital navigation procedure is illustrated in figure 3-3. The program is arranged such that one member of the ensemble is carried through the simulation,* concurrently with the linearized statistical computations.

In this analysis, factors which can complicate the simulation are sidestepped wherever it is apparant that the outcome would not depend upon the analytical model. Applied thrust is treated as a velocity impulse and the cartesian components of thrust error are assumed to be independent normally distributed random variables with zero mean and equal variance. Components of all simulation input error vectors are assumed to be independent and Gaussian with zero mean. Space geometry is idealized wherever permissible. No consideration is given here to measurement bias or astrodynamical uncertainties, since these items are covered in previously mentioned references, The possibility of instrument failure or gross measurement error is beyond the scope of this analysis.

3.4 RESULTS

The first series of runs (Series A) simulated three revolutions in the parking orbit (with the descent guidance tentatively omitted), for the purpose of investigating requirements involving data processing procedures, observables, and allowable errors. For standard conditions the rms input errors in each coordinate are:

---

* That is, a single Monte Carlo trial is included, in which all input errors are randomly selected and the true values of observables, vehicle position, and velocity are determined from actual nonlinear equations.

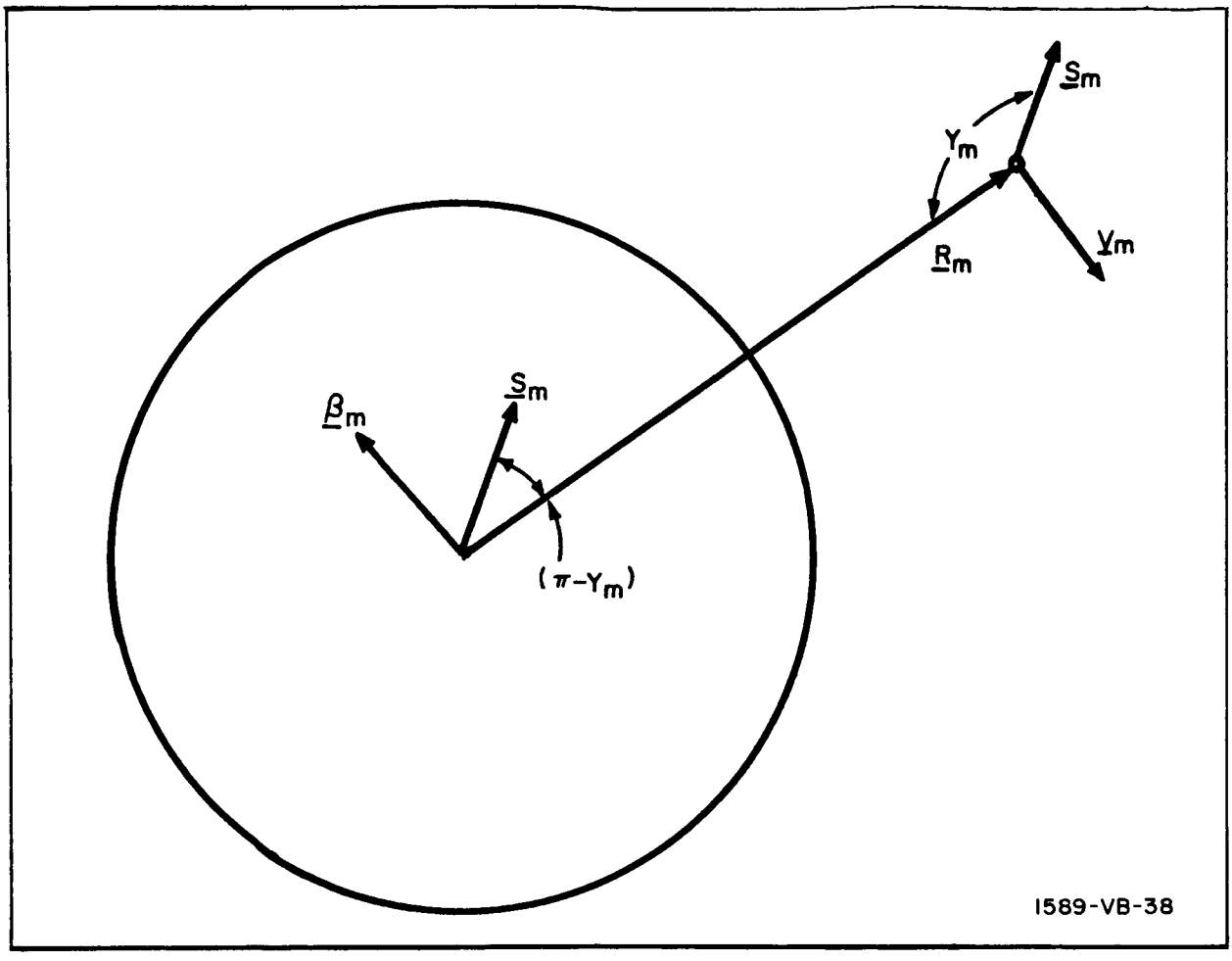

Figure 3-2. Angle Between Star and Local Vertical

- Initial deviation from nominal position: 10 km
- Initial deviation from nominal velocity: 10 m/sec
- Initial position uncertainty: 1 km
- Initial velocity uncertainty: 1 m/sec
- Error in applied impulse at injection: 5 m/sec
- Error in measured impulse at injection: 0.05 m/sec

The rms measurement error is 1 milliradian, with a 5-minute time interval between successive measurements. Standard observables are two stars near the orbital plane and one star near the pole of the orbit, which is

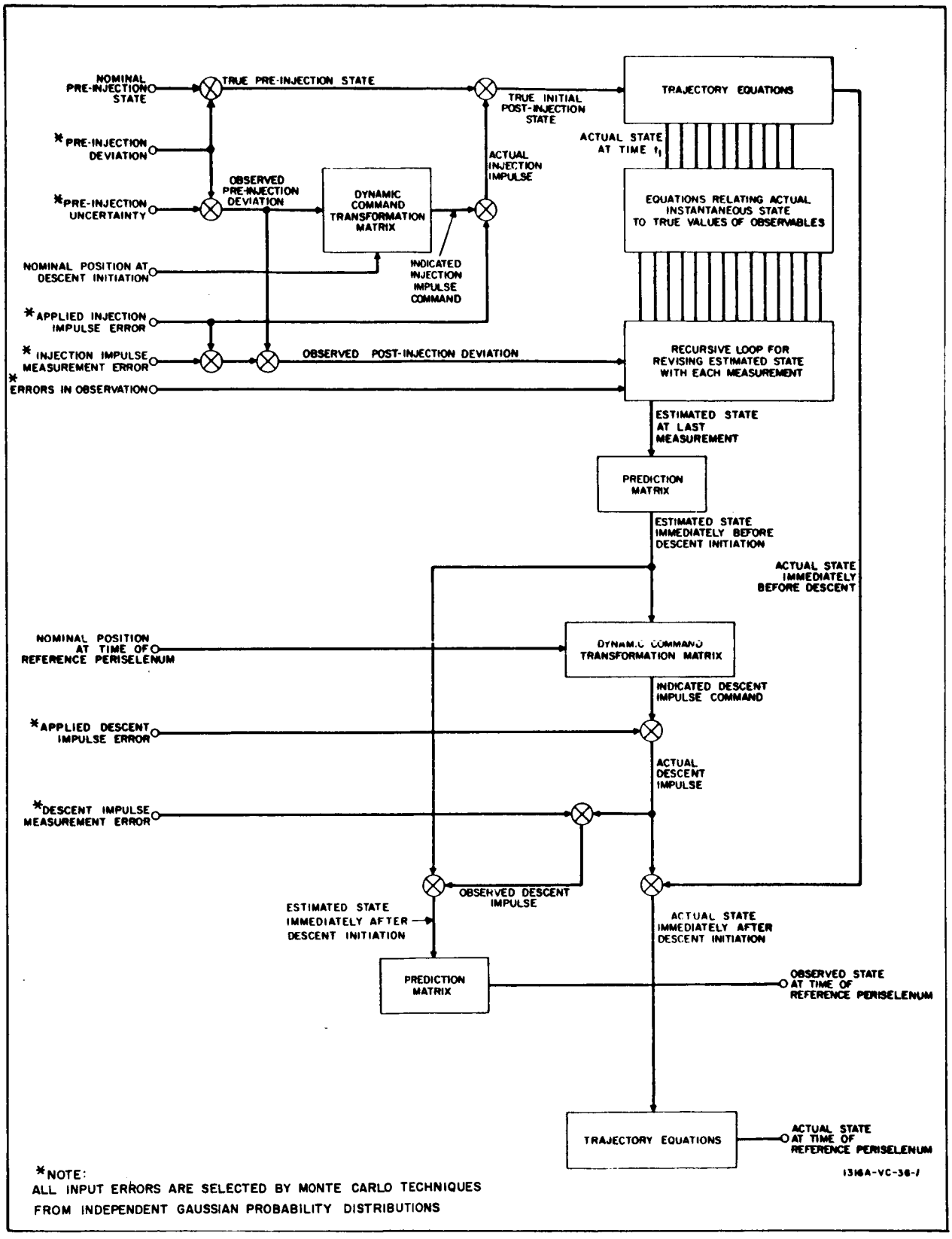

Figure 3-3 Schematic of Lunar Navigation Simulation

measured only when the visible in-plane star is nearly overhead (±25 degrees). In the standard case, all partial derivatives used as sensitivity coefficients are computed from the latest updated orbit estimate.

The earliest efforts in evaluating the navigation scheme were directed toward the specification of onboard computation procedures. With the above mentioned inputs the standard run (Case 1) was made, and the total position uncertainty (including both the square roots of the traces of the position uncertainty covariance matrices before and after each measurement, and the error as determined from the Monte Carlo simulation trial) was plotted at each measurement time. For the second run (Case 2), the program was modified such that the sensitivity coefficients used in processing the measurements were computed from the nominal orbit; the inputs and even the random number starters for Monte Carlo simulation, were matched to the first run. A third run (Case 3) was made in which the actual trajectory (but not the nominal or observed trajectory) was computed from the perturbed orbit equations, but all conditions were otherwise identical to those of the first run.

Since the covariance matrix analysis contains the inherent assumption that no errors are introduced by idealization of onboard computations, the above three runs do not exhibit any appreciable difference in linearized ensemble statistics. As shown by the simulation results plotted in figure 3-4, the three conditions are not equivalent.[1/] In particular, the use of a preselected nominal trajectory suffers from the persistent increase in the departure from that nominal, due to period variations. Whenever the vehicle reaches about 100 kilometers off nominal, the measured partial derivatives, as computed from the nominal orbit, were not in agreement with those of the actual and observed orbits. This causes a divergence between simulated and linearized results, as shown in figure 3-4. The use of two-body equations in the onboard computer, however, shows considerable promise, in spite of the presence of orbital perturbations.

The first run of this series was then repeated with various modifications for comparison of performance provided by different sets of observables. Four basic variations in the field of observables were investigated:

- The in-plane stars initially chosen for navigation were replaced by a pair which lie about 30 degrees out of the nominal orbital plane. (Case 4).

- The twenty first magnitude stars were all made available, and an optimum star selection technique, based upon the principal direction of navigation error, was used. (Case 5).

[1/] The simulation results, of course, do not form a smooth curve, since they do not represent the average of a large number of trials.

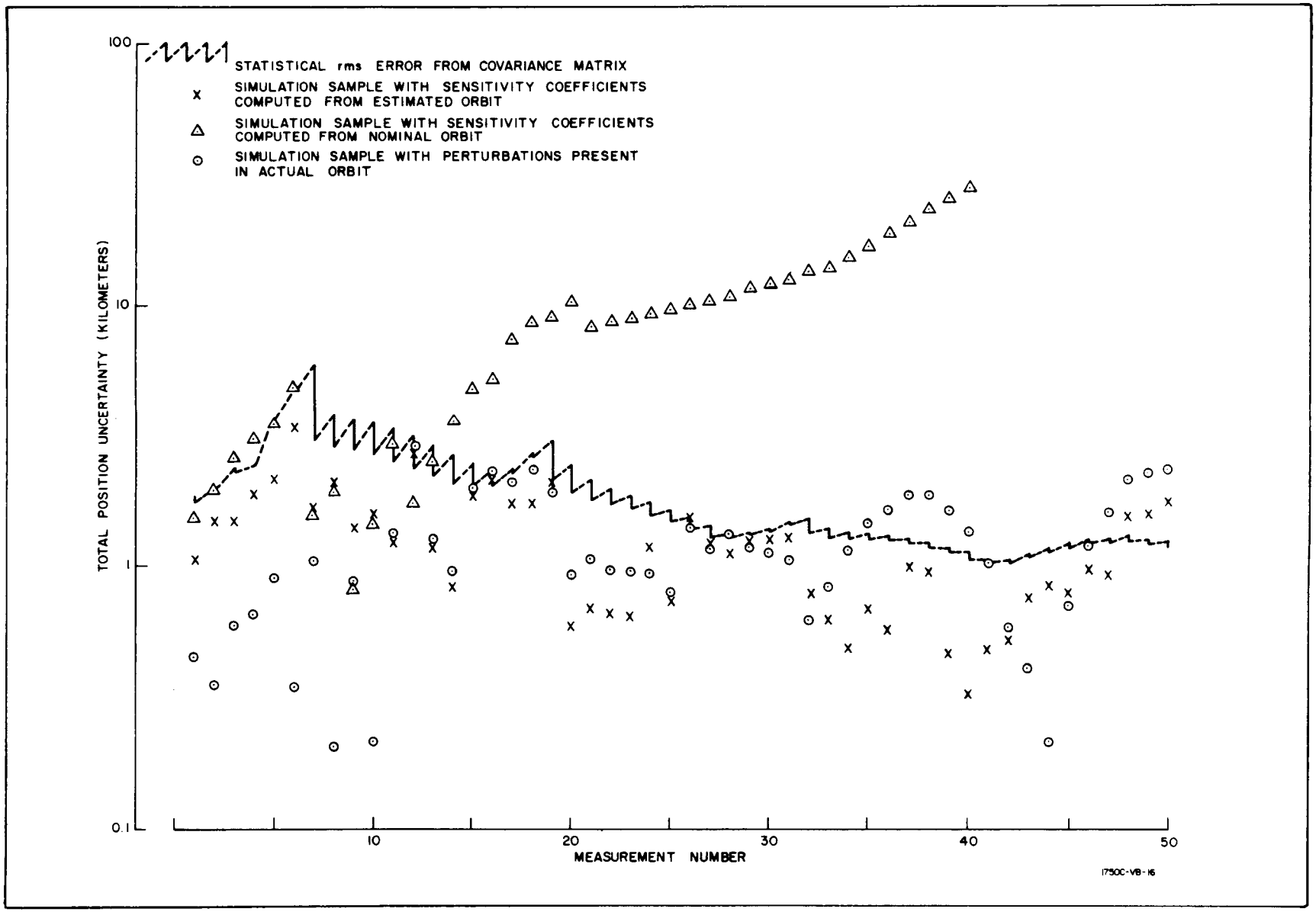

Figure 3-4. Total Position Uncertainty Versus Time (Cases 1, 2, and 3)

- All 57 navigation stars were used with the above mentioned selection technique. (Case 6).

- An altimeter, with an rms error (including terrain uncertainties) of 1 kilometer, was added to the runs with 57 stars, and an optimum measurement preselection technique was used. (Case 7).

The results of Case 4 are shown in figure 3-5. With only three stars available the ultimate effect of selecting stars which are farther removed from the orbital plane is a degradation in performance.

From figure 3-6 it is concluded that a selection of 20 stars offers little more than a properly chosen set of 3. A similar statement can be made in regard to the complete selection of 57 navigation stars; the statistical results of Cases 5 and 6 were essentially the same. The addition of an altimeter, as in figure 3-7 provides a temporary advantage which would be significant for translunar missions with coasting segments.[2/]

The next computer run (Case 8) was made to determine the effects of very large displacements from the computational reference. The standard conditions, with all sensitivity coefficients computed from the observed trajectory, were simulated with the rms initial position uncertainty changed to 100 km in each coordinate. The extent of agreement between the simulation and the linearized analysis, shown in figure 3-8, is an indication of the wide range of tolerable initial error. It is the safety of the vehicle, and not some limit of mathematical convergance, which determines the allowable translunar midcourse terminal errors.

The above run was then repeated with the pole star removed (Case 9), permitting measurement of the in-plane star as the angle approaches 180 degrees. As shown in figure 3-9, the simulation results are near the 3σ level at several points. This illustrates that overhead stars should not be used for navigation.

It is appropriate to mention at this point that all data shown here were obtained with the same random number starter and that subsequent runs with other random numbers exhibited a behavior consistent with the original conclusions.

2/ The altitude measurements were not needed after the early portion of the trajectory. This seems to indicate that a more realistic initial uncertainty covariance matrix would have eliminated the transient rise in initial position uncertainty, without the use of altitude information. Nevertheless, the utility of additional observables will remain significant in some applications.

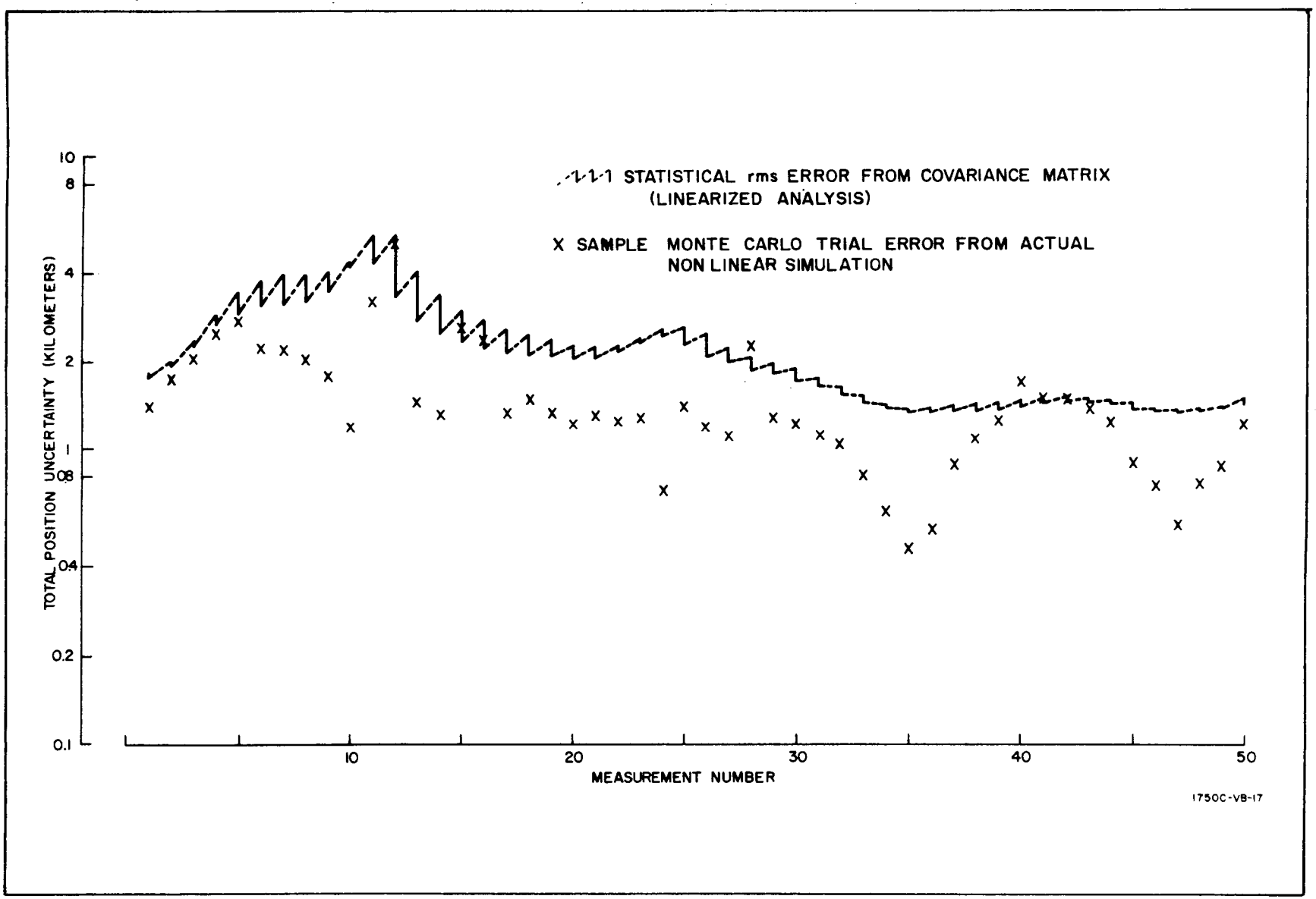

Figure 3-5 Total Position Uncertainty Versus Time (Case 4)

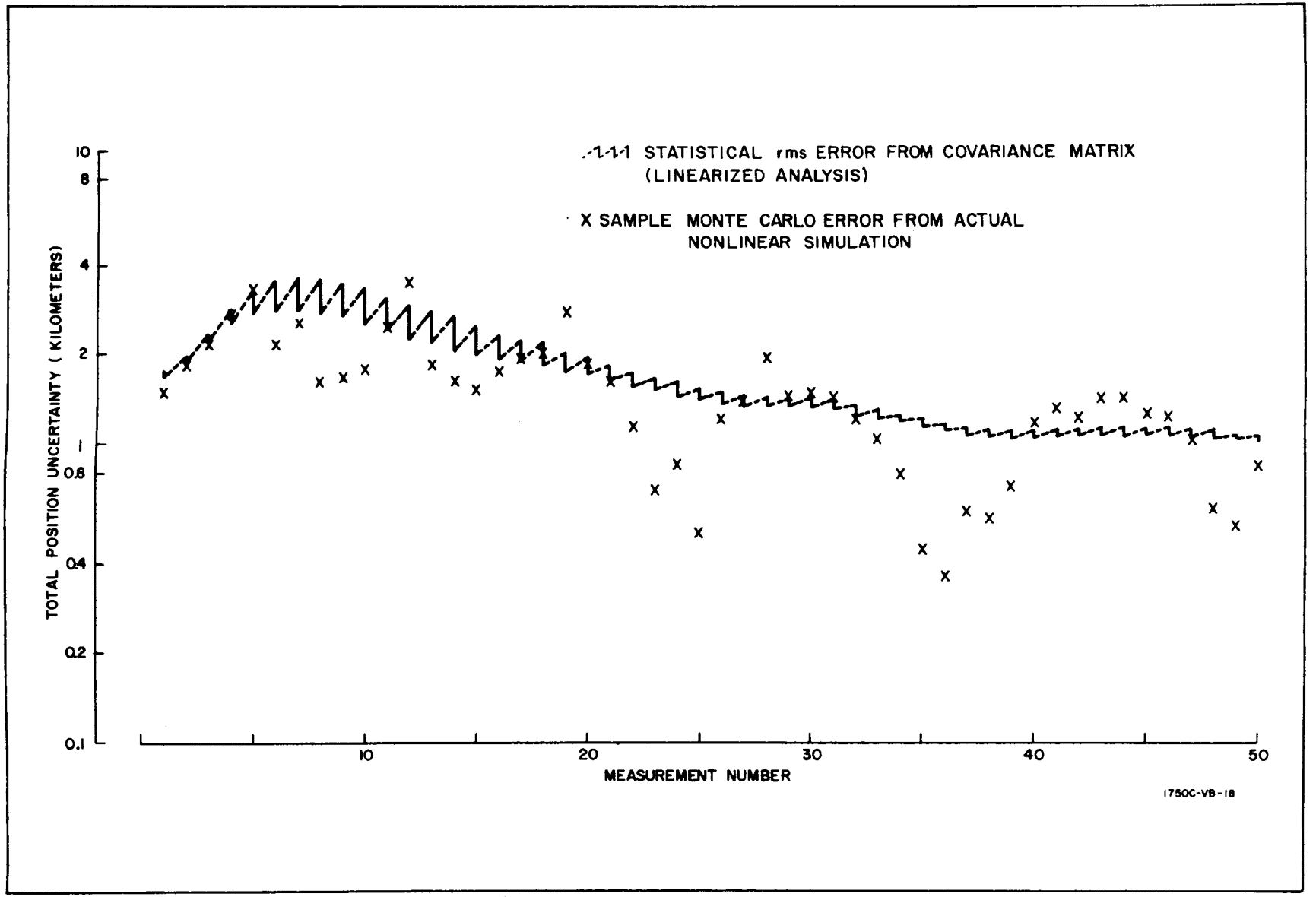

Figure 3-6 Total Position Uncertainty Versus Time (Case 5)

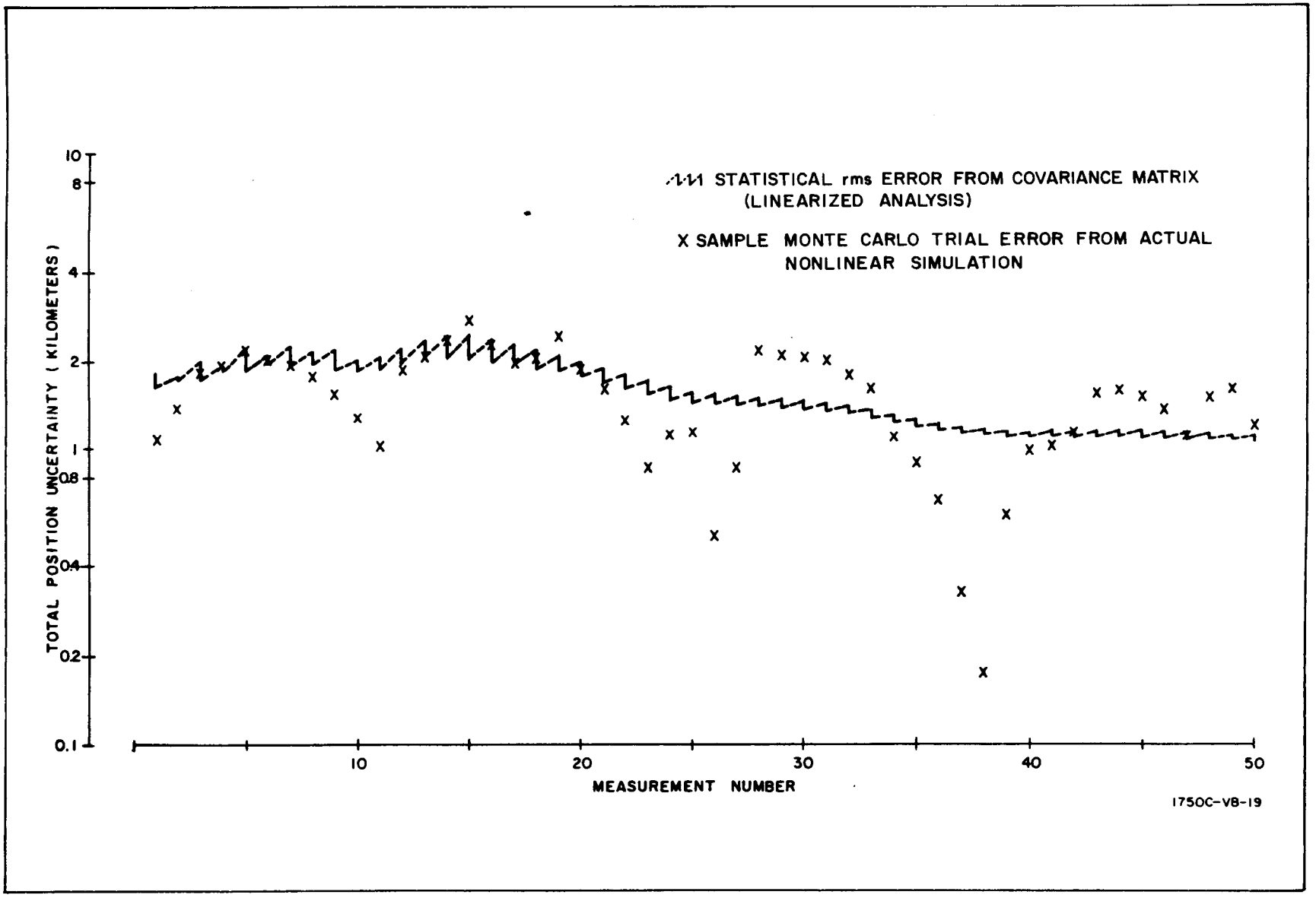

Figure 3-7 Total Position Uncertainty Versus Time (Case 7)

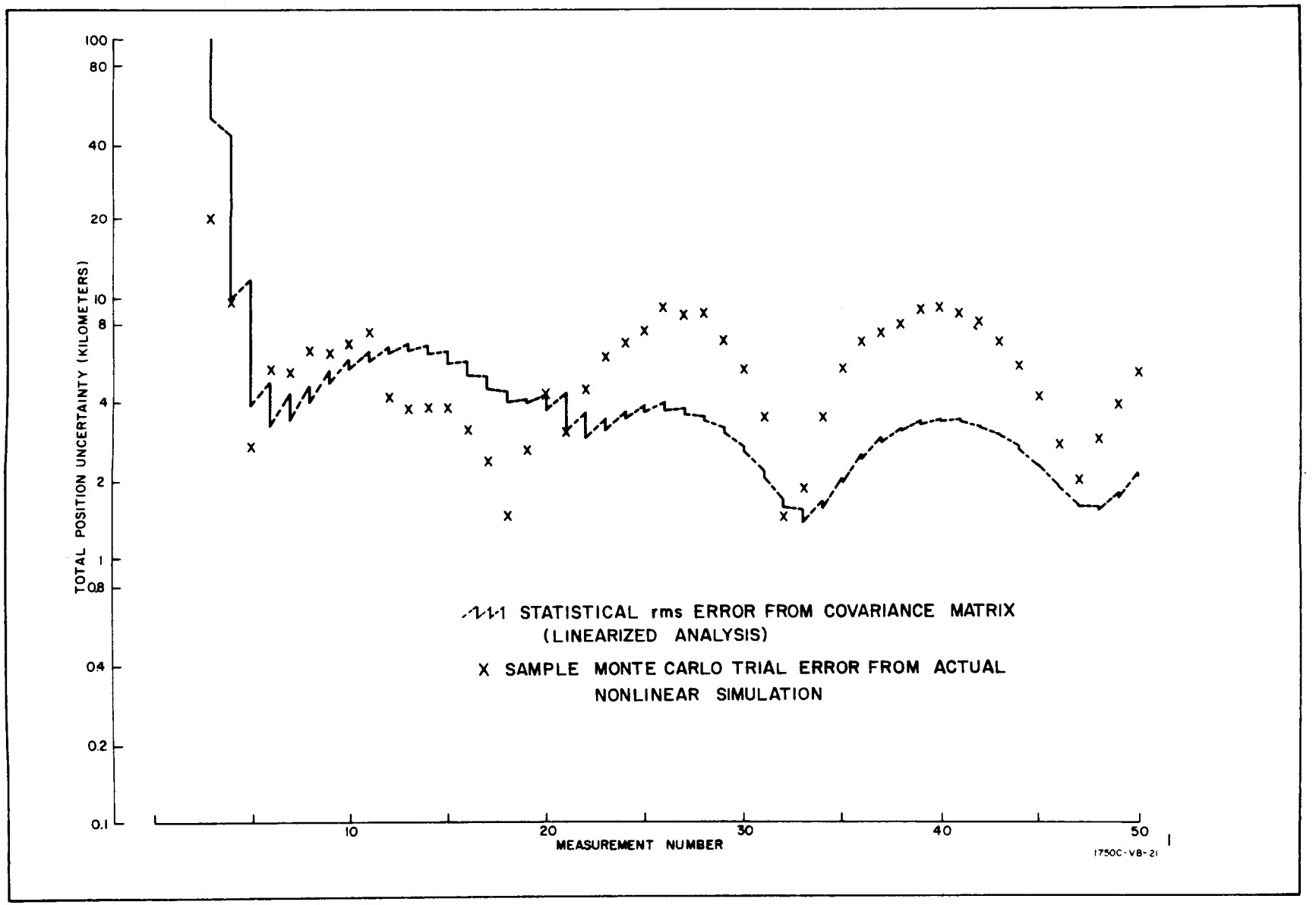

Figure 3-8 Total Position Uncertainty Versus Time (Case 8)

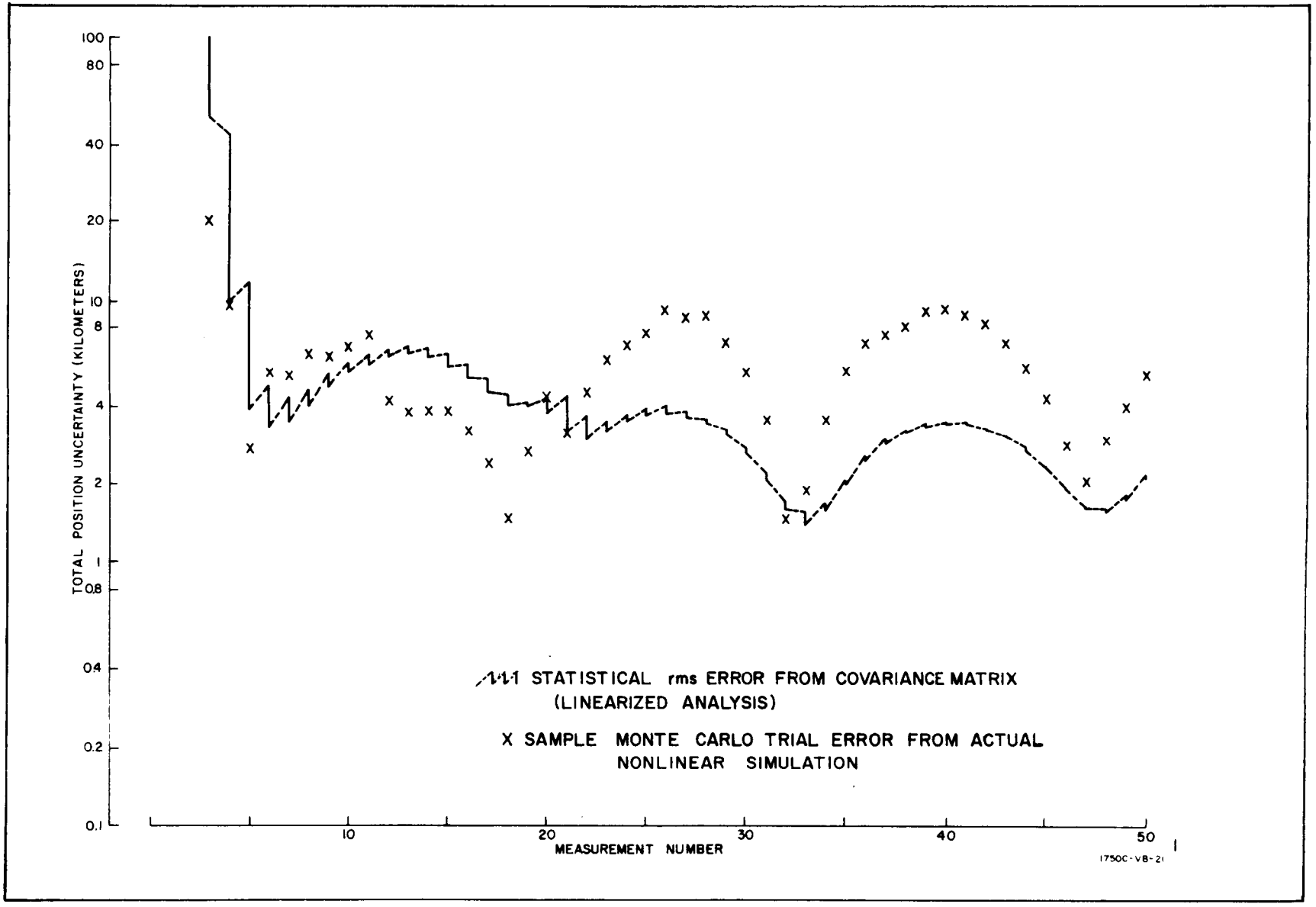

Figure 3-9 Total Position Uncertainty Versus Time (Case 9)

For the next series of runs (Series B), the single parking orbit revolution and descent arc of figure 3-1 were simulated to determine the required measurement accuracy. The standard conditions and inputs were used throughout, except for the time interval (τ) between successive measurements and the rms angle measurement error (σ_m). Fifteen runs were made including all combinations of angle measurement error and interval given below:

- Measurement Error: 0.5; 1.0; 1.5; 2.0; 3.0 milliradians
- Time between measurements: 120, 180, 240 seconds

The descent thrust measurement error was assumed equal to the thrust measurement error at injection. For applied thrust at descent, however, the error was assumed to be 0.1 meter per second in each axis.[3/]

The results of this simulation series are summarized as follows:

- The extra velocity impulse needed for FTOA guidance (typically a few hundred meters per second) is excessive; a variable time guidance law will undoubtedly take perference.
- The rms miss distance at the time of reference periselenum is very nearly directly proportional to the rms measurement error and to the square root of the measurement interval, as shown in figure 3-10.[4/] This is to be expected, since the deviation from the desired final position is (nearly) a linear function of the state uncertainty prior to the guidance command. This uncertainty, in turn, is proportional to the rms measurement error divided by the square root of the number of observations.

[3/] It should be noted that this stringent engine tolerance is not a system requirement but an assumed value used to render the thrust error small in comparison with navigation error effects. The FTOA guidance law, an unneccessary restriction in itself, results in a high sensitivity of final miss distance to applied thrust errors.

[4/] It should be noted that, due to descent thrust errors, the extrapolated curve would not pass through the origin.

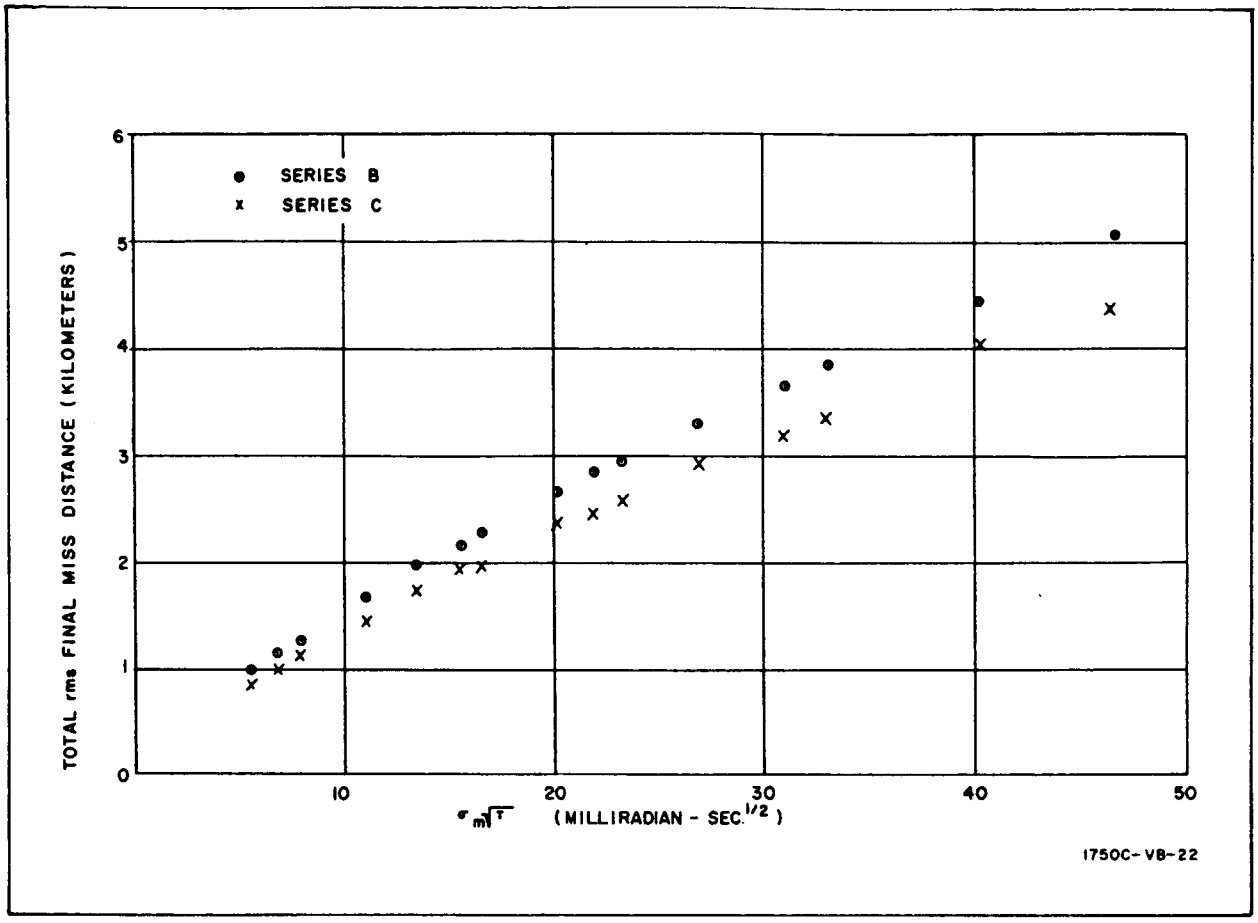

Figure 3-10 Final Miss Distance as a Function of Instrument Error and Measurement Frequency

- The tangential, vertical, and transverse components of final miss distance are not equally sensitive to the measurement parameters. The tangential error predominates, particularly at values near the maximum allowable miss distance.

- In view of the maximum allowable 3-σ-tangential miss distance of 5 kilometers, the combination of a 2-minute interval and about 1-1/4 milliradians rms error can be cited as safe specifications for the lunar navigation phase, with the three-star configuration of observables.

In seeking a set of conditions under which this last requirement can be relaxed, the entire run sequence was repeated (Series C), using all twenty first magnitude stars conditioned as in Case 6 of the first run sequence. As shown in figure 3-10, however, the improvement is appreciable but not profound. Futhermore, by selecting measurements to minimize the dominant error, the transverse errors are increased somewhat.

The case of a 3-milliradian rms error and a 2-minute interval was then repeated with the initial rms velocity uncertainty reduced by a factor of ten. Again, the effect was an appreciable (500 meter), but not drastic, reduction in rms terminal miss distance.[5/] Finally, a random number starter was found for which the displacement from nominal position at descent initiation time was relatively small, and the last simulation was repeated. The effect was a reduction of another 1100 meters from the rms miss distance, which brought the final figure (1750 meters rms) quite close to the originally specified allowable limit (5 km at 3σ). At the same time, the rms position and velocity uncertainty at descent initiation were virtually unchanged.

With FTOA guidance for a 1/2-hour descent arc, the sensitivity of the linearized final miss vector statistics to the parking orbit navigation errors (which is related to the slope in figure 3-10) is somewhat dependent upon the particular combination of initial errors occurring at injection. The reason for this dependence is clarified by considering the wide range of position displacements possible at descent initiation. For some of the larger values encountered (in the vicinity of 250 km), the position deviation to be compensated by guidance adjustments changes the total path length by a considerable percentage. Clearly, these variations in arc length, with fixed time at the endpoints, must change the average orbital velocity; the energy of the trajectory, in turn, influences the sensitivity of final errors to initial errors.

3.5 CONCLUSIONS

The highlights of the lunar parking and descent orbit analysis are summarized as follows:

- Provided that the parking orbit has a duration of 1/2 revolution or greater, it is permissible to limit the navigation observables to two or three known stars and the local vertical. A properly chosen set of three stars (two in the orbital plane and one near the pole of the orbit) provides navigation accuracy comparable to that obtainable with the 57 navigation stars (Ref. 3-10). Acceptable performance is also obtainable with two stars, both about 30 degrees out of the orbital plane.

- Overhead stars (i.e, stars near the local vertical line) are not acceptable navigation aids.

[5/] That is, the rms miss distance was reduced from about 3350 meters to 2850 meters. The low sensitivity of final errors to initial uncertainties indicates that reduction of midcourse navigation errors would be an inefficient means of improving the ultimate performance.

- The advantages of the star-vertical measurements are continuous accessibility (including the flight over the dark and unknown sides of the moon); low requirements for accompanying astrophysical data, power consumption, and field of view; insensitivity to lunar rotation; and ease of both manual and automatic implementation.

- With direct radial position information (i.e., altitude measurements), the navigation errors can in some cases be reduced more quickly. Because of the prominence of tangential errors, however, no appreciable premanent improvement is achieved.

- The measurement sensitivities and the state transition matrices used in the minimum variance equations must be computed from the updated trajectory estimate, rather than from a given nominal orbit.

- With repeatedly updated Keplerian equations used for navigation, the observed trajectory takes the form of a patched sequence of conic segments. Because this is a valid approximation to a perturbed orbit, and because actual navigation measurements include the effects of orbital perturbations, it is permissible to use two-body equations for navigation, even in the presence of perturbing forces.

- Complete knowledge of the initial uncertainty covariance matrix is not necessary; a pessimistic, diagonal (Ref. 3-11) initial matrix leads to a conservative result. Since final navigation errors are insensitive to initial navigation errors (Ref. 3-3), the result is only slightly pessimistic.

- Measurement timing uncertainties on the order of tenths of a second have little effect upon navigation accuracy in the cases under consideration here.

- Additional sources of error, not treated in this analysis, have been covered in other related studies. Lack of precise knowledge of sensor error statistics is apparently not critical (Ref. 3-8), and the effects of unknown measurement bias and astrodynamical uncertainties can be counteracted.(Ref. 3-7).

- The simulation conducted here is in accordance with the principle that terminal navigation errors (i.e., state vector uncertainties) are insensitive to initial errors. The guidance errors (i.e., final miss vector components), however, are somewhat sensitive to initial conditions. The reason is traceable to trajectory modifications necessitated by large displacements from reference position with fixed time guidance.

- The total rms final miss distance is directly proportional to the measurement error and to the square root of the interval between measurements.

- The slope of this line, however, is somewhat sensitive to initial errors, as explained by the above discussion of the guidance law.

- The fixed time guidance law, an unnecessary constraint, also leads to a high sensitivity of terminal miss distance to thrust errors.

- The fuel consumption accompanying the FTOA guidance scheme is excessive. This remark refers to the in-plane correction at descent initiation, plus any extra fuel required because of departures from the optimum (90-degree) arc for plane corrections, and also to the unwanted vertical velocity component at the intended powered landing initiation time. Total excess (i.e., above nominal) velocity impulse figures are typically on the order of a few hundred meters per second in the system analyzed here with FTOA guidance.

In view of the above items, it is reasonable to assert that the guidance technique to be selected for actual orbital flight will be superior to the FTOA scheme, and will complement the minimum variance navigation technique so that its full potential can be realized. The navigation scheme itself is able to perform adequately with state of the art horizon scanner accuracy, and will not be unduly degraded by nonlinearities, perturbations, imperfections in navigation computations, a limited field of observables, measurement timing uncertainties, or incomplete knowledge of parameters required for trajectory determination. In conclusion, the performance envisioned in the pioneering studies of minimum variance orbital navigation (Ref. 3-2, 3-3, 3-4) appears to be obtainable with a practical onboard system which lends itself readily to mechanization.

4. LUNAR LANDING PHASE

4.1 INTRODUCTION

This section summarizes the investigation of navigation and control sensor requirements for lunar landing. The total effort is divided into two parts, Problem Definition and Analytical Solution, which are reported in Volumes II and III respectively. The Analytical Solution is further subdivided into:

- A general background section linking Volumes II and III, and containing information pertinent to both guidance concepts selected for analysis in Volume II (linear predictive guidance, and proportional navigation).
- Several sections of background analysis for each of the two guidance schemes. These sections are required to define specific characteristics of the guidance and control system models in sufficient detail so that the investigation of sensor error effects can proceed. Typical discussions pertain to navigation equations, guidance equations, and trajectory characteristics.
- A discussion of the sensor error analysis performed for each of the two guidance concepts.
- Presentation and discussion of the results obtained for each guidance concept.
- Presentation of conclusions for each guidance concept.
- A comparative section discussing the relative merits of the two guidance concepts studied as illustrated by the analytical results.

4.2 BACKGROUND

The following subsections provide background information which facilitated discussion of the analytical effort which facilitated discussion of the analytical effort.

4.2.1 Mission Profile

The overall mission follows a profile similar to that planned for the Project Apollo manned landings. The vehicle is injected into a circular lunar parking orbit immediately following midcourse and into a synchronous, elliptical descent orbit prior to the actual landing phase. The landing phase as discussed in this report commences with ignition of the landing engine at periselenum of the synchronous descent orbit and terminates at vehicle touchdown. In portions of the investigation, the principal portion of the landing maneuver terminates with the vehicle in a hover condition at some specified altitude above the desired landing site. When this is the case, the terminal portion of landing (hover-to-touchdown) is assumed to be under manual guidance and control.

4.2.2 State Variables

Throughout this report, the instantaneous position and velocity of the space vehicle define the vehicle state at that instant. The state is described by a vector (column matrix) of state variables denoted $\underline{X}(t)$. (The time argument is often omitted.)

$$\underline{X} = \begin{bmatrix} X_1 \\ X_2 \\ \cdot \\ \cdot \\ \cdot \\ X_N \end{bmatrix} \qquad (4\text{-}1)$$

The total number of state variables (N) is 6 for three-dimensional space, and 4 for two-dimensional space. Much of the analytical effort is discussed in terms of the general state vector $\underline{X}$.

4.2.3 Control Vector

Throughout powered flight, the space vehicle is acted upon by a controllable force vector (the thrust vector), denoted $\underline{F}$. In three dimensional space this vector has three components:

$$\underline{F} = \begin{bmatrix} F_1 \\ F_2 \\ F_3 \end{bmatrix} \tag{4-2}$$

4.2.4 Navigation Observables

Specific delineation of the navigational quantities which can be observed during the landing phase is accompanied by discussion of the navigational requirements for various types of lunar missions. Finally, combinations of observables providing sufficient information for position and velocity determination are specified, and two of these are selected for analysis in the analytical solution. The two selected are referred to as beacon tracking navigation and doppler navigation respectively. Beacon tracking observables are line-of-sight range, angle, and their time derivatives from the vehicle to a beacon located at the desired landing site. Doppler navigation is so-named because the velocity vector is determined by making doppler measurements to the lunar surface in known directions. Positional information for the doppler navigation system is obtained by measuring altitude and the line-of-sight angle to the desired landing site.

In addition, a general vector of observables is defined to be $\underline{Y}(t)$:

$$\underline{Y} = \begin{bmatrix} Y_1 \\ Y_2 \\ \cdot \\ \cdot \\ \cdot \\ Y_M \end{bmatrix} \quad \text{(with the time argument omitted)} \tag{4-3}$$

where M is the total number of observables used. This vector representation is often used in the formal presentation of the analytical study.

4.2.5 Trajectory Considerations

Trajectory optimization is not considered to be within the scope of this study. However, certain trajectory characteristics are desirable for the landing maneuver, and an effort is made to use trajectories exhibiting these characteristics. Principal among the desired properties are a continuous, constant-level thrust program, and vertical approach to the landing site.

4.2.6 Analytical Assumptions

Several general analytical assumptions are made which apply throughout the lunar landing analysis.

- The vehicle is moving in an ideal central force field.
- The translational motion is accurately described by restricted two-body equations of motion.
- The moon is considered to be stationary in inertial space during the landing phase.
- The landing analyses are performed in two-dimensional space. The desired landing site is assumed to be in the vehicle plane of motion at all times.

4.2.7 Definition of Sensor Error Model

The main objective of the study is the evaluation of the effects of navigation and control sensor errors on the performance of two selected lunar landing navigation and guidance techniques. It is clear then, that the analytical model or characterization of the sensor error constitutes an important input to the analytical study. The following definitions will facilitate discussion:

$Y(t)$ = an observable quantity at time t.

$\tilde{y}(t)$ = the total error in observing $Y(t)$.

The total measurement error is considered to be the sum of four components - two bias components and two zero-mean random noise components.

$$\tilde{y}(t) = \tilde{y}_b + {}_Y p_b \frac{Y(t)}{100} + \tilde{y}_n(t) + {}_Y p_n(t) \frac{Y(t)}{100} \qquad (4\text{-}4)$$

The characteristics of each component are summarized below:

- $\tilde{y}_b$ is a bias error which is constant over the duration of the landing maneuver.

- ${}_Yp_b \frac{Y(t)}{100}$ is a time varying bias error component obtained by multiplying a scale factor bias coefficient, ${}_Yp_b/100$ times the value of the observable quantity. The coefficient ${}_Yp_b$ has the units of percent and is constant over the landing phase.

- $\tilde{y}_n(t)$ is a random error component characterized as being a stationary, Gaussian random variable with zero-mean value and mean squared value denoted ${}_n\sigma_Y{}^2$. The units of $y_n(t)$ are the same as those of $Y(t)$.

- ${}_Yp_n(t) \frac{Y(t)}{100}$ is a nonstationary random error which is seen to be the product of ${}_Yp_n(t)$ and $Y(t)/100$. The scale factor coefficient, ${}_Yp_n(t)$, is defined to be a stationary, Gaussian random variable with zero-mean value, and mean squared value ${}_p\sigma_Y{}^2$. The units of ${}_Yp_n(t)$ are percent.

Bias error quantities, y_b and ${}_Yp_b$ are constant over any given mission, but random over the ensemble of all possible missions. Random error components are random over any single mission as well as over the ensemble of missions. In addition, the four components of each observation error are assumed to be independent; when more than one observable is measured, all observation errors are independent.

4.3 ANALYTICAL SOLUTION

The Analytical Solution is divided into two main sections which constitute essentially independent analyses of the two guidance concepts which were selected for analysis in the Problem Definition; i.e., linear predictive guidance and modified proportional navigation. Each of these major divisions is subdivided into four parts:

- Background analyses: These analyses begin with the system concept generated in Volume II and end with a specific system model that can be used in the analysis of sensor error effects. Typical subjects discussed are: selection of state variables and formulation of the equations of motion; determination of navigation equations; discussion of the guidance law

and determination of the guidance equations; trajectory characteristics; specification of vehicle characteristics (as required); and further discussion of the sensor error model.

- Error analysis: The techniques used and their application to the problem of determining sensor error effects are discussed.

- Results: The results sections include presentations of numerical results obtained from the error analysis, a sample computation illustrating the use of the analytical results, and discussion and interpretation of the analytical results with regard to sensor accuracy requirements.

- Conclusions: Conclusions applicable to each guidance concept are presented. Finally, the two independent analyses are drawn together by a section comparing the relative characteristics of the two guidance systems as determined on the basis of analyses presented in Volume III.

4.3.1 Analysis of Lunar Landing Using Linear Predictive Guidance (LPG)

4.3.1.1 Background Analyses

a. State Variables - The state variables used during the analysis of linear predictive guidance are defined below and illustrated in figure 4-1.

$X_1 = h$: Spacecraft altitude above the lunar surface.

$X_2 = \theta$: The angular displacement of the spacecraft from the desired landing site in lunar central coordinates.

$X_3 = \gamma$: The vehicle flight path angle relative to vehicle local horizontal (in the plane of motion).

$X_4 = V$: The magnitude of the spacecraft velocity vector.

where X is the general state variable.

Quantities h and θ define position while γ and V define velocity in the two-dimensional space used for analysis. The vehicle position and velocity at any time is referred to as its "state".

b. Control Variables - The control variables are the magnitude, T, and the direction, α, of the thrust vector. Only two are used because a two-dimensional analysis is performed

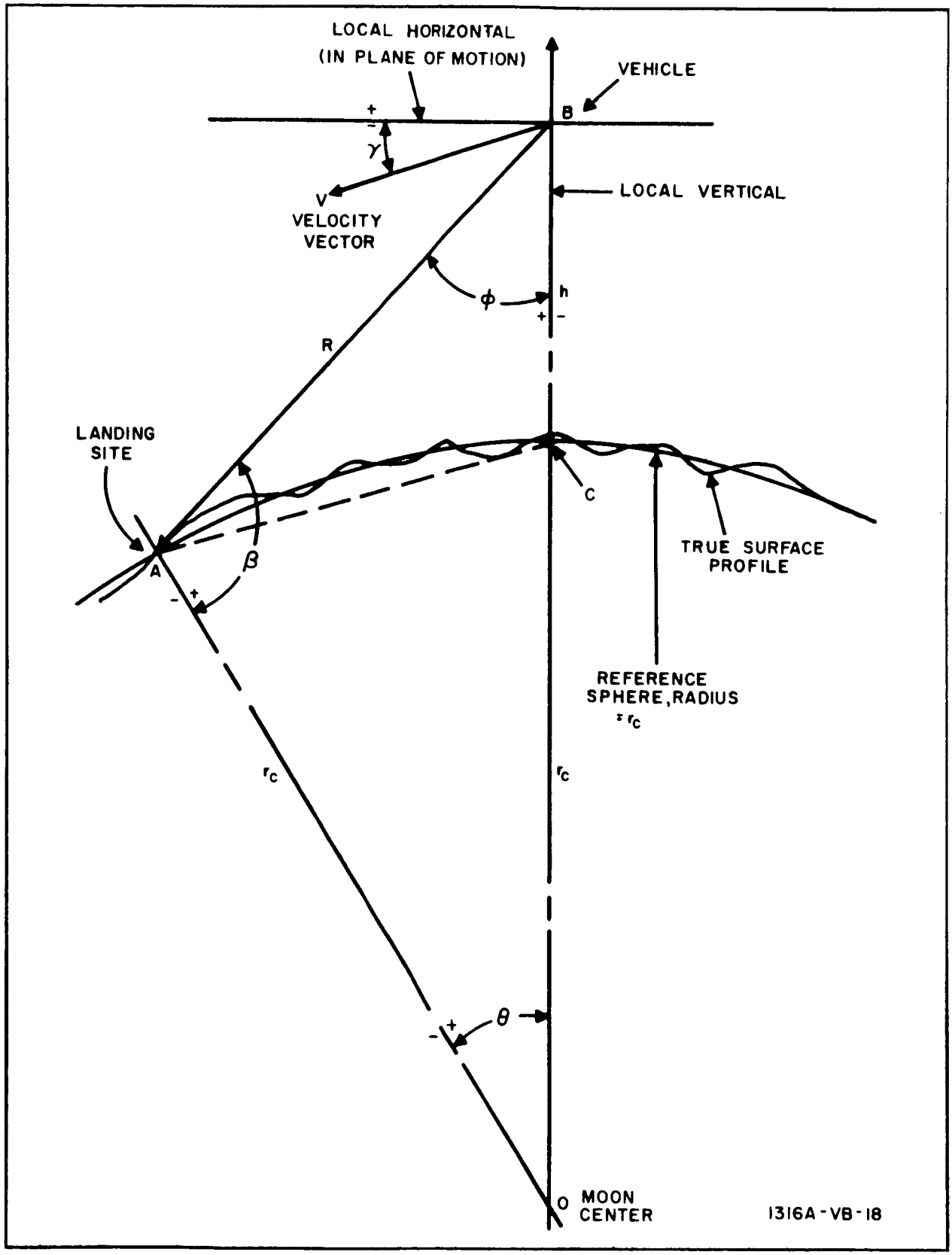

Figure 4-1. Lunar Landing Geometry

$$\underline{F} = \begin{bmatrix} F_1 \\ F_2 \end{bmatrix} = \begin{bmatrix} T \\ \alpha \end{bmatrix} \qquad (4\text{-}5)$$

c. Navigation - Navigation in this context refers to the process of estimating vehicle state on the basis of observed information. The measured quantities are termed "observables". When operating in the vicinity of a massive gravitational body, such as the moon, several quantities are considered observable. These are summarized below:

- Line-of-sight range, angle, and their time derivatives to a beacon on the surface: R, $\dot{R}$, ϕ, $\dot{\phi}$.
- Altitude and altitude rate: h, $\dot{h}$.
- Line-of-sight range, range rate, and angle to an arbitrary point on the surface: R_p, $\dot{R}_p$, ϕ_p.
- Vehicle accelerations in three orthogonal axes.
- Direction of local vertical.

From the list, two separate combinations of observables, each providing sufficient information for navigation, are selected for analysis. The first combination includes observation of line-of-sight range, angle, and their time derivatives, (denoted R, $\dot{R}$, ϕ, and $\dot{\phi}$) with respect to a beacon located at the desired landing site. This is referred to as beacon tracker navigation. These observables compose the observable vector $\underline{Y}_B$:

$$\underline{Y}_B = \begin{bmatrix} R \\ \dot{R} \\ \phi \\ \dot{\phi} \end{bmatrix} \qquad (4\text{-}6)$$

In addition, a navigation scheme observing altitude (h), line-of-sight angle to the landing site (ϕ), and two components of range rate to the surface in

known directions ($\dot{R}_1$ and $\dot{R}_2$) is investigated. These observables compose the observable vector $\underline{Y}_D$:

$$\underline{Y}_D = \begin{bmatrix} h \\ \dot{R}_1 \\ \phi \\ \dot{R}_2 \end{bmatrix} \qquad (4\text{-}7)$$

This is referred to as doppler navigation because of the method of velocity determination.

d. Guidance Technique - A linear predictive guidance technique is used and functions in the following manner. Linearized equations operating on observed deviations from a reference trajectory are used to estimate the terminal errors that would exist if no deviation from the reference thrust program were made. Then, deviations from the reference thrust program which will reduce selected terminal deviations to zero are determined. All terminal errors cannot be controlled because there is not a sufficient number of control quantities available. The particular terminal errors selected for control are said to define the guidance mode. Two guidance modes, termed H-θ guidance and H-V guidance respectively, are investigated in this study.

The important characteristics of this guidance concept are:

- It provides capability for successful landing with large, known, initial deviations from the reference trajectory.
- It is an endpoint guidance scheme, and does not waste fuel by trying to return to the reference trajectory prior to the endpoint.
- It requires storage of reference trajectory information on board the landing vehicle.
- The trajectory characteristics are not determined by the guidance law and can be selected independently.

Because of linearization error, trajectories flown using this guidance scheme in a noise-free environment (no sensor errors) do not quite return to the reference trajectory at the endpoint. For each particular set of initial deviations from the reference case, there is a particular path that would be

flown if perfect sensors were available. This is called the "pseudonominal" trajectory and it terminates in the "pseudonominal endpoint" t_f seconds after engine ignition (t_f is the nominal time-of-flight).

e. Reference Trajectory - The reference trajectory used is a constant-thrust gravity turn commencing at the periselenum of the synchronous descent orbit and terminating in a hover point 500 meters above the desired landing site. The desirable characteristics of this type of trajectory are:

- Continuous constant thrust generates minimum engine sizing, reliability, and throttling requirements.
- The gravity turn thrust program provides near minimum fuel expenditure.
- The gravity turn approach offers good terrain clearance and visibility characteristics. Final approach to the landing site is nearly vertical.
- The nominal thrust program automatically rotates the vehicle to the proper hover attitude for touchdown.

During this study, several trajectories of this type were generated corresponding to different periselenum altitudes. Geometrical and fuel characteristics of these trajectories are presented in subsection 2.2 of Appendix D (Volume V).

f. Characterization of Engine Control Subsystem - Lunar landing using linear predictive guidance is analyzed assuming essentially perfect control. This is done to eliminate consideration of mechanization characteristics of the vehicle attitude and engine control subsystems. To take into account the fact that these subsystems can include information sensors, control sensor errors are injected. The general characteristics of these errors are discussed in the problem definition portion of this summary.

One limiting characteristic related to bandwidth is applied to the engine control subsystem. The autocorrelation function of white noise passed through the control subsystem, denoted $\psi(\tau)$, is considered to have its first zero at $\tau = \tau_o$. Quantity τ_o is then referred to as the correlation interval of white noise passed through the subsystem.

g. Error Model - The navigation sensor error model used in the analysis of linear predictive guidance consists of only the random components of the general error model discussed in subsection 4.2. In addition, control sensor errors of the same general characteristics are introduced. No bias errors are considered.

4.3.1.2 Error Analysis

Of the two basic error analysis techniques, Monte Carlo simulation and linearized ensemble error analysis, the latter approach is selected for use in the investigation of lunar landing using linear predictive guidance. The two primary reasons for selecting linearized analysis are:

- Linearization is a mathematical technique and tends to deemphasize mechanization considerations, which is in keeping with the intent of the study.

- Linearized analysis produces statistical information directly. Since sensor errors can only be defined statistically, these effects must also be described statistically.

In addition, the linearized analysis is found to be quite flexible in that navigation, guidance, and control system parameters can be varied with little difficulty.

The background analysis sections include discussion of the various components of the overall navigation, guidance, and control system. Also included are descriptions of the linearized models of each major system block which are used to make up the overall system analytical model.

After linearization of the overall system, the resulting system model is still not amenable to ordinary analytical techniques, the reason being that many of the subsystems are characterized by time varying gain parameters. The approach taken to this problem is quite commonly used in the investigation of time varying control systems. Basically, the technique is to quantize time, or subdivide the flight into a sequence of small time intervals. Within each interval the system is allowed to be both linear and time invariant. All time varying parameters are sampled at the beginning of each interval and held at the sample value until the next sampling time, one quantization interval later. Then, all parameters are updated and sampled again. System characteristics are updated according to stored data evaluated on the reference trajectory, and vehicle state information is updated by using the linearized equations of motion and vehicle forces commanded at the previous sample time.

The numerical results of the error analysis are matrices of error sensitivity coefficients which yield upper bounds on the terminal mean squared errors when the mean squared values of the random components of the navigation and control sensor errors are given. The effects of bias errors on the performance of linear predictive guidance are not investigated.

4.3.1.3 Results

a. Presentation of Numercial Results - The numercial results obtained are presented graphically in Volume III. In these graphs each element of the three matrices of sensitivity coefficients which result from the error analysis is plotted as a function of nominal initial altitude for three values of τ_o (the engine subsystem correlation interval) and for two guidance modes.

The matrices of sensitivity coefficients $[K]$, $[K']$, and $[K'']$ are used to relate terminal mean squared errors to navigation and control sensor mean squared errors according to the matrix expression

$$\begin{bmatrix} \sigma^2_{X_1 f} \\ \sigma^2_{X_2 f} \\ \sigma^2_{X_3 f} \\ \sigma^2_{X_4 f} \end{bmatrix} = [K] \begin{bmatrix} {}_n\sigma^2_{Y_1} \\ {}_n\sigma^2_{Y_2} \\ {}_n\sigma^2_{Y_3} \\ {}_n\sigma^2_{Y_4} \end{bmatrix} + [K'] \begin{bmatrix} {}_p\sigma^2_{Y_1} \\ {}_p\sigma^2_{Y_2} \\ {}_p\sigma^2_{Y_3} \\ {}_p\sigma^2_{Y_4} \end{bmatrix} + [K''] \begin{bmatrix} {}_n\sigma^2_{F_1} \\ {}_n\sigma^2_{F_2} \end{bmatrix} \qquad (4\text{-}8)$$

where

$\sigma^2_{X_i f}$ is the mean squared value of the final error in X_i, the i^{th} state variable.

${}_n\sigma^2_{Y_i}$ is the mean squared value of $(\tilde{y}_i)_n$ which is one of the two random components of the total navigation sensor error $\tilde{y}_i$.

${}_p\sigma^2_{Y_i}$ is the mean squared value of ${}_{Y_i}p_n$, a random scale factor which when multiplied by $\frac{Y_i}{100}$ yields the second random component of $\tilde{y}_i$.

$_{n}\sigma_{F_i}^2$ is the mean squared value of $(\tilde{f}_i)_n$, which is the random error contribution of the control sensor measuring F_i, the i^{th} component of the control vector.

b. Sample Computation - To illustrate the use of the sensitivity coefficient matrices, a set of values for rms navigation and control sensor errors were selected and a sample calculation was performed for τ_o = 1 second and h_o = 20 km. The selected sensor error parameters and the resulting error components are summarized in tables 4-1, 4-2, and 4-3. Table 4-1 gives the estimated terminal position and velocity errors resulting from the assumed control sensor errors, while tables 4-2 and 4-3 contain similar data for the two sets of navigation sensors. Tables 4-2 and 4-3 also present overall error estimates. The sensor capabilities are typical of the state of the art, assuming a 1-second smoothing time, which is compatible with the value of τ_o used in the sample.

Typical conclusions concerning results of the sample computation are:

- The dominant error source in the beacon tracking navigation scheme is the line-of-sight angle rate measuring device.
- No error source can be regarded as dominant with the set of doppler navigation sensor errors.
- Switching from the H-θ to the H-V guidance mode increases all three terminal error components in the system using beacon tracking observables, and two out of three (all but velocity) components when doppler navigation observables are used. Since velocity errors are critical, H-θ guidance is indicated with beacon tracking and H-V guidance with doppler navigation.
- In general, rms terminal errors are smaller with doppler navigation observables than with beacon tracker observables (assuming state of the art capability).

Thus, the desired system configuration, based on the sample computation, uses doppler navigation observables and the H-V guidance mode. This conclusion is based entirely on the magnitude of the terminal errors and does not consider mechanization, fuel consumption characteristics, or any other factors which also must be considered before final system design is attained.

c. Results of Parameter Variations - During the error analysis of linear predictive guidance, several system parameters are treated as variables:

TABLE 4-1

MEAN SQUARED TERMINAL ERRORS CAUSED BY CONTROL SENSOR ERRORS (SAMPLE COMPUTATION, h_o = 20 km, τ_o = 1 sec.)

Error Source	RMS Sensor Error (Symbol and Magnitude)	Resulting Terminal Mean Squared Error Components		
		Altitude Error $L(\sigma^2_{h\ f_i})_M$ (meters)	Central Angle Error $L(\sigma^2_{\theta\ f_i})_M$ $(\text{radians})^2$	Velocity Error $L(\sigma^2_{V\ f_i})_M$
Thrust Magnitude Control Sensor	${}_n\sigma_{F_1} = {}_n\sigma_T$ = 500 new.	0.0239	7.90×10^{-14}	1.23
	${}_p\sigma_{F_1} = {}_p\sigma_T = 0.0$	0.0	0.0	0.0
Thrust Direction Control Sensor	${}_n\sigma_{F_2} = {}_n\sigma_\alpha$ = 0.035 rad.	2.73	9.25×10^{-14}	0.0
	${}_n\sigma_{F_2} = {}_p\sigma_\alpha = 0.0$	0.0	0.0	0.0
Total Mean Squared Terminal Error Caused by Control Sensor Errors[a]		2.75	17.15×10^{-14}	1.23

a. Results presented in this table are applicable to all four possible combinations of observation (navigation) systems and guidance modes.

guidance mode (H-θ or H-V); observables (beacon tracker or doppler navigator); quantization interval (τ_o = 1, 2, or 3 seconds); nominal trajectory initial attitude (10, 15, 20, 25, and 30 km). The results of these investigations are summarized below:

- Guidance mode: It is found that terminal velocity errors are reduced by changing from H-θ guidance to H-V guidance when doppler navigation is in use. A reduction in velocity error is also realized when using beacon tracking navigation so long as angle rate measurement error is not the dominant contributor to terminal state errors.

TABLE 4-2

MEAN SQUARED TERMINAL ERRORS CAUSED BY NAVIGATION SENSOR ERRORS (SAMPLE COMPUTATION: OBSERVABLES $R\ \dot{R}\ \phi\ \dot{\phi}$, h_o = 20 km; τ_o = 1 second)

Error Source	RMS Sensor Error (Symbol and Magnitude)	Resulting Terminal Mean Squared Error Components					
		H-θ Guidance Mode			H-V Guidance Mode		
		Altitude Error $L^{(\sigma^2_{h\,Y_i})}{}_M$ $(\text{meters})^2$	Central Angle Error $L^{(\sigma^2_{\theta\,Y_i})}{}_M$ $(\text{radians})^2$	Velocity Error $L^{(\sigma^2_{V\,Y_i})}{}_M$ $(\text{m/sec})^2$	Altitude Error $L^{(\sigma^2_{h\,Y_i})}{}_M$ $(\text{meters})^2$	Central Angle Error $L^{(\sigma^2_{\theta\,Y_i})}{}_M$ $(\text{radians})^2$	Velocity Error $L^{(\sigma_{V\,Y_i})}{}_M$ $(\text{m/sec})^2$
Range Measurement ($_BY_1 = R$)	$_n\sigma_{Y_1} = {}_n\sigma_R = 5.0$ m	0.0675	0.675×10^{-14}	0.063	0.198	17.3×10^{-14}	0.0445
	$_p\sigma_{Y_1} = {}_p\sigma_R = 0.1\%$	0.00129	0.0777×10^{-14}	0.00103	0.0059	0.276×10^{-14}	0.00115
Range rate measurement ($_BY_2 = \dot{R}$)	$_n\sigma_{Y_2} = {}_n\sigma_{\dot{R}} = 0.5$ m/sec.	0.0772	1.51×10^{-14}	0.165	0.131	7.72×10^{-14}	0.0102
	$_p\sigma_{Y_2} = {}_p\sigma_{\dot{R}} = 0.5\%$	0.0165	6.90×10^{-14}	0.850	0.066	1.17×10^{-14}	0.133
Angle measurement ($_BY_3 = \phi$)	$_n\sigma_{Y_3} = {}_n\sigma_\phi = 0.001$ rad.	0.0001	0.034×10^{-14}	0.00174	0.00007	0.0107×10^{-14}	0.0005
	$_p\sigma_{Y_3} = {}_p\sigma_\phi = 0.0$	0.0	0.0	0.0	0.0	0.0	0.0
Angle rate measurement ($_BY_4 = \dot{\phi}$)	$_n\sigma_{Y_4} = {}_n\sigma_{\dot{\phi}} = 0.001$ rad./sec	85.0	42.6×10^{-14}	1.78	94.4	115.0×10^{-14}	7.09
	$_p\sigma_{Y_4} = {}_p\sigma_{\dot{\phi}} = 0.0$	0.0	0.0	0.0	0.0	0.0	0.0
Total Mean Squared Terminal Error Caused By Navigation Sensor Errors		85.16	51.80×10^{-14}	2.86	94.80	138.0×10^{-14}	7.28
Total Mean Squared Terminal Error Caused By Control Sensor Errors (Table 4-1)		2.75	17.15×10^{-14}	1.23	2.75	17.15×10^{-14}	1.23
Total Mean Squared Terminal Errors $L^{(\sigma^2_{X_i})}{}_M$		87.91	68.95×10^{-14}	4.09	97.55	155.1×10^{-14}	8.51
Total Root Mean Squared Terminal Errors $L^{(\sigma^2_{X_i})}{}_M$		9.38 (meters)	8.30×10^{-7} (radians)	2.02 (m/sec)	9.87 (meters)	12.5×10^{-7} (radians)	2.92 (m/sec)

TABLE 4-3

MEAN SQUARED TERMINAL ERRORS CAUSED BY NAVIGATION SENSOR ERRORS (SAMPLE COMPUTATION: OBSERVABLES $h\dot{R}_1$ $\phi\dot{R}_2$; h_o = 20 km; τ_o = 1 second)

Error Source	RMS Sensor Error (Symbol and Magnitude)	Resulting Terminal Mean Squared Error Components					
		H-θ Guidance Mode			H-V Guidance Mode		
		Altitude Error $L^{(\sigma^2_{h\,Y_i})_M}$ $(\text{meters})^2$	Central Angle Error $L^{(\sigma^2_{\theta\,Y_i})_M}$ $(\text{radians})^2$	Velocity Error $L^{(\sigma^2_{V\,Y_i})_M}$ $(\text{m/sec})^2$	Altitude Error $L^{(\sigma^2_{h\,Y_i})_M}$ $(\text{meters})^2$	Central Angle Error $L^{(\sigma^2_{\theta\,Y_i})_M}$ $(\text{radians})^2$	Velocity Error $L^{(\sigma^2_{V\,Y_i})_M}$ $(\text{m/sec})^2$
Altitude measurement ($_DY_1 = h$)	$_n\sigma_{Y_1} = {}_n\sigma_h = 5.0$ m	0.0234	1.94×10^{-14}	0.298	0.177	6.58×10^{-14}	0.0362
	$_p\sigma_{Y_1} = {}_p\sigma_h = 0.1\%$	0.000595	0.048×10^{-14}	0.00709	0.00525	0.238×10^{-14}	0.000795
Range rate measurement ($_DY_2 = \dot{R}_1$)	$_n\sigma_{Y_2} = {}_n\sigma_{\dot{R}_1} = 0.2$ m/sec	0.0264	3.25×10^{-14}	0.0152	0.0264	5.91×10^{-14}	0.00895
	$_p\sigma_{Y_2} = {}_p\sigma_{\dot{R}_1} = 0.5\%$	0.0190	1.99×10^{-14}	0.222	0.00790	0.500×10^{-14}	0.0500
Angle measurement ($_DY_3 = \phi$)	$_n\sigma_{Y_3} = {}_n\sigma_\phi = 0.001$ rad.	0.0103	1.42×10^{-14}	0.159	0.0	0.0	0.0
	$_p\sigma_{Y_3} = {}_p\sigma_\phi = 0.0$	0.0	0.0	0.0	0.0	0.0	0.0
Range rate measurement ($_DY_4 = \dot{R}_2$)	$_n\sigma_{Y_4} = {}_n\sigma_{\dot{R}_2} = 0.2$ m/sec.	0.00568	2.00×10^{-14}	0.0651	0.0179	1.63×10^{-14}	0.0106
	$_p\sigma_{Y_4} = {}_p\sigma_{\dot{R}_2} = 0.5\%$	0.00675	2.65×10^{-14}	0.345	0.0500	0.210×10^{-14}	0.0398
Total Mean Squared Terminal Error Caused By Navigation Sensor Errors		0.092	13.30×10^{-14}	1.11	0.284	15.07×10^{-14}	0.146
Total Mean Squared Terminal Error Caused By Control Sensor Errors (Table 4-1)		2.75	17.15×10^{-14}	1.23	2.75	17.15×10^{-14}	1.23
Total Mean Squared Terminal Errors $L^{(\sigma^2_{X_i})_M}$		2.84	30.45×10^{-14}	2.34	3.03	32.22×10^{-14}	1.38
Total Root Mean Squared Terminal Errors $L^{(\sigma_{X_i})_M}$		1.69 (meters)	5.52×10^{-7} (radians)	1.53 (m/sec)	1.74 (meters)	5.68×10^{-7} (radians)	1.18 (m/sec)

- Observation scheme: On the basis of state-of-the-art sensor capability, it is found that the doppler navigation scheme yields consistently smaller terminal error components than the beacon tracking scheme.

- Quantization interval (τ_o): It is found that the vast majority of terminal error components increase in magnitude as τ_o increases from 1 to 3 seconds. There are exceptions, and these are pointed out.

- Nominal trajectory initial altitude: No generalization can be made concerning the effect of changing initial altitude (h_o) on the terminal errors. Nearly as many of the error sensitivity coefficients decrease as increase with increasing h_o.

4.3.1.4 Conclusions

The following conclusions are based on analytical results obtained:

- Characteristics of terminal state error distributions for any given group of sensors are highly dependent on which sensor is the dominant error source.

- Generally, increasing τ_o results in increased terminal mean squared errors.

- When state of the art sensor capabilities are assumed for both navigation sensor schemes, doppler navigation results in smaller terminal errors.

- Changing from the H-θ to the H-V guidance mode does result in reduced terminal velocity errors when doppler navigation is used; however, the reduction is not very significant. In addition, it is possible for this guidance mode switch to result in increased terminal velocity error when beacon tracking navigation is employed.

- Terminal position errors caused by navigation and control sensor errors are not serious, being on the order of a few meters (based on sample computation results). The situation with regard to velocity errors is not so clear-cut. The landing mission profile as envisioned in this study is made up of two subphases: descent-to-hover and hover-to-touchdown. Linear predictive guidance is considered to be used down to the hover point with some undefined terminal guidance system controlling the actual touchdown. For manned flights, this touchdown

maneuver is considered to be under manual control. For this case, velocity errors at hover of the magnitude indicated in tables 4-2 and 4-3 are felt to be satisfactory. For the unmanned case, relaxed touchdown velocity requirements can be expected, so that the terminal (hover point) velocity errors resulting from state of the art sensor capability are expected to be satisfactory even if the hover-to-touchdown guidance system offers no improvement in touchdown velocity uncertainty. (This is the case if thrust is simply terminated at the hover point, allowing the vehicle to descend to the surface under gravitational acceleration.)

4.3.2 Analysis of Lunar Landing Using Modified Proportional Navigation

4.3.2.1 Background Analysis

a. State Variables - The principal state variables used during the analysis of linear predictive guidance are defined below, and illustrated in figure 4-2.

$X_1 = R$ = line-of-sight range from spacecraft to the desired landing site.

$X_2 = \dot{R}$ = the time derivative of R.

$X_3 = \Omega$ line-of-sight angle to the desired landing site measured with respect to landing site local vertical.

$X_4 = \dot{\Omega}$ = the time derivative of Ω.

b. Control Variables - The control quantities are accelerations along the vehicle roll and yaw axes respectively. However, the attitude control system is assumed to keep the roll axis aligned with the line-of-sight to the desired landing site, so that the command accelerations are along and perpendicular to the line-of-sight. These accelerations are denoted a_R and a_Ω respectively. The control vector $\underline{F}$ is:

$$\underline{F} = m \begin{bmatrix} a_R \\ a_\Omega \end{bmatrix} \qquad (4\text{-}9)$$

where m is the vehicle mass.

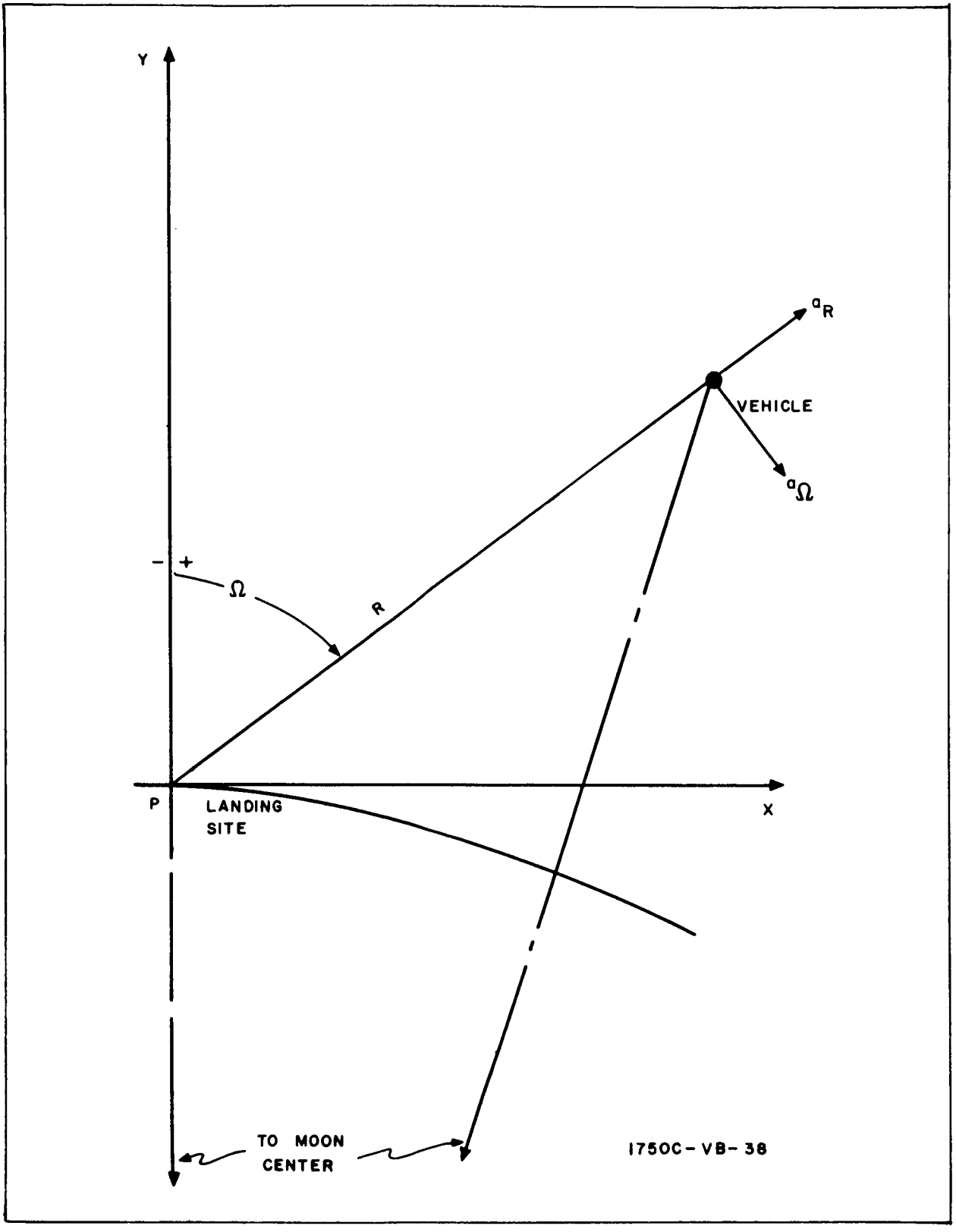

Figure 4-2. Geometry

c. Navigation Observables - Navigation information is obtained by a beacon tracking sensor system. The observables are considered to be identical to the state variables. Thus,

$$\underline{Y} = \begin{bmatrix} R \\ \dot{R} \\ \Omega \\ \dot{\Omega} \end{bmatrix} \qquad (4\text{-}10)$$

d. Guidance Technique - The guidance concept finally selected is a hybrid combination of two modified proportional navigation guidance laws and is referred to as the MPN/VT - B guidance concept for reasons discussed in Volume III. Over the majority of the landing maneuver, the vehicle moves according to the accelerations commanded by the first modified proportional navigation guidance law (denoted simply MPN guidance) which is defined by the following expressions:

$$a_{R_1} = \frac{K-1}{K} \frac{(\dot{R}_1)^2}{R_1} + \frac{\mu \cos \Omega_1}{r_c^2}$$

$$a_{\Omega_1} = (S + \frac{K-1}{K}) \dot{R}_1 \dot{\Omega}_1 - \frac{\mu \sin \Omega_1}{r_c^2} \qquad (4\text{-}11)$$

where

S and K are guidance parameters equal to 1.5 and 2.0 respectively

μ is the lunar gravitational constant

r_c is the mean lunar radius

R_1 and Ω_1 are the line-of-sight range and angle to a fictitious landing site located 305 meters (1000 feet) directly above the desired landing site.

The trajectory flown by the vehicle using this guidance law is found to be very similar to a class of minimum fuel trajectories. However, this guidance law does not produce a vertical touchdown. Therefore, when the range to the fictitious landing site (R_1) is reduced to 305 meters, the above guidance law

is replaced by a second modification of proportional navigation denoted MPN/VT which does provide a vertical approach to the landing site. These guidance equations are:

$$a_R = \frac{K_1 - 1}{K_1} \frac{(\dot{R})^2}{R}$$

$$a_\Omega = S_1 \dot{R} \dot{\Omega} - S_2 \frac{(\dot{R})^2}{R} \Omega \qquad (4\text{-}12)$$

where K_1, S_1, and S_2 are guidance parameters equal to 3.0, 3.1, and 0.8 respectively.

e. Vehicle Characteristics - Several assumptions concerning vehicle characteristics are made:

- Initial mass: 31,066 kg.
- Fuel specific impulse: 420 sec.
- Engine and sensor transfer functions are characterized by linear second order filters.
- The thrust is assumed to be provided by 2 RL-10 type engines each limited to 66,765 newtons (15000 pounds) maximum, and throttleable over a 10:1 range.

f. Trajectory - One is not free to choose the type of trajectory that will be flown when using this guidance concept. The trajectory characteristics are determined by the initial conditions and guidance parameter values used. The guidance parameter values specified during the guidance technique discussion are found to yield a trajectory with characteristics that are very similar to those of a class of minimum fuel trajectories. The nominal initial conditions selected are:

- Range to the landing site: 312.7 km.
- Horizontal velocity: 1723 meter/second
- Vertical velocity: 0.0 meters/second
- Altitude: 38.1 km.

g. Sensor Error Model - All four components of the general error model discussed in subsection 4.2 are considered in the analysis of modified proportional navigation guidance. Only navigation sensor errors are evaluated.

4.3.2.2 Error Analysis

The complete error analysis of lunar landing using the hybrid guidance concept MPN/VT-B is performed in two parts. Bias errors are treated using digital simulation of the nonlinear navigation, guidance, and control system, and the effects of random fluctuation errors are evaluated using the adjoint error analysis technique.

a. Bias Errors - The degradation of the MPN/VT-B guidance concept by the two types of bias errors (constant magnitude and constant percent) is determined by means of a digital simulation program. For this analysis, the values of R, $\dot{R}$, Ω, and $\dot{\Omega}$ used in the guidance equations are replaced by the measured values of these quantities denoted $\hat{R}$, $\hat{\dot{R}}$, $\hat{\Omega}$, and $\hat{\dot{\Omega}}$.

For this part of the analysis, sensor dynamics are characterized by a simple time lag. In general, the measured value of the i^{th} observable can be obtained from the expression:

$$\hat{Y}_i(s) = \left[\frac{1}{1 + \tau_{Y_i} s}\right]\left[Y_i(s) + (\tilde{y}_i)_b + {}_{Y_i}p_b \frac{Y_i(s)}{100}\right] \qquad (4\text{-}13)$$

where $(\tilde{y}_i)_b$ and ${}_{Y_i}p_b$ are defined in subsection 4.2. Then,

$$\left[1 + \tau_{Y_i} s\right] \hat{Y}_i(s) = Y_i(s) + (\tilde{y}_i)_b + {}_{Y_i}p_b \frac{Y_i(s)}{100}$$

and

$$\hat{Y}_i(s) = \frac{Y_i(s) - \hat{Y}_i(s) + (\tilde{y}_i)_b + {}_{Y_i}p_b \frac{Y_i(s)}{100}}{\tau_{Y_i} s} \qquad (4\text{-}14)$$

The factor s in the denominator indicates an integration. Therefore,

$$\hat{Y}_i(t) = \int_0^t \left[\frac{Y_i(t) - \hat{Y}_i(t) + (\tilde{y}_i)_b + Y_i p_b \frac{Y_i(t)}{100}}{\tau_{Y_i}} \right] dt \qquad (4\text{-}15)$$

The digital simulation program integrates the equations of motion forward (starting with the nominal initial values of the state variables) until altitude equals zero. At this time position and velocity deviations from the nominal case are printed out and the effects of the bias errors are ascertained by comparison with error free performance.

The analysis technique is to assign values to the bias error components of one of the measurement errors (e.g., the range measurement errors). All other bias error components are set equal to zero. Then the simulation program is run and the terminal errors that result are the terminal errors produced by the assumed bias errors.

b. Random Fluctuation Errors - Random fluctuation errors are evaluated by computing error sensitivity coefficients using the adjoint analysis technique. The adjoint analytical technique is applied only to that portion of the landing maneuver employing MPN/VT guidance equations (R_1 less than 305 meters, or R less than 497 meters). Terminal position and velocity errors are caused primarily by random sensor errors occurring in the final portion of the landing maneuver because of the self-correcting character of the closed loop guidance and control system. (Past experience supports this statement.) This is the reason that only the MPN/VT guided portion of the landing maneuver is analyzed using the adjoint technique.

In the adjoint analysis, sensor dynamics are represented by second order filters. When error analysis results are discussed, input random fluctuation errors will be characterized by their rms values: ${}_n\sigma_{Y_i}$ and ${}_p\sigma_{Y_i}$. These quantities refer to sensor noise characteristics at the output of the filter representing the i^{th} sensor. (For the adjoint analysis, white noise is assumed at the sensor inputs.)

4.3.2.3 Results

This paragraph demonstrates the methodology developed to obtain estimates of sensor error effects and indicates dynamic range requirements for the nominal lunar landing mission considered herein. The results and discussion of the

error analysis presented in this paragraph are pertinent only to the guidance scheme and the nominal mission profile selected in paragraph 4.3.2.1. Since the effect of random errors will be governed by the performance of the guidance system during the final phase of the landing trajectory, random error sensitivity coefficients are generated for only the MPN/VT portion of the trajectory. Bias errors and dynamic lags are evaluated by simulating specific bias error levels in the forward trajectory program, which considers the entire trajectory. Consequently, the effect of bias errors on fuel consumption are available.

a. Sensor Error Effects for the MPN/VT-B Guidance Concept - The first results presented are the sensitivity coefficients generated by the adjoint error analysis. These coefficients relate the mean squared terminal deviations in Y, $\dot{Y}$, X, and $\dot{X}$ to the mean squared values of the random sensor errors which cause them according to the matrix equation given below.

$$\begin{bmatrix} \sigma_Y^2 \\ \sigma_{\dot{Y}}^2 \\ \sigma_X^2 \\ \sigma_{\dot{X}}^2 \end{bmatrix} = \begin{bmatrix} k_{11} & k_{12} & k_{13} & k_{14} \\ k_{21} & k_{22} & k_{23} & k_{24} \\ k_{31} & k_{32} & k_{33} & k_{34} \\ k_{41} & k_{42} & k_{43} & k_{44} \end{bmatrix} \begin{bmatrix} {}_n\sigma_R^2 \\ {}_n\sigma_{\dot{R}}^2 \\ {}_n\sigma_\Omega^2 \\ {}_n\sigma_{\dot{\Omega}}^2 \end{bmatrix} + \begin{bmatrix} k'_{11} & k'_{12} & k'_{13} & k'_{14} \\ k'_{21} & k'_{22} & k'_{23} & k'_{24} \\ k'_{31} & k'_{32} & k'_{33} & k'_{34} \\ k'_{41} & k'_{42} & k'_{43} & k'_{44} \end{bmatrix} \begin{bmatrix} {}_p\sigma_R^2 \\ {}_p\sigma_{\dot{R}}^2 \\ {}_p\sigma_\Omega^2 \\ {}_p\sigma_{\dot{\Omega}}^2 \end{bmatrix} \qquad (4\text{-}16)$$

In this discussion, X and Y are the horizontal and vertical axes respectively of an inertial cartesian coordinate system with origin at the desired landing site (see figure 4-2).

Since the quantities ${}_p\sigma_\Omega^2$ and ${}_p\sigma_{\dot{\Omega}}^2$ are set equal to zero for this analysis, the third and fourth columns of the matrix of primed coefficients are not computed. With this fact taken into account, the numerical values of the two sensitivity coefficients are as follows:

$$\begin{bmatrix} k_{11} & k_{12} & k_{13} & k_{14} \\ k_{21} & k_{22} & k_{23} & k_{24} \\ k_{31} & k_{32} & k_{33} & k_{34} \\ k_{41} & k_{42} & k_{43} & k_{44} \end{bmatrix} = \begin{bmatrix} 1.59\times10^{-1} & 1.98\times10^{-1} & 3.49\times10^{-2} & 5.40\times10^{1} \\ 1.08\times10^{0} & 1.25\times10^{0} & 8.64\times10^{-2} & 1.32\times10^{2} \\ 9.54\times10^{-15} & 1.10\times10^{-13} & 5.63\times10^{-9} & 3.39\times10^{-7} \\ 1.69\times10^{-14} & 5.29\times10^{-14} & 5.29\times10^{-10} & 5.11\times10^{-8} \end{bmatrix} \qquad (4\text{-}17)$$

$$\begin{bmatrix} k'_{11} & k'_{12} \\ k'_{21} & k'_{22} \\ k'_{31} & k'_{32} \\ k'_{41} & k'_{42} \end{bmatrix} = \begin{bmatrix} 7.78 \times 10^{-6} & 1.23 \times 10^{-5} \\ 3.78 \times 10^{-3} & 3.54 \times 10^{-5} \\ 1.62 \times 10^{-17} & 6.48 \times 10^{-17} \\ 4.45 \times 10^{-18} & 9.49 \times 10^{-18} \end{bmatrix} \quad (4\text{-}18)$$

These coefficients are used to evaluate sensor capability expected to exist in the 1970 time period. These typical sensor error levels are presented in table 4-4. Three degrees of sensor error are postulated: low, medium, and high.

Table 4-5 gives the individual contributions of each random error source to the total terminal mean squared position and velocity deviations for each of the three levels of sensor capability. In general, it can be seen that the horizontal error components, σ_X^2 and $\sigma_{\dot{X}}^2$ are small enough to be considered negligible. However, the vertical error components, especially $\sigma_{\dot{Y}}^2$ (vertical velocity) are not negligible. Table 4-5 shows that the rms terminal velocity error increases sharply as the sensor error level increases, as expected. In addition, the most significant contributors to the terminal velocity errors are range measurements and line-of-sight angular rate measurements. This is true for all three sample levels of sensor capability.

Next, the effect of the bias components of sensor error are considered. Estimates of bias error effects can be obtained through the use of the adjoint analysis technique, but they are not in this study. Rather, the forward digital simulation program is used with the bias errors introduced as indicated in paragraph 4.3.2.2a. Thus, the bias error analysis is not subject to the assumptions attendant to linearization and provides the effect of sensor bias error components on X, $\dot{X}$, and $\dot{Y}$ at the true touchdown point, Y = 0. This analysis technique also allows one to determine the effects of bias error components on fuel consumption. The degrees of sensor capability are selected. (These are given in table 4-4.) The bias error components indicated in table 4-4 are applied to the landing vehicle during the entire landing trajectory (periselenum to touchdown) and the values of X, $\dot{X}$, $\dot{Y}$ and the total fuel consumed are determined at the point Y = 0. The results are given in tables 4-6, 4-7, and 4-8 which show dynamic errors (X, $\dot{X}$, and $\dot{Y}$) and the total fuel consumption respectively.

TABLE 4-4

TYPICAL SENSOR ERROR LEVELS (USED FOR SAMPLE COMPUTATION)

Error Source	Symbolic Designation And Units		Random Errors (1σ)			Bias Errors (1σ)		
			Error Level			Error Level		
			Low	Medium	High	Low	Medium	High
Range observation	$_{n}\sigma_{R}$	(m)	0.61	1.52	3.05	-	-	-
	$_{p}\sigma_{R}$	(%)	0.2	0.5	1.0	-	-	-
	R_{b}	(m)	-	-	-	0.305	0.61	3.05
	$_{b}p_{R}$	(%)	-	-	-	0.2	0.5	2.0
Range rate observation	$_{n}\sigma_{\dot{R}}$	(m/sec)	0.0305	0.152	0.61	-	-	-
	$_{p}\sigma_{\dot{R}}$	(%)	0.05	0.20	0.50	-	-	-
	$\dot{R}_{b}$	(m/sec)	-	-	-	0.0305	0.152	0.61
	$_{b}p_{\dot{R}}$	(%)	-	-	-	0.05	0.20	0.50

TABLE 4-4 (Continued)

Error Source	Symbolic Designation And Units		Random Errors (1σ)			Bias Errors (1σ)		
			Error Level			Error Level		
			Low	Medium	High	Low	Medium	High
Line-of-sight angle observation	$_{n}\sigma_{\Omega}$	(rad)	0.0001	0.0002	0.001	-	-	-
	$_{p}\sigma_{\Omega}$	(%)	0.0	0.0	0.0	-	-	-
	Ω_{b}	(rad)	-	-	-	0.001	0.005	0.010
	$_{b}p_{\Omega}$	(%)	-	-	-	0.0	0.0	0.0
Line-of-sight angle rate observation	$_{n}\sigma_{\dot{\Omega}}$	(rad/sec)	0.00003	0.0001	0.0002	-	-	-
	$_{p}\sigma_{\dot{\Omega}}$	(%)	0.0	0.0	0.0	-	-	-
	$\dot{\Omega}_{b}$	(rad/sec)	-	-	-	0.00003	0.0001	0.0002
	$_{b}p_{\dot{\Omega}}$	(%)	-	-	-	0.0	0.0	0.0

TABLE 4-5

RESULTS OF SAMPLE COMPUTATION SHOWING TERMINAL EFFECTS OF RANDOM SENSOR ERRORS

Error Source		Terminal Mean Squared Error Components											
		Low Sensor Error Level				Medium Sensor Error Level				High Sensor Error Level			
		σ_Y^2	$\sigma_{\dot{Y}}^2$	σ_X^2	$\sigma_{\dot{X}}^2$	σ_Y^2	$\sigma_{\dot{Y}}^2$	σ_X^2	$\sigma_{\dot{X}}^2$	σ_Y^2	$\sigma_{\dot{Y}}^2$	σ_X^2	$\sigma_{\dot{X}}^2$
Range measurement	$_n\sigma_R^2$	0.059	0.400	3.54×10^{-15}	6.26×10^{-15}	0.366	2.48	2.20×10^{-14}	3.88×10^{-14}	1.48	10.0	8.90×10^{-14}	1.57×10^{-13}
	$_p\sigma_R^2$	3.11×10^{-5}	1.51×10^{-4}	6.48×10^{-19}	1.78×10^{-19}	1.94×10^{-4}	9.42×10^{-4}	4.05×10^{-18}	1.11×10^{-18}	7.75×10^{-4}	3.77×10^{-3}	1.62×10^{-17}	4.44×10^{-15}
Range rate measurement	$_n\sigma_{\dot{R}}^2$	1.84×10^{-4}	1.16×10^{-3}	1.02×10^{-16}	4.92×10^{-17}	4.60×10^{-3}	2.90×10^{-2}	2.55×10^{-15}	1.23×10^{-15}	7.35×10^{-2}	4.65×10^{-1}	4.08×10^{-14}	1.97×10^{-14}
	$_p\sigma_{\dot{R}}^2$	3.08×10^{-8}	8.85×10^{-8}	1.62×10^{-19}	2.37×10^{-20}	4.93×10^{-7}	1.42×10^{-6}	2.59×10^{-18}	3.85×10^{-19}	3.08×10^{-6}	8.86×10^{-6}	1.62×10^{-17}	2.41×10^{-15}
Angle measurement	$_n\sigma_\Omega^2$	3.49×10^{-4}	8.64×10^{-4}	5.63×10^{-11}	5.29×10^{-12}	1.40×10^{-3}	3.45×10^{-3}	2.25×10^{-10}	2.11×10^{-11}	3.50×10^{-2}	8.62×10^{-2}	5.62×10^{-9}	5.27×10^{-10}
Angle rate measurement	$_n\sigma_{\dot{\Omega}}^2$	4.86×10^{-2}	1.19×10^{-1}	3.05×10^{-10}	4.60×10^{-11}	5.40×10^{-1}	1.32×10^{0}	3.38×10^{-9}	5.10×10^{-10}	2.16×10^{0}	5.28×10^{0}	1.35×10^{-8}	2.04×10^{-9}
Total mean squared error (rss)		0.108 $(\text{meters})^2$	0.521 $(\text{m/sec})^2$	3.61×10^{-10} $(\text{meters})^2$	0.513×10^{-10} $(\text{m/sec})^2$	0.912 $(\text{meters})^2$	3.83 $(\text{m/sec})^2$	36.0×10^{-10} $(\text{meters})^2$	5.31×10^{-10} $(\text{m/sec})^2$	3.76 $(\text{meters})^2$	15.8 $(\text{m/sec})^2$	1.91×10^{-8} $(\text{meters})^2$	25.7×10^{-10} $(\text{m/sec})^2$
Total rms Error		0.329 meters	0.722 m/sec	1.90×10^{-5} meters	7.16×10^{-6} m/sec	0.955 meters	1.96 m/sec	6.00×10^{-5} meters	2.31×10^{-5} m/sec	1.94 meters	3.98 m/sec	1.38×10^{-4} meters	5.07×10^{-5} m/sec

TABLE 4-6

BREAKDOWN OF TOUCHDOWN ERRORS CAUSED BY SENSOR BIAS ERRORS

Error Level	Error Source	Symbolic Designation, Value, and Unit	Touchdown Errors		
			$\dot{Y}$ (m/sec)	X(m)	$\dot{X}$ (m/sec)
	Range Observation	$R_b + {}_R P_b \left(\frac{R}{100}\right) = 0.305 + 0.002\ R$ (meters)	-0.915	0.0	0.0915
Low	Range Rate Observation	$\dot{R}_b + {}_{\dot{R}} P_b \left(\frac{\dot{R}}{100}\right) = 0.0305 + 0.005\ \dot{R}$ (meters/sec)	-0.336	0.0	0.0153
	Angle Observation	$\Omega_b + {}_{\Omega} P_b \left(\frac{\Omega}{100}\right) = 0.00003 + 0$ (radians)	0.0	0.0	0.0
	Angle Rate Observation	$\dot{\Omega}_b + {}_{\dot{\Omega}} P_b \left(\frac{\Omega}{100}\right) = 0.00003 + 0$ (rad/sec)	0.0	0.0	0.0
	Root Sum Square Errors		-0.975	0.0	0.0915
Medium	Range Observation	$R_b + {}_R P_b \left(\frac{R}{100}\right) = 0.61 + 0.005\ R$ (meters)	-1.68	0.0	0.0915
	Range Rate Observation	$\dot{R}_b + {}_{\dot{R}} P_b \left(\frac{\dot{R}}{100}\right) = 0.1525 + 0.002\ \dot{R}$ (meters/sec)	-0.746	0.0	0.0153
	Angle Observation	$\Omega_b + {}_{\Omega} P_b \left(\frac{\Omega}{100}\right) = 0.0001 + 0$ (radians)	0.0	0.0	0.0
	Angle Rate Observation	$\dot{\Omega}_b + {}_{\dot{\Omega}} P_b \left(\frac{\dot{\Omega}}{100}\right) = 0.0001 + 0$ (rad/sec)	-0.061	0.0	0.0
	Root Sum Square Errors		-1.83	0.0	0.0915

TABLE 4-6 (Continued)

Error Level	Error Source	Symbolic Designation, Value, and Unit	Touchdown Errors		
			$\dot{Y}$ (m/sec)	X (m)	$\dot{X}$ (m/sec)
High	Range Observation	$R_b + {}_R p_b \left(\frac{R}{100}\right) = 3.05 + 0.02\,R$ (meters)	-5.19	0.0	0.244
	Range Rate Observation	$\dot{R}_b + {}_{\dot{R}} p_b \left(\frac{\dot{R}}{100}\right) = 0.61 + 0.005\,\dot{R}$ (meters/sec)	-2.08	0.0	0.0762
	Angle Observation	$\Omega_b + {}_{\Omega} p_b \left(\frac{\Omega}{100}\right) = 0.1 + 0$ (radians)	-0.061	0.0	0.0
	Angle Rate Observation	$\dot{\Omega}_b + {}_{\dot{\Omega}} p_b \left(\frac{\dot{\Omega}}{100}\right) = 0.0002 + 0$ (rad/sec)	-0.122	0.0	0.0
	Root Sum Square Errors		-5.55	0.0	0.256

Using the numerical results given in tables 4-5 and 4-6, the touchdown velocity standard deviations are computed for each sensor error level. These represent velocity deviations. The 99-percent level is 2.5 times the 1σ deviation. Maximum touchdown velocities with 99-percent confidence level for all three sensor error levels are summarized in table 4-9.

Table 4-8 shows the effect of sensor bias error components and engine dynamic lag upon total fuel consumption. In all cases the fuel usage figure has been adjusted, in the event that a hard landing is indicated, by the magnitude of $\dot{Y}$. That is, if ΔV is 1800 meters/second to the point $Y = 0$ with $\dot{Y}$ at the corresponding time equal to -15 meters/second then the ΔV recorded in table 4-8 is 1815 meters/second. The digital simulation program is run once for each bias error level listed in table 4-8.

b. Sensor Dynamic Range Requirements. - If it is necessary to obtain relative measurements from the spacecraft to the landing site prior to the time of landing engine ignition to avoid gross errors in the initial conditions for descent, then the navigation sensor system must be able to acquire the landing site beacon prior to reaching periselenum of the synchronous descent orbit. Since the nominal range from periselenum to the landing site depends on the initial thrust-to-mass ratio, the acquisition range requirement is also a function of this quantity. For the nominal case investigated herein (periselenum altitude equal 38.1 km (125,000 ft)), line-of-sight range at periselenum is approximately 300 km (10^6 ft). Consequently, the sensor is to be capable of 99-percent probability of acquisition at approximately 300-km range.

Table 4-10 indicates the sensor dynamic range requirements for navigation and guidance from periselenum to touchdown for the nominal trajectory.

4.3.2.4 Conclusions

Results and conclusions drawn from the preceding effort are summarized in the following statements.

- A combination of two proportional navigation guidance laws provides a guidance concept which approaches an optimum fuel trajectory over most of the flight and then makes a vertical approach to touchdown.

- Terminal vertical velocity errors are significant for all three assumed levels of sensor capability. Terminal vertical position, and horizontal position and velocity errors are not critical even at the high sensor error level assumed.

TABLE 4-7

TOUCHDOWN ERRORS CAUSED BY ENGINE LAG

Engine Dynamic Lag τ	Touchdown Errors		
	$\dot{Y}$ (m/sec)	X (m)	$\dot{X}$ (m/sec)
0 (no lag)	0	0	0
1 second	0.762	0	0
2 second	0.381	0	0

TABLE 4-8

EFFECTS OF SENSOR BIAS ERRORS AND ENGINE LAGS ON FUEL CONSUMPTION. (AS MEASURED BY THE PARAMETER ΔV.)

Sensor Bias Errors (1σ) or Engine Lay	Total ΔV Required, (mps) Periselenum to Touchdown
Nominal: no error, no lag	1871
Dynamic Lag: τ = 2 sec	1874
Range bias: $R_b + {}_R p_b \left(\frac{R}{100}\right) = 0.305 + 0.002\ R$ (m)	1873
Range bias: $R_b + {}_R p_b \left(\frac{R}{100}\right) = 0.61 + 0.005\ R$ (m)	1874
Range bias: $R_b + {}_R p_b \left(\frac{R}{100}\right) = 3.05 + 0.02\ R$ (m)	1872
Range Rate bias: $\dot{R}_b + {}_{\dot{R}} p_b \left(\frac{\dot{R}}{100}\right) = 0.0305 + 0.0005\ \dot{R}$ (m/sec)	1874
Range Rate bias: $\dot{R}_b + {}_{\dot{R}} p_b \left(\frac{\dot{R}}{100}\right) = 0.152 + 0.002\ \dot{R}$ (m/sec)	1875
Range Rate bias: $\dot{R}_b + {}_{\dot{R}} p_b \left(\frac{\dot{R}}{100}\right) = 0.61 + 0.005\ \dot{R}$ (m/sec)	1874
Angle bias: $\Omega_b + {}_{\Omega} p_b \left(\frac{\Omega}{100}\right) = 0.00003 + 0$ (rad)	1875
Angle bias: $\Omega_b + {}_{\Omega} p_b \left(\frac{\Omega}{100}\right) = 0.1 + 0$ (rad)	1872
Angle Rate bias: $\dot{\Omega}_b + {}_{\dot{\Omega}} p_b \left(\frac{\dot{\Omega}}{100}\right) = 0.00003 + 0$ (rad/sec)	1875
Angle Rate bias: $\dot{\Omega}_b + {}_{\dot{\Omega}} p_b \left(\frac{\dot{\Omega}}{100}\right) = 0.0001 + 0$ (rad/sec)	1878

TABLE 4-9

MAXIMUM TOUCHDOWN VELOCITY (99 PERCENT CONFIDENCE LEVEL)

Sensor Error Level	1 σ Velocity Errors Caused By Bias Error (meters/sec)	1 σ Velocity Errors Caused By Random Error (meters/sec)	Combined Velocity Error, (1σ) (meters/sec)	99 Percent Maximum Touchdown Error Confidence Level (2.5 σ)* (meters/sec)	Velocity Error Caused By Engine Lag (2 sec) (meters/sec)	Overall 99 Percent Touchdown Velocity Confidence Level (meters/sec)
Low	0.975	0.721	1.21	3.03	0.381	3.41
Medium	1.83	1.97	2.69	6.73	0.381	7.13
High	5.55	3.98	6.82	17.1	0.381	17.5

* Because the bias errors represent "worst case" 1σ values, the 99 percent confidence level is assumed to correspond to the 2.5σ error level. Actually, 99 percent of all events are included between ±2.65σ for the normal distribution.

TABLE 4-10

SENSOR DYNAMIC RANGE REQUIREMENTS

Observable	Dynamic Range	
	High	Low
Range	300 km	0 km
Range Rate	2000 m/sec	0 m/sec
LOS Angle*	120 deg	0 deg
LOS Angle Rate	50 mr/sec	0 mr/sec

*This depends upon the method of LOS angle determination over the horizon

- The most significant random error contribution to the terminal velocity error are range observation and line-of-sight angle observation. This suggests the use of "low" error level sensors for these observations and higher error level sensors for the remaining observables.

- Sensor bias errors contribute significantly to the terminal velocity error at all three assumed levels and must be kept as low as possible. Bias errors in the observation of range and range rate are the most critical.

- The increase in fuel consumption caused by engine lag and sensor bias errors is not particularly significant. If the largest increases for each error source in table 4-8 are added directly (this is pessimistic) the total increase in ΔV is 21 meters/second or approximately 1 percent of the nominal ΔV requirement.

4.4 COMPARATIVE DISCUSSION OF GUIDANCE CONCEPTS

This subsection summarizes a comparative discussion of the two landing guidance concepts analyzed: linear predictive guidance and modified proportional navigation with vertical touchdown capability. Direct comparison of the two system models is not possible in many areas because

of differences in system parameters and analytical constraints (e.g., initial mass and engine size constraints). As a result, the material presented in this subsection is restricted to a comparison of nominal fuel consumption (as indicated by the quantity ΔV) and a comparison of mean squared terminal errors resulting when identical navigation sensors and sensor accuracies are assumed. In addition, brief consideration is given to the relative computational requirements and sensor dynamic range requirements of the two approaches.

The discussions in each of these areas are summarized below.

- Nominal fuel consumption: On the basis of information presented it is found that the gravity turn trajectory flown by the linear predictive guidance concept is somewhat more economical at low initial altitudes, and that this advantage decreases and eventually reverses sign as the initial altitude is increased.

- Comparison of terminal errors: When identical navigation sensor accuracies are used in the two guidance concepts, linear predictive guidance is found to result in smaller rms terminal attitude and velocity errors. Horizontal position errors are apparently much smaller with MPN/VT-B guidance; however, this cannot be stated positively because of the pessimistic nature of linear predictive guidance error estimates. In any event, neither estimate of terminal horizonal deviations is significantly large.

- Onboard computation: Overall, it is expected that the linear predictive guidance concept requires greater onboard computer capacity, primarily because of the need to store reference trajectory data.

- Sensor Dynamic Range: The overall similarity of the mission profiles followed indicates identical sensor dynamic range requirements for the two guidance concepts.

5. LUNAR ASCENT

5.1 INTRODUCTION

The ascent portion of the lunar missions study was made to ascertain the feasibility of a given guidance scheme used during the boost phase of the ascent trajectory and to establish the sensor specifications weighed against a given error allotment in position and velocity at thrust termination. The determination of the sensor specifications requires the selection of a guidance scheme and a specific type of system configuration. Consequently, the sensor specifications include actual hardware items in terms of types, numbers, and the sensing accuracy of the individual instruments.

The sensor specifications are based on the minimum accuracies required to perform the lunar ascent. The minimum accuracies in turn are based on the maximum errors tolerated in the guidance system and the maximum error expectation in determining the launch position coordinates at the lunar surface.

5.2 ASCENT TRAJECTORY

This study considers three different trajectories by which the lunar ascent may be accomplished. These are:

a. A powered ascent from launch to terminal rendezvous. This maneuver accomplishes the lunar ascent in a minimum time but requires a maximum fuel expenditure.

b. A powered ascent from launch to an intermediate 30-kilometer orbit followed by a Hohmann transfer which terminates at target acquisition.

c. A powered ascent phase which yields an intermediate parking orbit which, after an arbitrary time delay, is followed by injection into a transfer orbit which terminates at target acquisition.

The above ascents have been grouped together in two categories for determining the sensors in this study. The first two maneuvers are classed as direct ascents. The third maneuver is the parking ascent. In keeping with the rendezvous portion of the lunar mission study, an altitude of 200 kilometers is chosen for the terminal rendezvous or target orbit.

Two intermediate orbits at nominal heights of 30 and 150 kilometers are considered. Both the target orbit and the intermediate orbits are assumed circular and coplanar with the ascent trajectory. The minimum time and the minimum energy (Hohmann transfer) direct ascents give an upper and lower bound on the ascent trajectories of this type of ascent. In a similar manner the nominal 30-150-kilometer parking orbits are chosen to ensure that the extremes of the parking ascents are covered. These two types of ascents are shown in figures 5-1 and 5-2.

The thrust portions of both the direct and parking ascents employ an optimized boost trajectory. In essence, a boost trajectory is determined which results in a maximum tangential orbit velocity at a specific height. This is equivalent to maximizing the mass in orbit.

5.3 GUIDANCE MECHANIZATION

The guidance and navigation functions for the lunar ascent are performed in a selenocentric reference frame. It is assumed in the analysis that such a reference frame can be considered as an inertial reference since the orbital motion of the moon relative to the earth and sun will not induce any measurable errors into the guidance system during the ascent. Position and velocity within the navigational reference frame are obtained from three orthogonally oriented accelerometers mounted on a gyro stabilized platform. The platform is space stabilized by three single degree-of-freedom gyros. The orientation of the accelerometers and gyros, with respect to the navigational (selenocentric) reference frame and boost trajectory, are shown in figure 5-3.

To perform the error analysis, a definite guidance scheme (inertial guidance) and a specific type of mechanization (space stabilized platform) must be chosen. The choice of inertial guidance was influenced by the following factors:

- The ascent is essentially a ballistic trajectory.
- Inertial systems are well developed and have been used extensively on ballistic missiles.
- Such systems are self-contained since they require no external monitoring during the ascent.
- The vehicle requires attitude stabilization regardless of the choice of system.

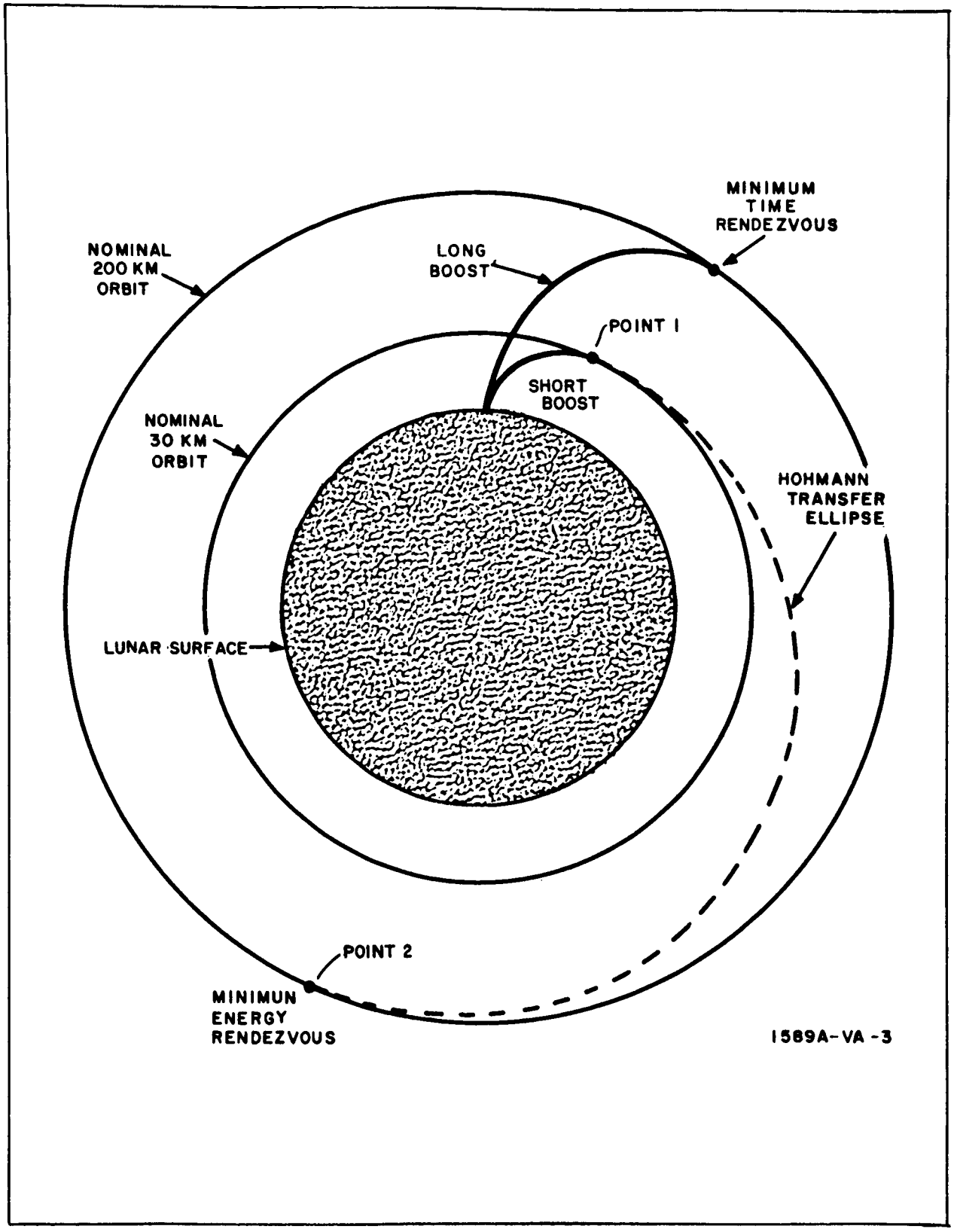

Figure 5-1. Direct Ascent to Rendezvous

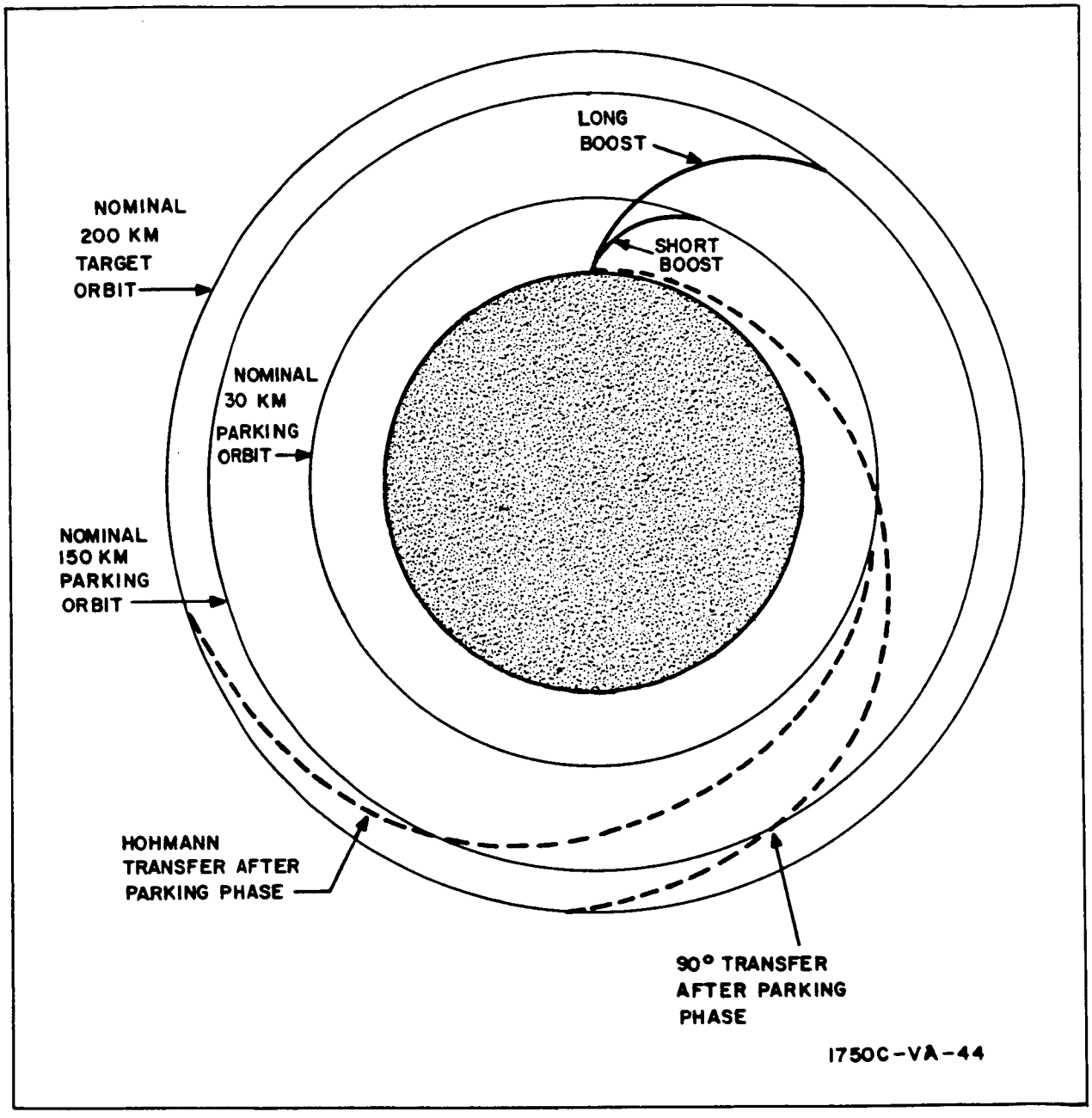

Figure 5-2. Parking Ascent to Rendevous

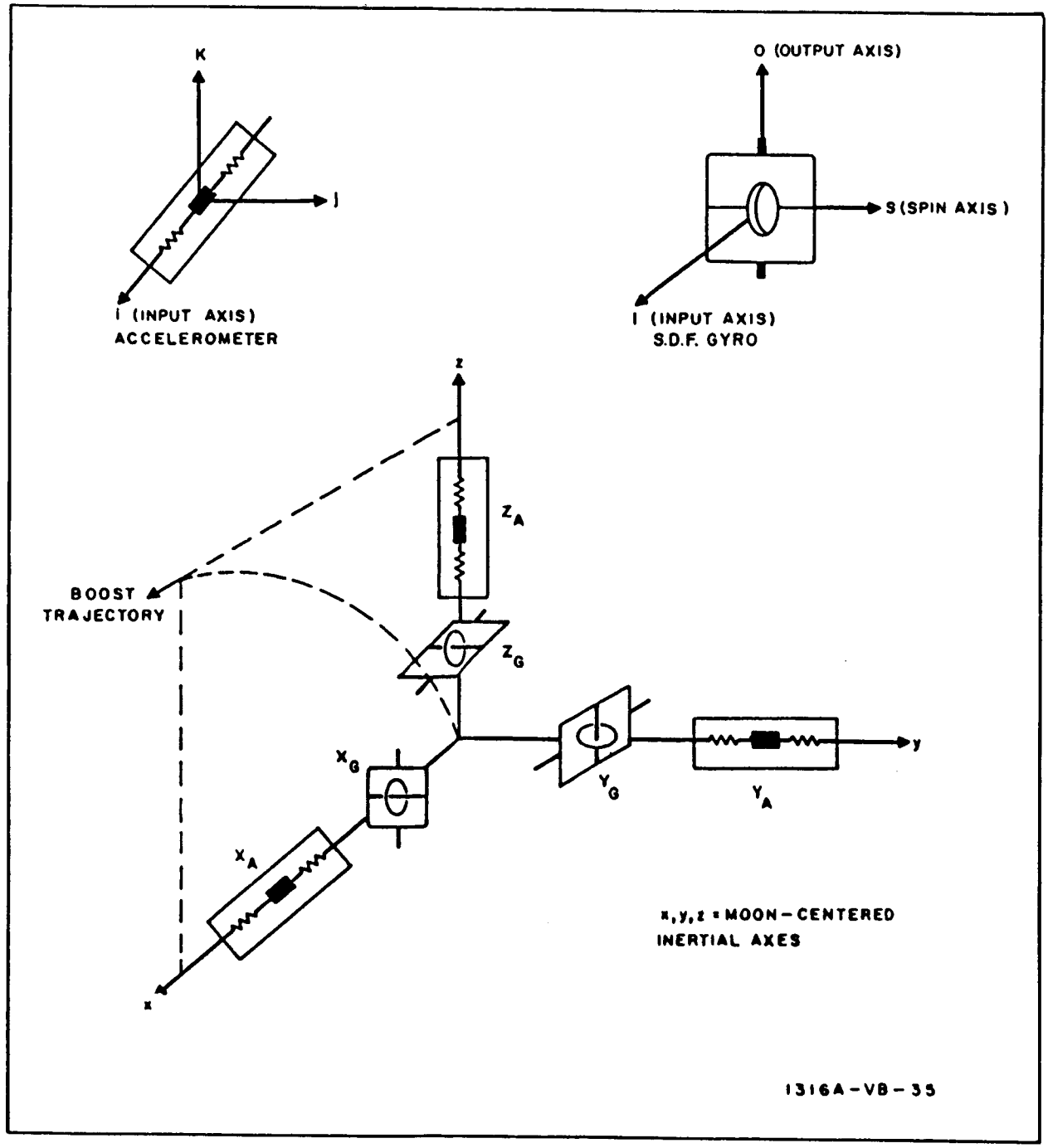

Figure 5-3. Orientation of Inertial Sensors and Navigation Reference Frame

The inertial guidance system could be implemented along several different lines. For example, the platform could be stabilized by 2 two-degree-of-freedom gyros, or a gimballess inertial system could have been chosen. Consequently, the error analysis and the sensor specifications are valid only for a specific system.

5.4 ERROR CRITERION

The sensor requirements are based on the errors associated with position and velocity prediction. To perform an error analysis, some standard must be established as a reference upon which to base the final results. The standard used in this study is the maximum allowable error in position and velocity that can be tolerated at the initiation of the Hohmann transfer coast phase from the nominal 30-kilometer parking orbit. The assumption is arbitrarily made that a 3-σ error in any one injection parameter shall not result in more than a 20-percent increase in fuel consumption over the nominal case (zero error) utilizing the Hohmann orbit transfer. The total fuel consumption consists of the fuel required for injection at the initiation of the Hohmann transfer plus synchronization at terminal rendezvous. The 3-σ position and velocity errors are:

Δh = 1.4 kilometers (3-σ value)

ΔV = 1.5 meters/sec. (3-σ value)

These errors are extracted from table 1 of Appendix F (Volume V)

5.5 ERROR SOURCES

There are several sources of errors which cause the launch vehicle to deviate from the nominal trajectory during the lunar ascent. Three major error sources are guidance system errors, selenophysical errors, and transfer errors. Figure 5-4 shows schematically the relationship of these errors for a minimum energy direct ascent trajectory.

The guidance system errors comprise the sensor, computer, and thrust cutoff errors. In this study the sensors are the stable platform, gyros, and accelerometers. The other errors in the guidance system, which are predominately the computer and thrust cutoff errors, are assumed to be second order effects and are, therefore, neglected. The guidance system errors, then, comprise the sensor errors.

The second major error source is referred to collectively as selenophysical errors which manifest themselves as errors in the launch site position coordinates and can accrue from rotational effects, lunar oblateness, and gravity anomalies. The nature of the lunar rotation practically eliminates

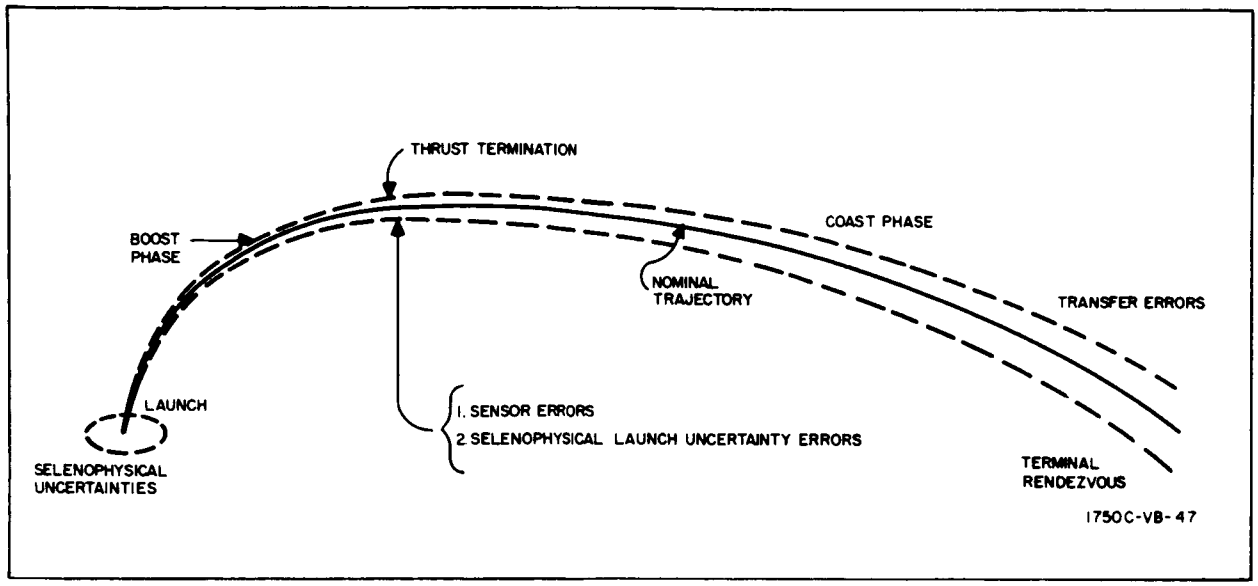

Figure 5-4 Ascent Trajectory

the effects of centripetal acceleration on gravity measurements. It has been further concluded that the lunar oblateness, which is less than that of the earth, contributes essentially second order effects to the launch position errors.

The major contribution to selenophysical errors is expected to be from gravity anomalies which affect the determination of the magnitude and direction of the gravity vector.

The transfer errors are simply the errors which accrue in position and velocity during the coast phase of the ascent. These errors are not considered in the sensor specification; however, they are listed here since they ultimately affect terminal rendezvous conditions except for the minimum time powered boost.

5.6 ERROR ANALYSIS

The method used in this study to determine the sensor requirements involves initially determining the maximum error expectation in the launch position coordinates and the contribution that this position error makes to the position and velocity errors at thrust termination. The total error allotment at thrust termination (see subsection 5.4) is then partitioned with the remaining error portion being given to the guidance system. The error analysis then consists of formulating mathematical models of the acceleration errors associated with the accelerometers, gyros, and platform as a function of the thrust accelerations. The subsequent procedure is to evaluate each term in the error model to determine its effect on the position

and velocity of the vehicle at thrust termination. The error contribution from each sensor is then adjusted to be compatible with the total error allotted to the guidance system.

The errors in position coordinates of the navigation reference come from uncertainties in the location of the launch site on the lunar surface and errors in determining the lunar radius. The maximum launch site position error and the error associated with the lunar radius are taken as 1 kilometer (3-σvalue).

5.7 RESULTS

Table 5-1 shows the position and velocity error contributions from the guidance system and the selenophysical errors at thrust termination at 30 kilometers. It is apparent that at thrust termination the selenophysical errors or launch position coordinate errors contribute primarily to the position errors, whereas the guidance system's contribution is primarily velocity errors.

TABLE 5-1
3-σ ERRORS AT THRUST TERMINATION (30 KILOMETERS)

Error	Position (km)	Velocity (m/sec)
Guidance system errors	0.131	1.264
Selenophysical errors	1.380	0.598
Guidance plus selenophysical errors	1.383	1.398
Total allowable error	1.400	1.500

The sensor specifications for the direct and parking ascents are listed in table 5-2.

TABLE 5-2
SENSOR SPECIFICATIONS FOR LUNAR ASCENT

Sensor	Direct Ascent 3-σ Values	Parking Ascent 3-σ Values	Units
Accelerometer			
Number	3	3	
Range	±1.5	±1.5	g
Bias	6×10^{-5}	6×10^{-5}	g
Scale factor	6×10^{-5}	6×10^{-5}	g/g
Nonlinear effect	3×10^{-5}	3×10^{-5}	g/g^2
Nonlinear effect	3×10^{-5}	3×10^{-5}	g/g^3
Cross axis bias sensitivity	3×10^{-5}	3×10^{-5}	g/cross-g
Cross axis scale factor	3×10^{-5}	3×10^{-5}	g/g cross-g
Gyro			
Single-degree-of-freedom-integrating			
Number	3	3	
Drift rate	0.3	0.06	o/hr
Mass unbalance	1.2	0.06	o/hr/g
Anisoelasticity	1.2	0.06	$o/hr/g^2$
Platform			
Initial misalignment	60	60	arc-sec
Servo bias	60	60	arc-sec
Deformation	60	60	arc-sec

$g = 9.8 \times 10^{-3}$ km/sec^2

Type - All inertial, space stabilized platform - all sensors orthogonally oriented

5.8 CONCLUSIONS

The sensor specifications for the boost phase of the lunar ascent are based on the allowable injection errors at the initiation of the Hohmann transfer from the nominal 30-kilometer parking orbit. The same error criterion was applied to both the direct and parking ascents; however, because the initial errors at thrust termination for the parking orbit do not remain constant but propagate with both secular and periodic characteristics, the sensors for the parking orbit are required to be more accurate.

The launch site uncertainties, which represent the maximum error expectation in position coordinates, do not pose a major problem for the lunar ascent. The sensor specifications obtained in this study are well within the present state of the art.

This study does not recommend one type of ascent over the other since the sensor specifications are not sufficiently different to dictate this choice. It is felt that the mission requirements will be the key factors which will decide the type of ascent.

6. LUNAR RENDEZVOUS

A representative rendezvous model has been investigated in which a nominal cotangential (Hohmann) transfer is used. A representative guidance and control method was studied and the system has been implemented on the IBM 7094 computer to generate the data used for establishing the sensor accuracy requirements for the injection phase and the terminal rendezvous phase.

6.1 TYPE OF RENDEZVOUS

Either the direct ascent or the parking orbit is suitable for rendezvous but, due to the launch window sensitivity of the direct launch, the parking orbit is preferred. Also, the circular parking orbit offers a "phasing" capability between the chaser and target. The cotangential transfer provides a smooth terminal approach as well as the minimum energy transfer. The geometry is shown in figure 6-1.

Based on the knowledge of its own altitude, the orbital elements of both vehicles, and the phase angle between the two vehicles, the chaser computes the incremental velocity vector required to inject itself into the desired elliptical ascent to intercept the target and then, at the proper time, applies the incremental velocity by means of rocket thrust. Injection sensors are required to observe chaser altitude and phase relationship. Sensors are also needed for attitude stabilization and velocity cutoff.

Upon traveling the ascent ellipse, when the chaser to target range has decreased to a preset enabling range, R_1, terminal rendezvous maneuvers are initiated as required to smoothly close with the orbiting target and to match target velocity at the approximate apo-apsis of the transfer orbit. Terminal rendezvous sensors are required to observe relative target motion in terms of the following observables: range, range rate, and line-of-sight rates. Chaser vehicle attitude references and vehicle stabilization also play a vital part in the rendezvous.

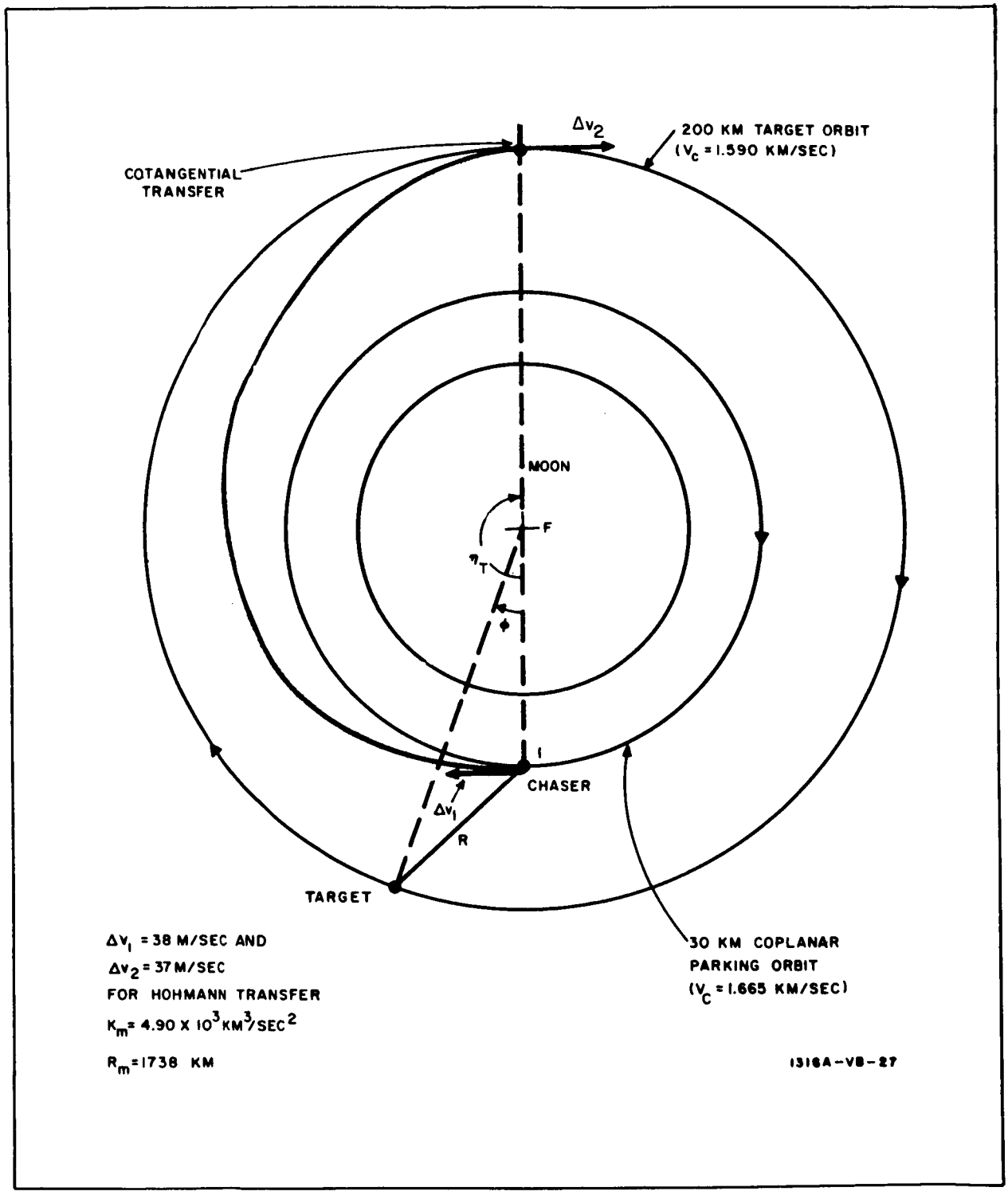

Figure 6-1. Lunar Orbital Rendezvous

6.2 INJECTION ERRORS

Injection errors not only create a dispersion in terminal conditions (and thereby increase the burden on the terminal rendezvous system) but also result in increased propellant consumption.

The miss distance sensitivity coefficients for the 180-degree lunar transfer without rendezvous maneuvering are indicated by table 6-1. These values are pessimistic since they do not generally represent the minimum miss condition but rather the miss distance that develops at the desired transfer angle.

TABLE 6-1

MISS DISTANCE SENSITIVITY COEFFICIENTS
(FOR 30/200-KM LUNAR ORBIT TRANSFER)

Error	Horizontal Coefficients	Vertical Coefficients 180°	Units
altitude	$\partial M_x/\partial h_1$ 4.94	$\partial M_z/\partial r_1$ 1.14	$\frac{km}{km}$
velocity	$\partial M_x/\partial V_1$ 11.0	$\partial M_z/\partial V_1$ 4.77	$\frac{km}{m/sec}$
attitude	$\partial M_x/\partial \gamma_1$ -2.94	$\partial M_z/\partial \gamma_1$ 0	$\frac{km}{deg.}$
target lead	$\partial M_x/\partial t_1$ 0.274	$\partial M_z/\partial t_1$ 0	$\frac{km}{sec}$

6.3 GUIDANCE AND CONTROL

The terminal rendezvous control method utilized in the study is briefly presented by figure 6-2, which indicates the inertial reference, vehicle attitude stabilization, type of maneuvering rockets, and the rocket firing schemes employed. The phase plane of figure 6-3, shows the short range coarse control of the longitudinal axis, while figure 6-4 demonstrates the subsequent vernier control used to enhance the terminal conditions (which form the initial conditions for docking). The chaser ends up ahead of the target at a desired standoff range at essentially zero range rate.

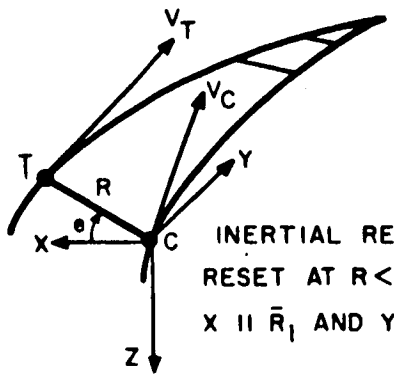

INERTIAL REFERENCE RESET AT $R < R_1$ TO: $X \parallel \bar{R}_1$ AND $Y \perp \bar{r}_m$

1. CHASER VEHICLE STABILIZED TO FIXED INERTIAL REFERENCE WHEN $R < R_1$.
2. RESTARTABLE DUAL THRUST LEVEL ROCKETS ALIGNED TO BODY AXES.

VERTICAL CONTROL

IF $|\dot{\theta}| > \epsilon$

COMPUTE FIRING TIME:

$$t_F = \frac{C\,|R\dot{\theta}|}{|a_z|}$$

IF $t_F \geq 2$ SEC, FIRE ROCKET TO REDUCE $\dot{\theta}$:

$a_z = -|a_z|\ \mathrm{sgn}\ (\dot{\theta})$

VERNIER CONTROL IS USED WHEN: $|R\dot{\theta}| \leq 2.5$ M/SEC

LATERAL CONTROL

SIMILAR TO VERTICAL

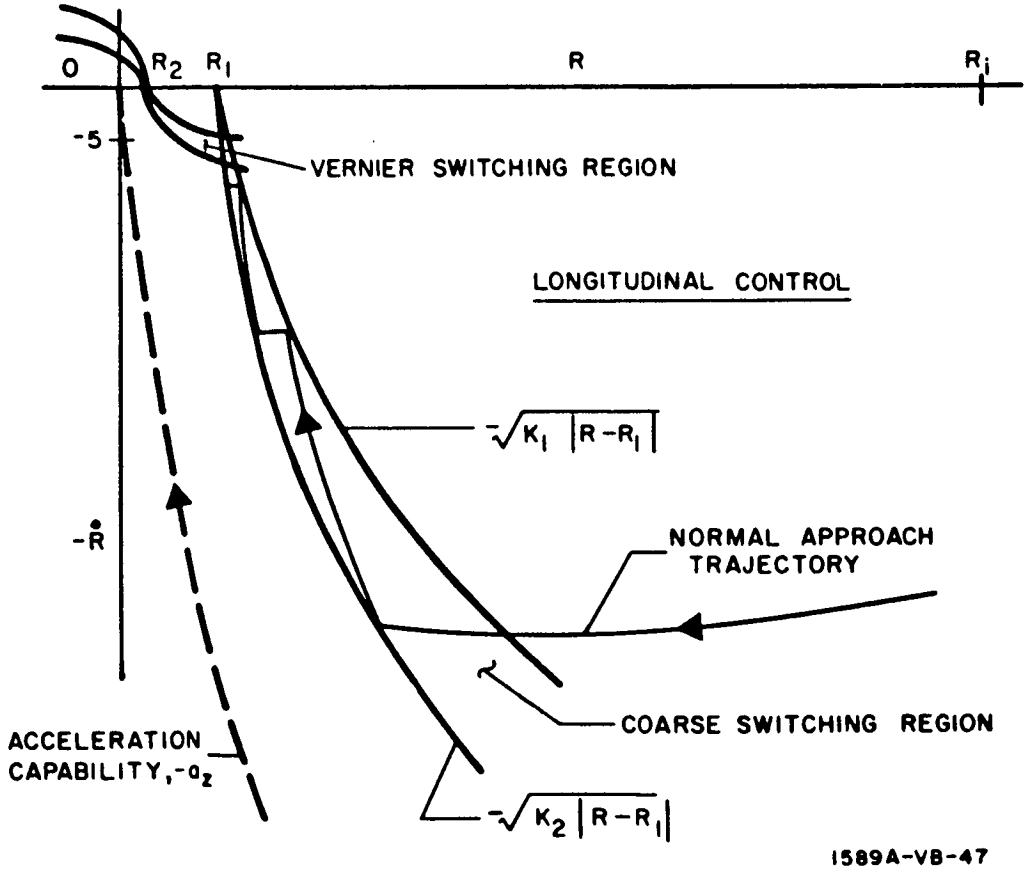

Figure 6-2. Rendezvous Guidance (Lunar Orbital Rendezvous)

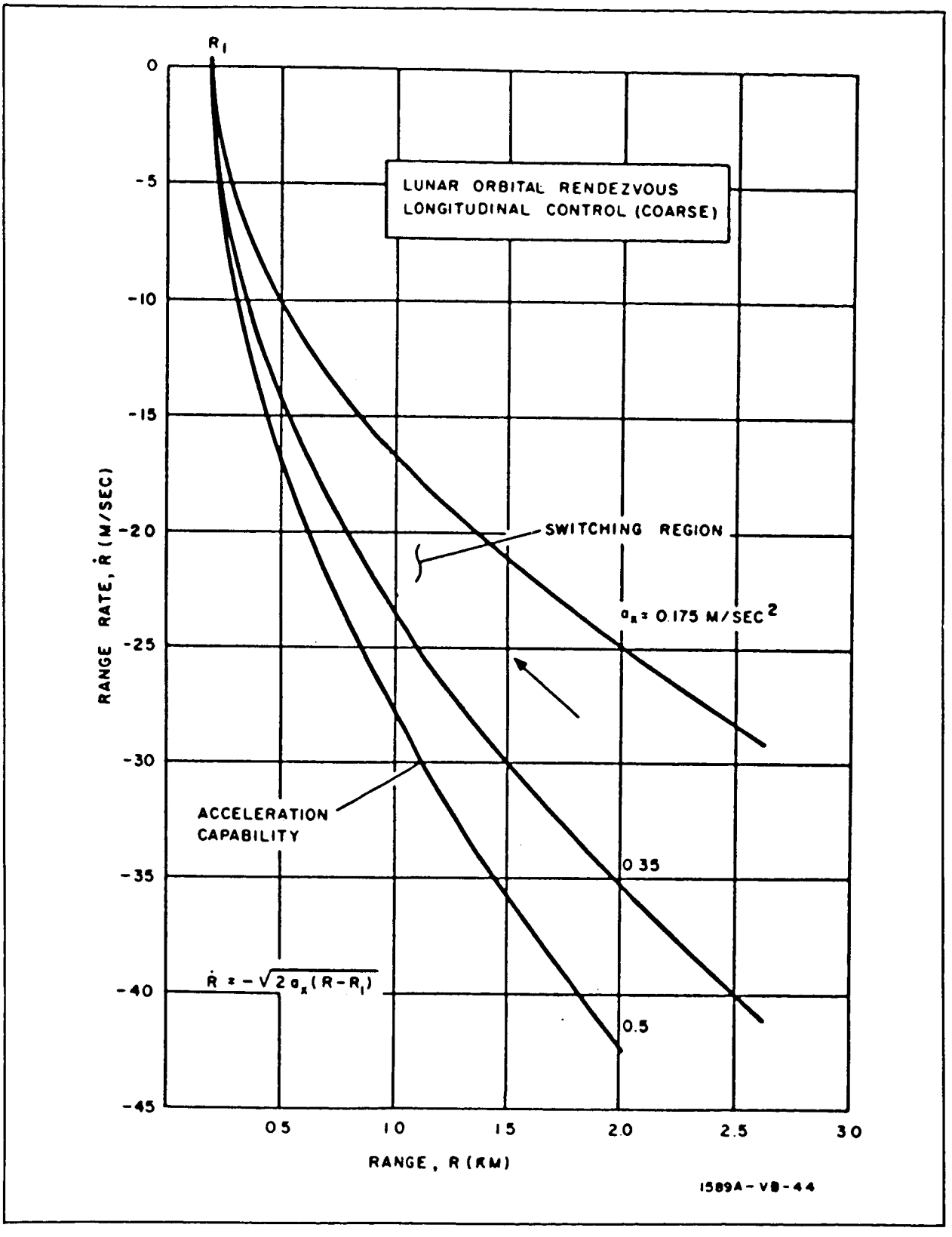

Figure 6-3. Longitudinal Control - Coarse

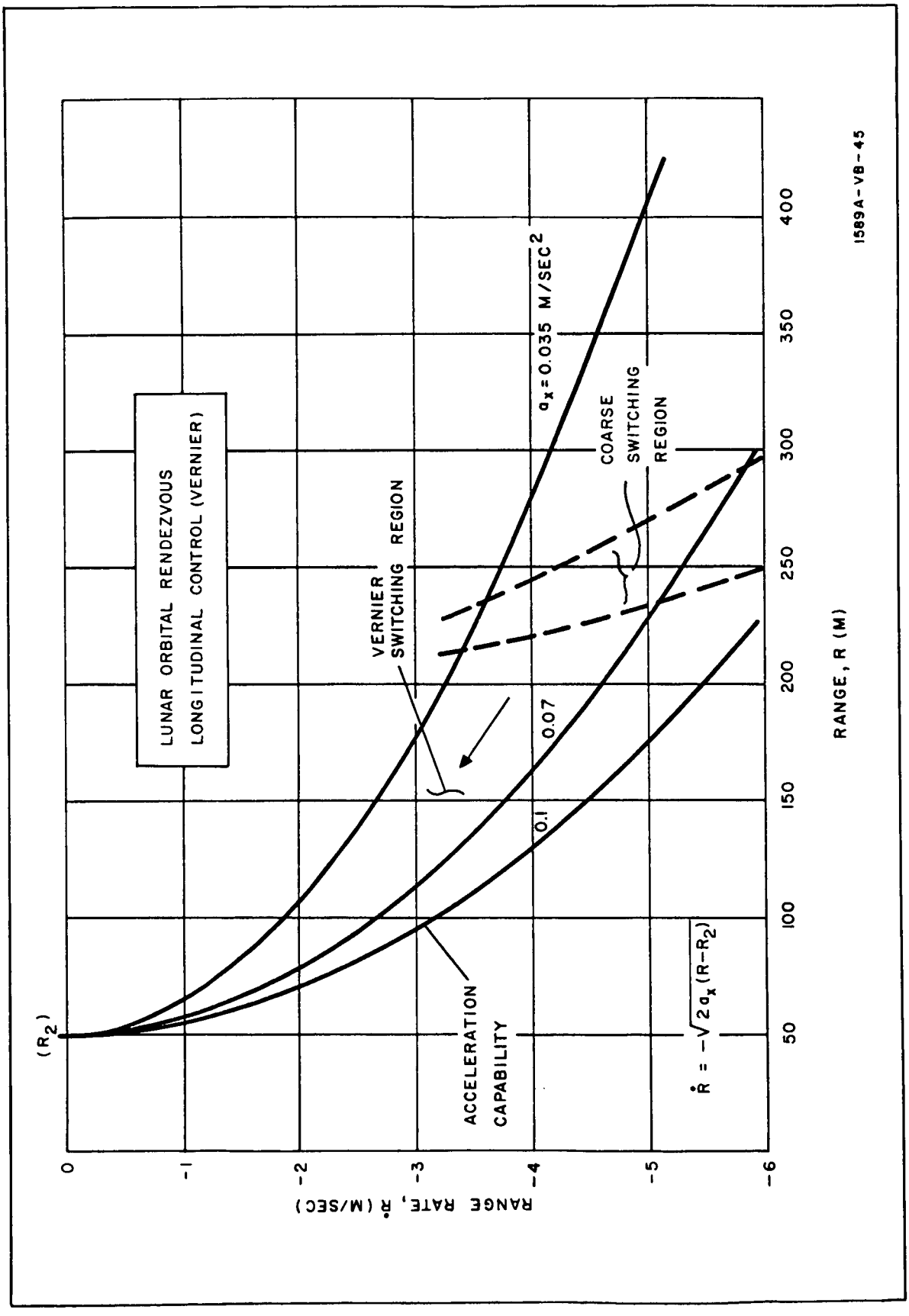

Figure 6-4. Longitudinal Control - Vernier

6.4 DATA PROCESSING

Vehicle trajectories, the propulsion system, the guidance and control method, and the sensors have been simulated on the IBM 7094 computer. Injection errors and rendezvous sensor errors were incorporated into the computer program.

Least-squares digital data smoothers with a smoothing time of 15 seconds and a 1-second computing interval were used to improve the accuracy of the "raw" observed data. Velocity compensation was afforded in the smoothers to permit tracking during rocket firing periods. The smoothed signals are then used for control purposes. A diagram is shown in figure 6-5.

6.5 EFFECTS OF INJECTION ERRORS

Errors of injection into the transfer orbit result in increased propellant consumption. For example, the curve of figure 6-6 illustrates for a typical active rendezvous system how the incremental velocity requirement (compared with the theoretical minimum of the Hohmann transfer) increases with the error in initial phase angle. In determining the tolerable level of injection sensor errors, the 3σ value of injection error is considered to be that error which results in a 20-percent ΔV increase over the Hohmann transfer.

Injection errors propagate along the ascent ellipse to produce dispersions in the terminal conditions. Figure 6-7, a typical rendezvous phase plane diagram, illustrates the dispersion introduced by injection errors. Correspondingly, the dispersion in elevation angle due to injection errors is shown in figure 6-8.

6.6 EFFECTS OF RENDEZVOUS SENSOR ERRORS

Errors in the terminal rendezvous sensors not only extend the uncertainty region of the terminal condition, but also increase the expenditure of rendezvous maneuvering propellant. The curves of figure 6-9 illustrate how propellant consumption (in terms of incremental velocity ratio) increases with rendezvous sensor errors for a particular rendezvous situation. For each ratio of error level, 25 computer runs are made with different random sensor errors inserted. The $+3\sigma$ deviation from the arithmetic mean is also shown and is used to establish the allowable level of sensor error. The point where the actual ΔV is 150-percent of the Hohmann ΔV (and intercepts the $x + 3\sigma$ curve) is considered to correspond to the 3σ level of sensor error. For the lunar case shown, the ΔV for the 30/200-km Hohmann transfer is 75 m/sec corresponding to a W_p/W_o of 0.008 for an I_{sp} of 300 seconds.

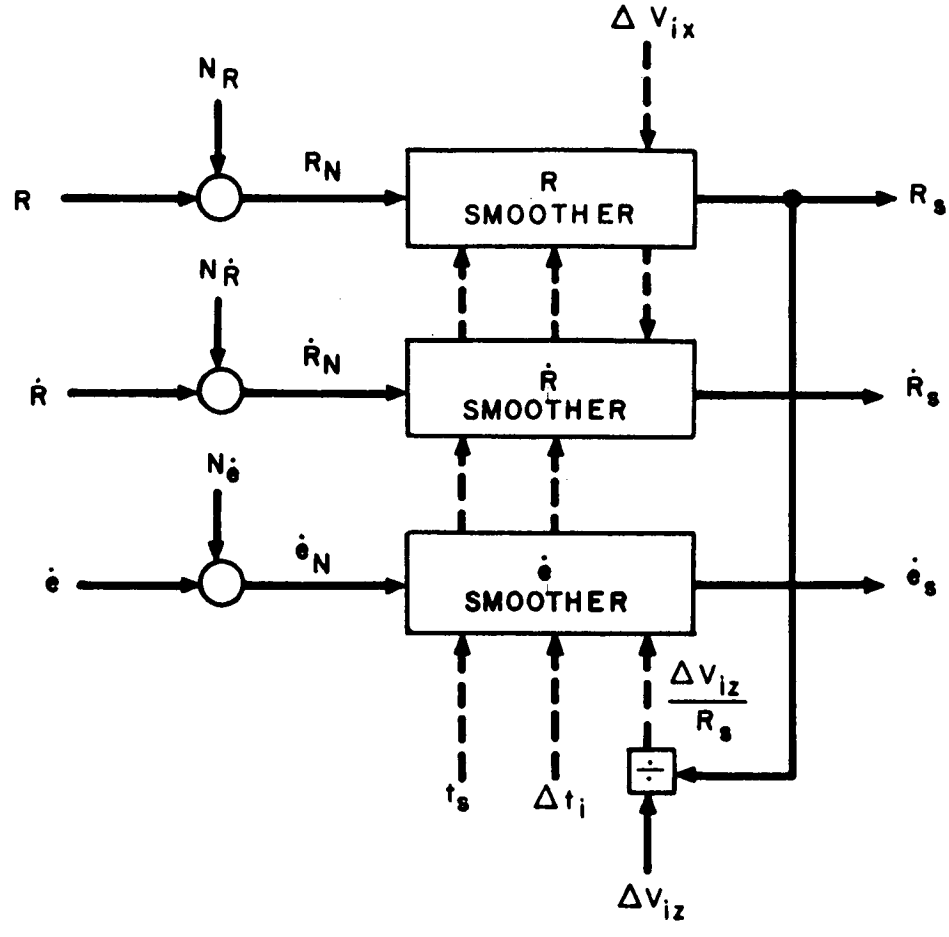

Figure 6-5. Digital Data Smoother

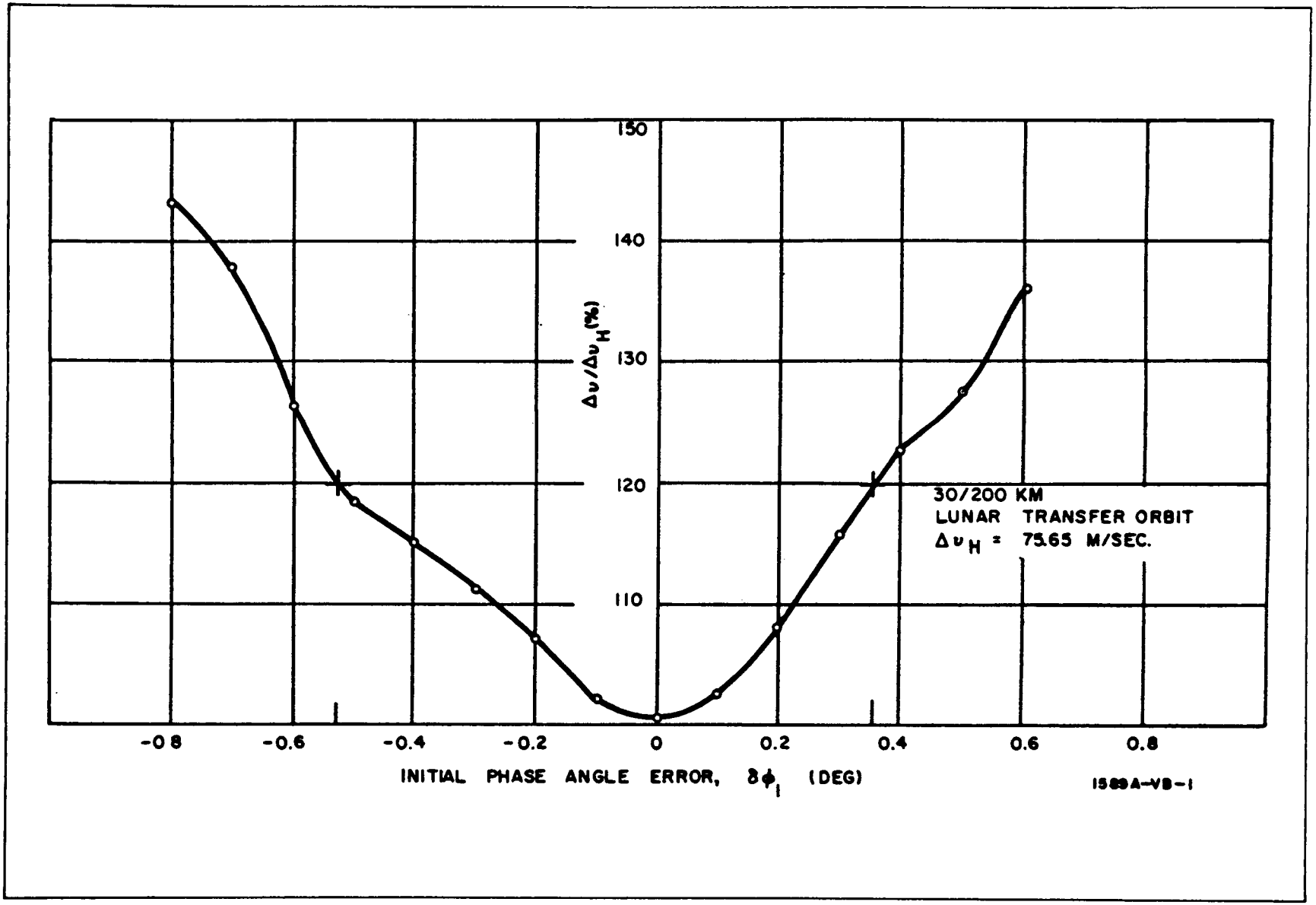

Figure 6-6. Effect of Initial Phasing Error on Propellant Consumption

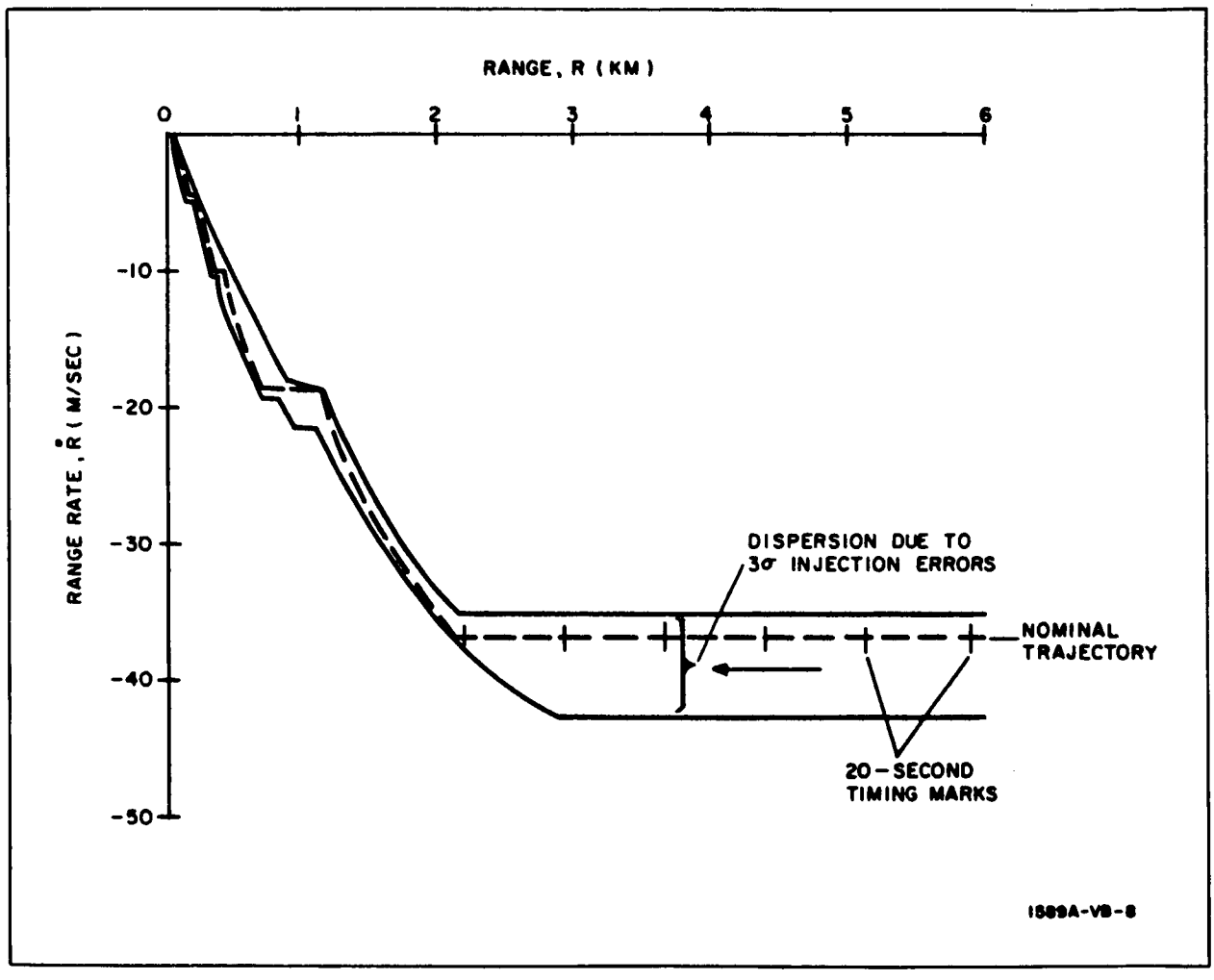

Figure 6-7. Rendezvous Phase Plane

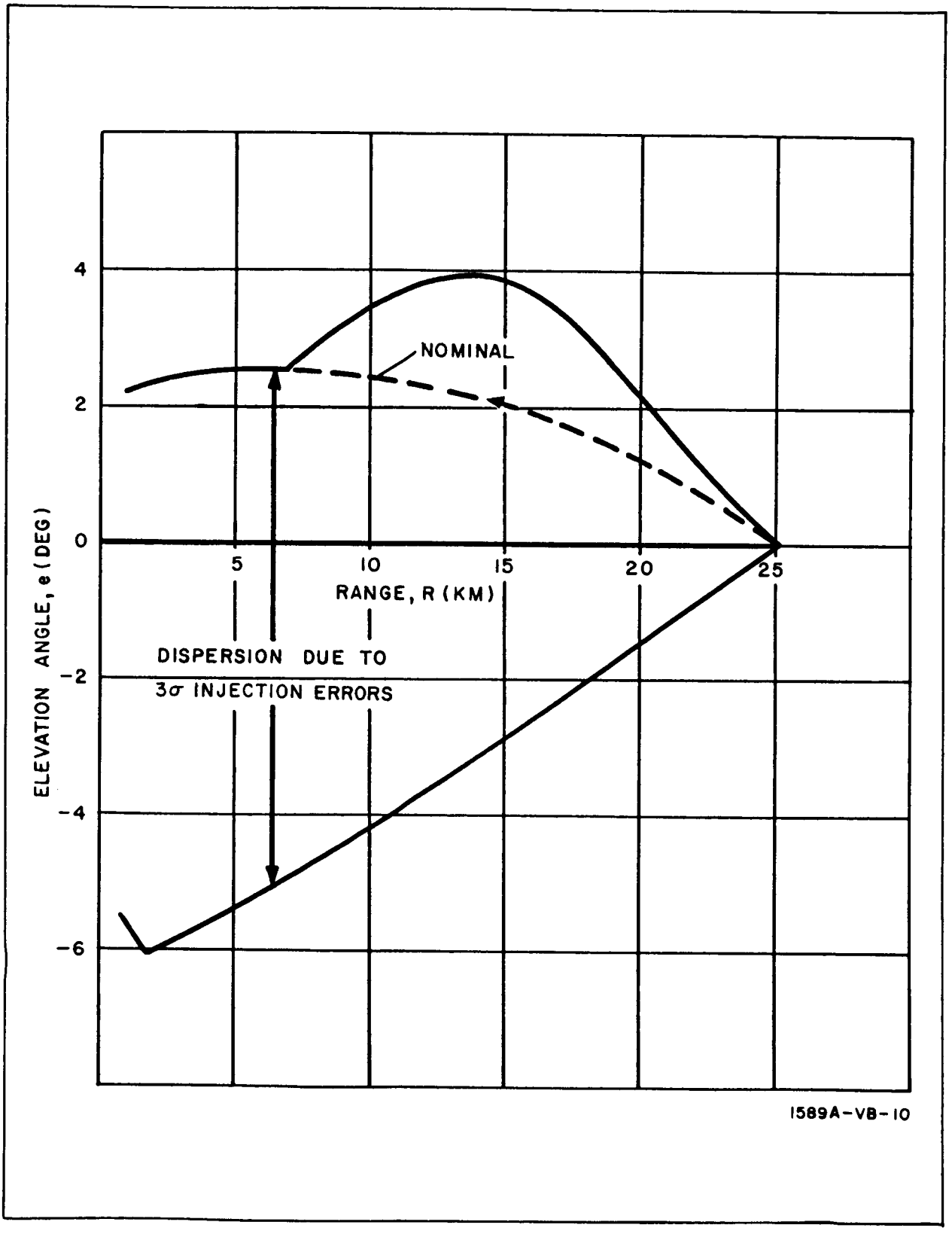

Figure 6-8. Variation in Elevation Angle With Range

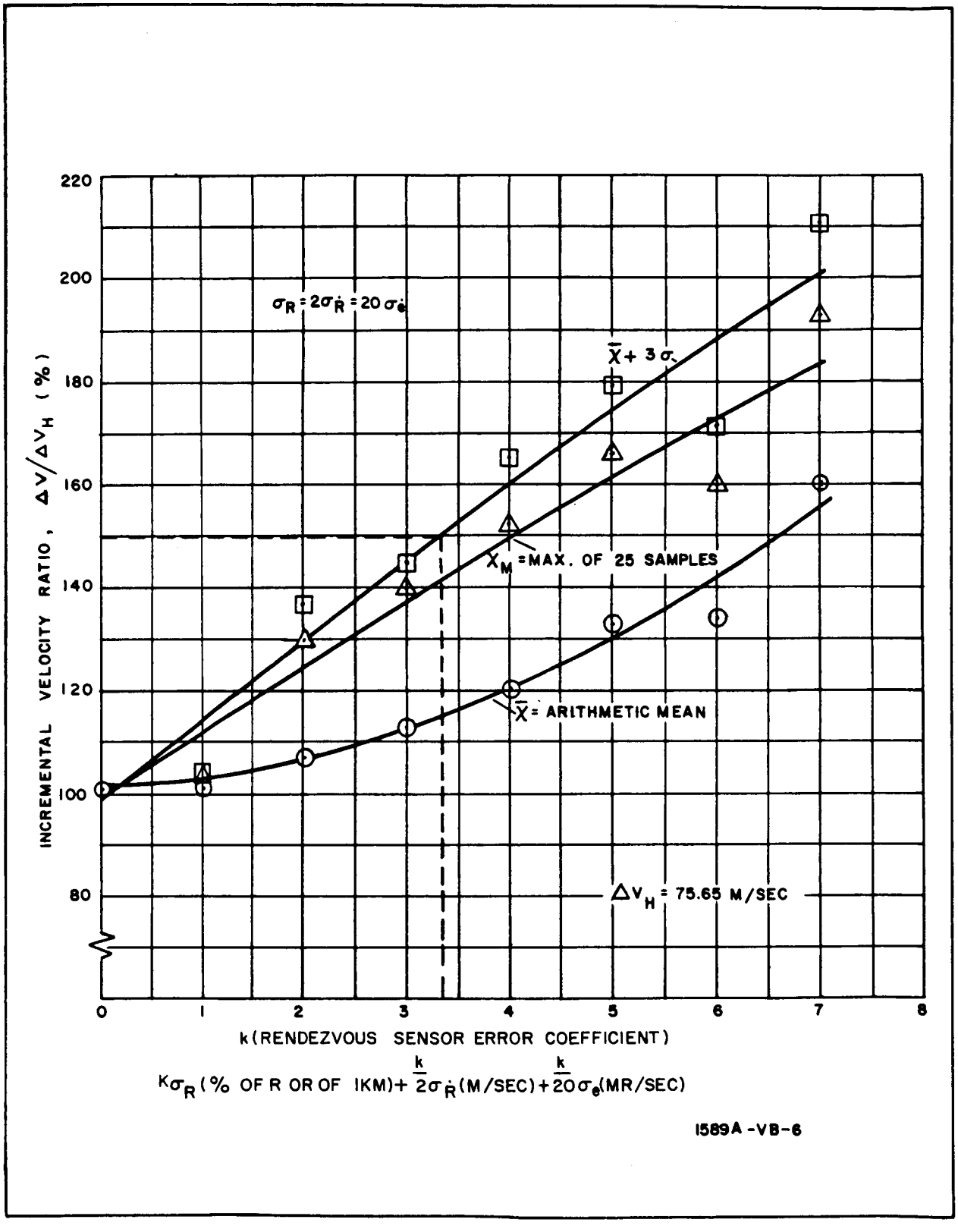

Figure 6-9. Effect of Rendezvous Sensor Errors on Propellant Consumption

7. EARTH RENDEZVOUS

7.1 INTRODUCTION

Rendezvous is the procedure of bringing two vehicles into close spatial proximity while in orbit about the earth. It will play a significant role in assembling large orbiting facilities which, because of energy restrictions, must be boosted in sections and assembled while in orbit. Logistical support of these facilities will also necessitate performance of the rendezvous procedure.

7.2 MISSION PROFILE

A nominal mission profile is assumed for the analyses in which the target (the vehicle with which rendezvous is to be performed) is in a circular orbit about the earth at an altitude of 500 to 1000 km. The chaser (the vehicle performing the rendezvous) is in a 185-km parking orbit coplanar with the target orbit. The overall rendezvous procedure comprises four sequential phases: injection, midcourse, active rendezvous, and docking.

7.2.1 Injection

At a predetermined point, the chaser imparts a computed velocity increment and assumes a transfer trajectory which is cotangential with the target orbit at the nominal rendezvous point. The transfer trajectory used as the nominal or reference is the 180-degree Hohmann transfer. This transfer is chosen on the basis of velocity considerations, the Hohmann being the minimum energy two-pulse transfer between orbits.

7.2.2 Midcourse

The major portion of the time that the chaser is traveling the transfer orbit, it is in a passive mode; i.e., no thrusting is performed. Measurements may be performed, however, to update the estimations of the state variables, position and velocity, of the chaser.

7.2.3 Active Rendezvous

When the chaser-to-target range has decreased to a predetermined value (25 to 50 km) the chaser commences a series of thrusting maneuvers which cause it to close upon the target in a manner defined by the guidance technique

used. The active phase ends when the chaser reaches a predetermined range and range rate relative to the target.

7.2.4 Docking

The docking phase covers the time from termination of active rendezvous to physical contact between the chaser and target. Since this phase will most likely be performed using manual control based upon visual observations, it is beyond the scope of this report.

7.3 ANALYSIS

As a means of determining sensor requirements for rendezvous, the mission profile is combined with various guidance and control methods and incorporated in various computer simulations (both digital and analog) of the rendezvous procedure. This procedure allows the effects of sensor errors on the system to be studied in a parametric manner.

7.3.1 Guidance and Control

- Injection: Since injection is essentially an impulsive maneuver, no specific guidance and control methods are assumed.

- Midcourse: No guidance techniques are required for this phase since the chaser assumes a coasting or passive mode during this time.

- Active Rendezvous: The active rendezvous phase takes place during the last several hundred seconds of travel of the transfer orbit. A guidance and control technique is used to effect the desired manner of closure on the target.

Three guidance and control systems studied for active rendezvous are utilized for the active phase:

a. An automatically controlled variable-thrust level guidance based on proportional navigation and referred to as modified proportional navigation (MPN)

b. An automatically controlled constant-thrust level on-off system

c. A pilot controlled constant-thrust level on-off system

Control is separated into longitudinal control and normal control for each system.

Longitudinal control is exercised by thrusting along the longitudinal axis, which is essentially aligned with the LOS, to decrease the chaser-to-target range rate in a specified manner as the range decreases. The range - range rate relationship is indicated in figure 7-1 by the heavy dashed line on the phase plane (range versus range rate). This phase plane trajectory is typical of that resulting when MPN guidance is used. For the constant-thrust level on-off system, a trajectory which approaches the terminal conditions between the switching boundaries results. Such a trajectory is indicated by the dotted line in figure 7-1.

Normal control is exercised by thrusting perpendicular to the LOS and in the plane of LOS rotation in a direction which nulls the LOS inertial rate. By nulling the LOS rate, the chaser is maintained on a closing course with the target. As is seen from figure 7-2, the LOS orientation with respect to

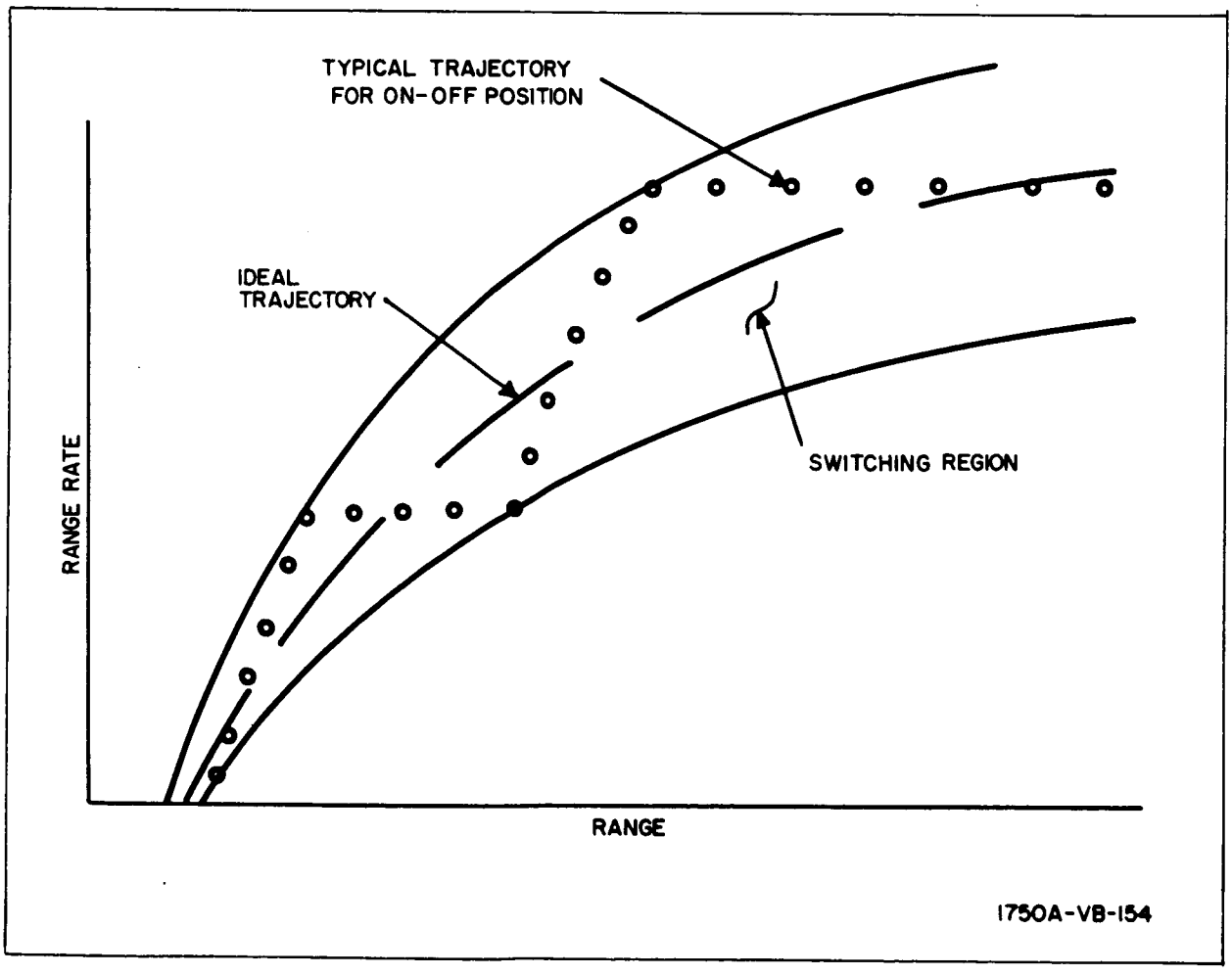

Figure 7-1. Phase Plane Relationship for Longitudinal Control

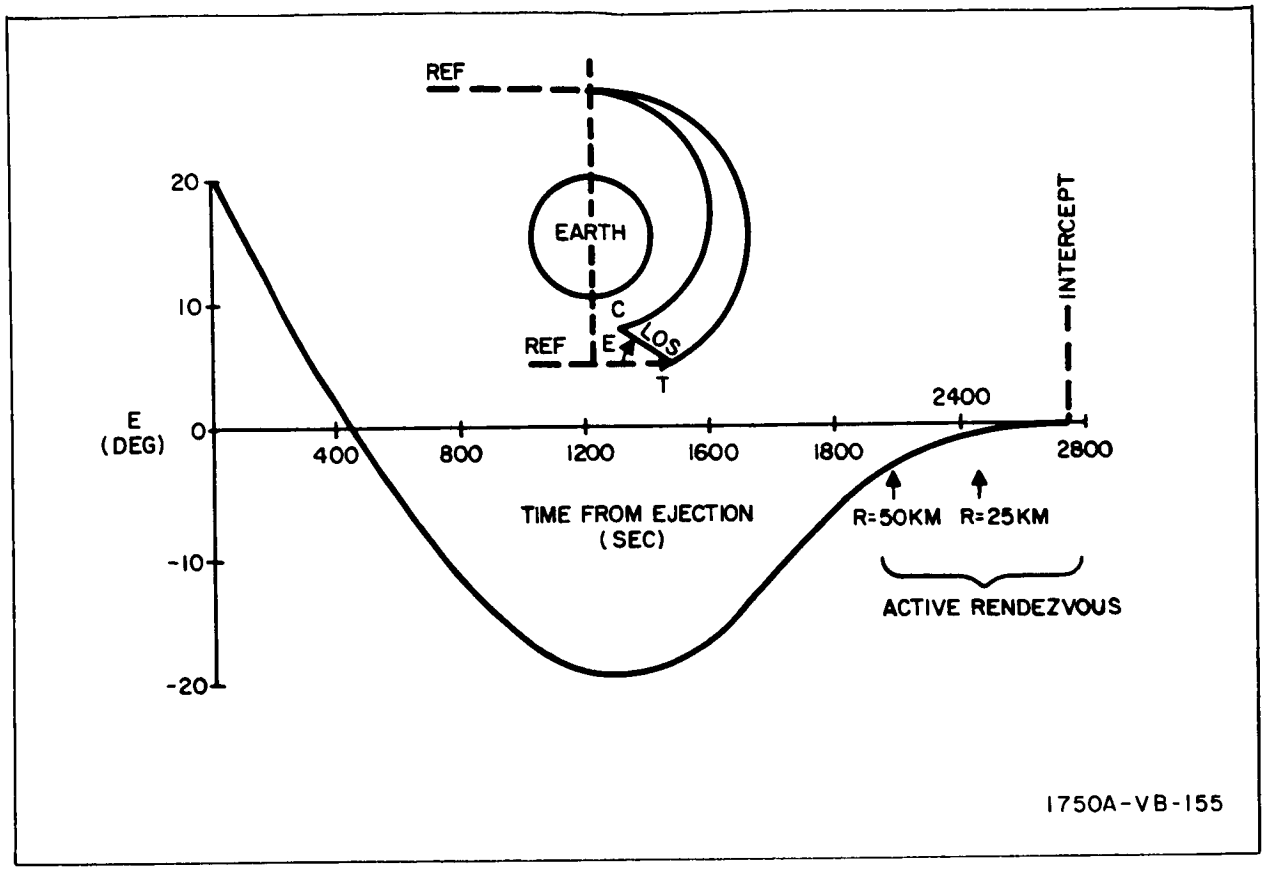

Figure 7-2. Orientation of LOS with Respect to Inertial Space During Nominal 185-555 km Hohmann Transfer

inertial space varies only slightly during the final portion of the nominal Hohmann transfer. Consequently, any LOS rates encountered are, essentially, the result of orbital perturbations and/or improper execution of the injection maneuver and are relatively minor (i.e., the normal control exercised is not required to alter the trajectory of the chaser significantly to effect rendezvous).

7.3.2 Reduction of Errors in Estimated State Variables

Because of errors at injection and orbital perturbations, the chaser deviates from the reference transfer orbit (the nominal Hohmann transfer) and the resulting state variables at the rendezvous point will deviate from the state variables which may be estimated at any point along the transfer orbit. Errors inherent in the estimation can be reduced by performing measurements of the relative dynamics between the chaser and target during the midcourse phase and updating the estimated state variables by a process utilizing the measured observables. Analysis of the correction procedure is

limited to determining the optimum combination of observables to be measured and the relative time at which to perform the measurements.

7.3.3 Observables Utilized

7.3.3.1 Observables for Injection

The injection maneuver may be based upon combinations of one or more of the following:

a. Altitude

b. Velocity

c. Central angle (between the radius vector of chaser and target)

d. Chaser-to-target range

e. Chaser-to-target range rate

f. Time

7.3.3.2 Observables for Midcourse Correction of State Variables and Active Rendezvous

Since the rendezvous procedure is one of controlling the relative geometry and dynamics of the two vehicles, both the midcourse correction of the state variables and the active rendezvous phases require combinations of one or more of the following:

a. Chaser-to-target range

b. Chaser-to-target range rate

c. LOS orientation with respect to an inertial reference

d. LOS angular rate with respect to inertial space

7.3.4 Error Analysis

7.3.4.1 Sources of Error

Errors are assumed to occur in the execution of the injection maneuver and in the sensor measurements during active rendezvous.

Injection errors may occur in measurement of the observables upon which the maneuver is based and/or in imparting the velocity impulse required to achieve the transfer orbit. The resultant errors occur in the chaser state variables as one or more of the following:

a. a position error

b. a velocity vector error (magnitude and/or direction)

c. a timing error

No attempt is made to separate the sources of the resulting errors (i.e., measurement errors or control errors).

Sensor measurement errors occurring in the measurement of observables during active rendezvous are assumed to have the following forms. Range and range rate measurement errors have either a bias error, a normally distributed random error, or both. Each error comprises a fixed component and a component which is a percentage of the observable being measured. Angle and angular rate measurements are each assumed to have a normally distributed random error.

7.3.4.2 Error Criteria

Two error criteria are postulated and used in the study. The first stipulates that any single 3σ error at injection shall not result in more than a 20-percent increase in ΔV (incremental velocity) over that required for both impulses of the nominal Hohmann transfer when the rendezvous is performed with zero sensor measurement errors during the active phase. It is further stipulated that any single $3\ \sigma$ rendezvous sensor measurement error shall result in no more than a 50-percent increase in total ΔV over the nominal Hohmann transfer. The second criterion allows no more than a 20-percent deviation in the postulated range and range rate at termination of active rendezvous when all errors are included on the measurements.

7.3.5 Midcourse Analysis

A two-dimensional analysis is conducted to determine the effect of a midcourse measurement in reducing the uncertainties in the state variables at rendezvous. Two factors are investigated: the most effective combination of observables to be utilized and the best time at which to perform the measurement.

The reference coordinate system used is a local vertical system centered at the target with the positive X-axis along the horizontal in the direction opposite the motion of the target. The Y-axis is along the radius vector from the earth.

Deviations of the chaser state variables from the reference are represented by

$$\left[\Delta_I\right] = \begin{bmatrix} \Delta X \\ \Delta Y \\ \Delta \dot{X} \\ \Delta \dot{Y} \end{bmatrix}$$

These deviations may be propagated to the point of measurement by a state transition matrix, $[M]$. The point of measurement is defined by the central angle of the target coordinate system from the nominal point of rendezvous. This angle is the product of the orbital angular velocity of the target and the time to go to rendezvous, $\omega_T T_1$. Deviations at the measurement point but prior to the measurement are expressed as

$$\left[\Delta_1 -\right] = \left[M\,(T_I,\ T_1)\right]\left[\Delta_I\right]$$

At this point, the observables are measured and the measurements are utilized in a correction matrix $[C]$. This matrix is used to premultiply the deviations $\left[\Delta_1 -\right]$, thereby yielding the updated deviations

$$\left[\Delta_1 +\right] = \left[C\right]\left[\Delta_1 -\right]$$

$$= \left[C\right]\left[M\,(T_I,\ T_1)\right]\left[\Delta_I\right]$$

These are then propagated to the nominal point of rendezvous to obtain the uncertainties in the state variables at that point.

$$\left[\Delta_f\right] = \left[M\,(T_1,\ T_f)\right]\left[\Delta_1 +\right]$$

$$= \left[M\,(T_1,\ T_f)\right]\left[C\right]\left[M\,(T_I,\ T_1)\right]\left[\Delta_I\right]$$

Measurement of the following combinations of observables, to be used in the correction matrix, is investigated.

- Range and range rate
- Angle and angular rate
- Range and angle
- Range rate and angle
- Range, range rate, and angle
- Range, angle, and angular rate.

7.4 RESULTS

As would be expected, the resulting sensor accuracies are dependent upon the analytical model used and the error criteria applied. Sample results using different models and criteria are presented below.

7.4.1 Sensor Requirements Obtained Using MPN System

7.4.1.1 Injection Sensor Requirements

It is determined that injection sensor requirements are dependent upon the relative chaser-to-target range at which the active rendezvous phase begins. Fuel consumption per unit injection error as a function of the initial range for active rendezvous is shown in figure 7-3. The fuel expenditures are based on the MPN system. As shown, greater injection errors can be tolerated as the active rendezvous starting range is increased.

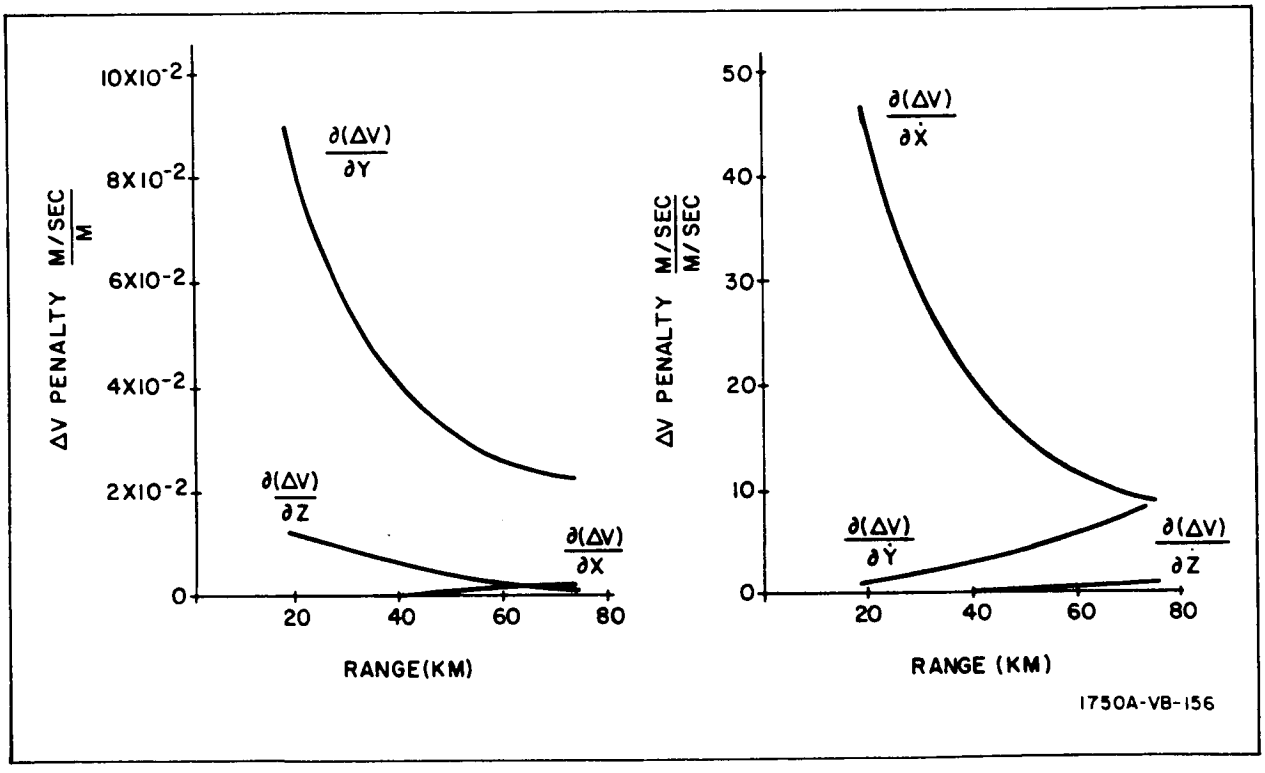

Figure 7-3. Injection Sensitivity Coefficients for Initial Range of Active Rendezvous (MPN System)

Applying the fuel criteria of paragraph 7.3.4.2 to the system for an initial range of 18.5 km (10 n.mi) the chaser position and velocity accuracies of table 7-1 are obtained. These quantities are measured in a rotating local-vertical coordinate system centered at the target.

TABLE 7-1
ALLOWABLE (3σ) POSITION AND VELOCITY ERRORS AT INJECTION

Position	Velocity
ΔX = ---	$\Delta \dot{X}$ = 0.9 m/sec
ΔY = 0.47 km	$\Delta \dot{Y}$ = 42.25 m/sec
ΔZ = 3.38 km	$\Delta \dot{Z}$ = ---

7.4.1.2 Rendezvous Sensor Requirements

In the MPN system, the following observables are measured by the sensors.

- Range
- Range rate
- LOS angular rate

The combined effects of dynamic errors and random and bias sensor errors on the active rendezvous phase are obtained. Three levels of sensor errors, considered representative of the 1970 time period, are investigated. These errors are presented in table 7-2.

Figure 7-4 illustrates the effect of the errors on final position. Bias errors are incorporated in a manner such that the effect of each adds "in the same direction", thereby providing a worst case. The total bias error is represented by a vector as shown. Random errors are indicated by the ellipses about the ends of the respective bias errors. The allowable final position error is indicated by the circle of radius 6.1 meters (20 ft).

In figure 7-5, the effects of sensor errors on final range rate are presented in a similar fashion with the allowable final velocity error set at 6.1 m/sec (20 ft/sec). It is seen that the medium level of errors allows the rendezvous to be performed with an acceptable level of accuracy while the high level of errors does not. The medium level is therefore stipulated as the measurement accuracies required of the rendezvous sensors.

TABLE 7-2
TYPICAL SENSOR ERROR LEVELS

(1970 Time Period)

RANDOM (FLUCTUATION) ERROR LEVELS (1σ)

Type / Range	Range (m)	% Range	Range Rate $\left(\frac{m}{sec}\right)$	% Range Rate	LOS Rate $\left(\frac{mr}{sec}\right)$
Low	0.61 (2 ft)	0.2	0.03 (0.1 ft/sec)	0.05	0.03
Medium	1.52 (5 ft)	0.5	0.15 (0.5 ft/sec)	0.20	0.10
High	3.04 (10 ft)	1.0	0.06 (2.0 ft/sec)	0.50	0.20

BIAS ERROR LEVELS (1σ)

Type / Range	Range (m)	% Range	Range Rate $\left(\frac{m}{sec}\right)$	% Range Rate	LOS Rate $\left(\frac{mr}{sec}\right)$
Low	0.305 (1 ft)	0.2	0.03 (0.1 ft/sec)	0.05	0.03
Medium	0.61 (2 ft)	0.5	0.15 (0.5 ft/sec)	0.20	0.10
High	3.05 (10 ft)	2.0	0.6 (2.0 ft/sec)	0.50	0.20

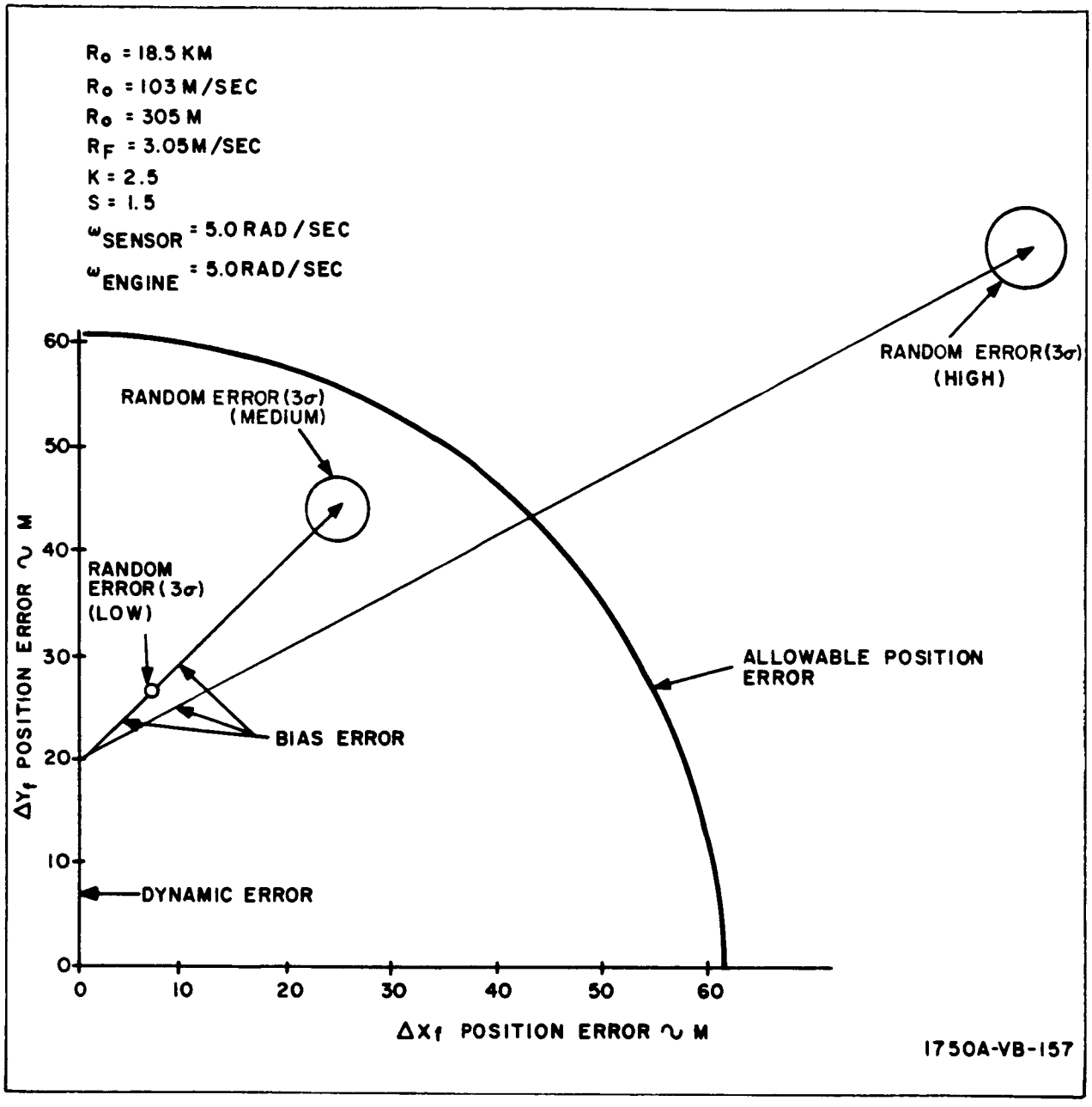

Figure 7-4. Rendezvous Terminal Position Error Versus Sensor Error Level for MPN

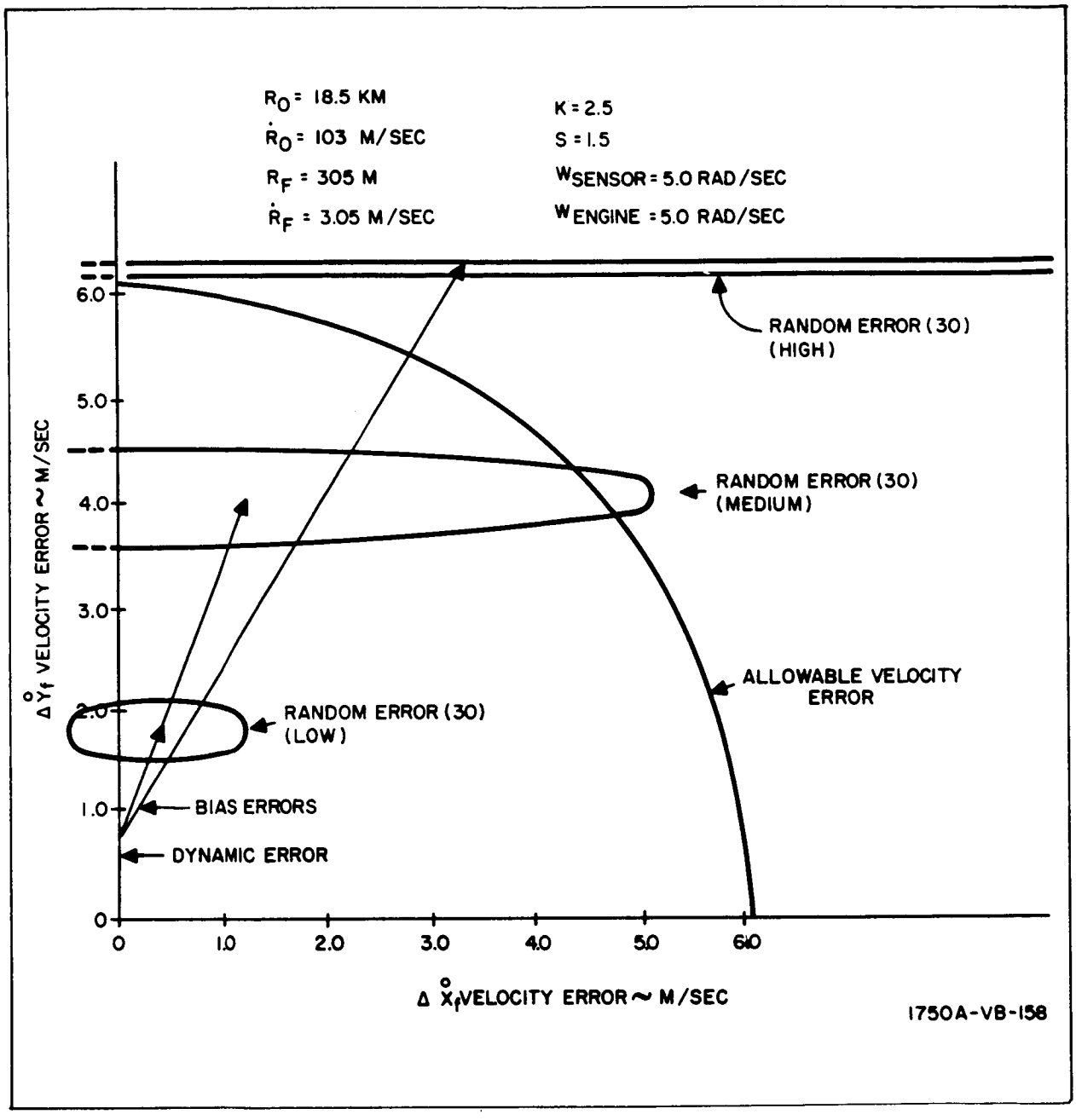

Figure 7-5. Rendezvous Terminal Velocity Error Versus Sensor Error Level for MPN

7.4.2 Sensor Requirements Using On-Off System

7.4.2.1 Injection Sensor Requirements

Injection errors determined by simulating the automatic control on-off system on a digital computer are presented in table 7-3. The program computes the velocity expenditures required during active rendezvous to compensate for the injection errors and the criteria of a 20-percent maximum velocity increase (paragraph 7.3.4.2) is applied. State of the art capabilities are also presented for comparison.

TABLE 7-3
INJECTION SENSOR ACCURACY REQUIREMENTS

Symbol	Quantity	Sensor Accuracy (3σ)	State of the art Accuracy (3σ)
Δh	Altitude	4.0 km (2% of R)	200 m (0.1% of R)*
ΔV	Velocity	2.0 m/sec	0.3 m/sec
Δr	Pitch Attitude	4.5 deg	0.3 deg
$\Delta \psi$	Yaw Attitude	26.6 deg	0.3 deg
$\Delta \phi$	Central Angle	0.19 deg	- - -
ΔR	Range	2.7% of R	0.1% of R
Δt	Timing	43.2 sec	3 sec
Δi	Inclination	0.26 deg	0.1 deg

* A radar altimeter can measure terrain altitude to this accuracy, but it cannot measure absolute altitude with this degree of precision.

7.4.2.2 Rendezvous Sensor Requirements

Range and LOS angle are measured by the automatic on-off system sensor. The time derivitives are then obtained by onboard computations.

To determine the effects of sensor errors during the active phase of rendezvous, a computer program is used to make a series of runs utilizing various noise levels on the sensor measurements. To provide a standard of comparison, all runs have a -0.3 m/sec velocity error at injection. Ten runs are made at each noise level with a different random number routine.

None of the noise levels degrades system performance sufficiently to prevent rendezvous. The ratio of angular noise to range noise is taken as

$$\sigma_e \text{ (mr)} = 30\ \sigma_R \text{ (\% of range)}$$

Comparison is made of the velocity expenditures for each run with the velocity required for the ideal Hohmann transfer. The results of this comparison are shown in figure 7-6 in the form of increased fuel required as a

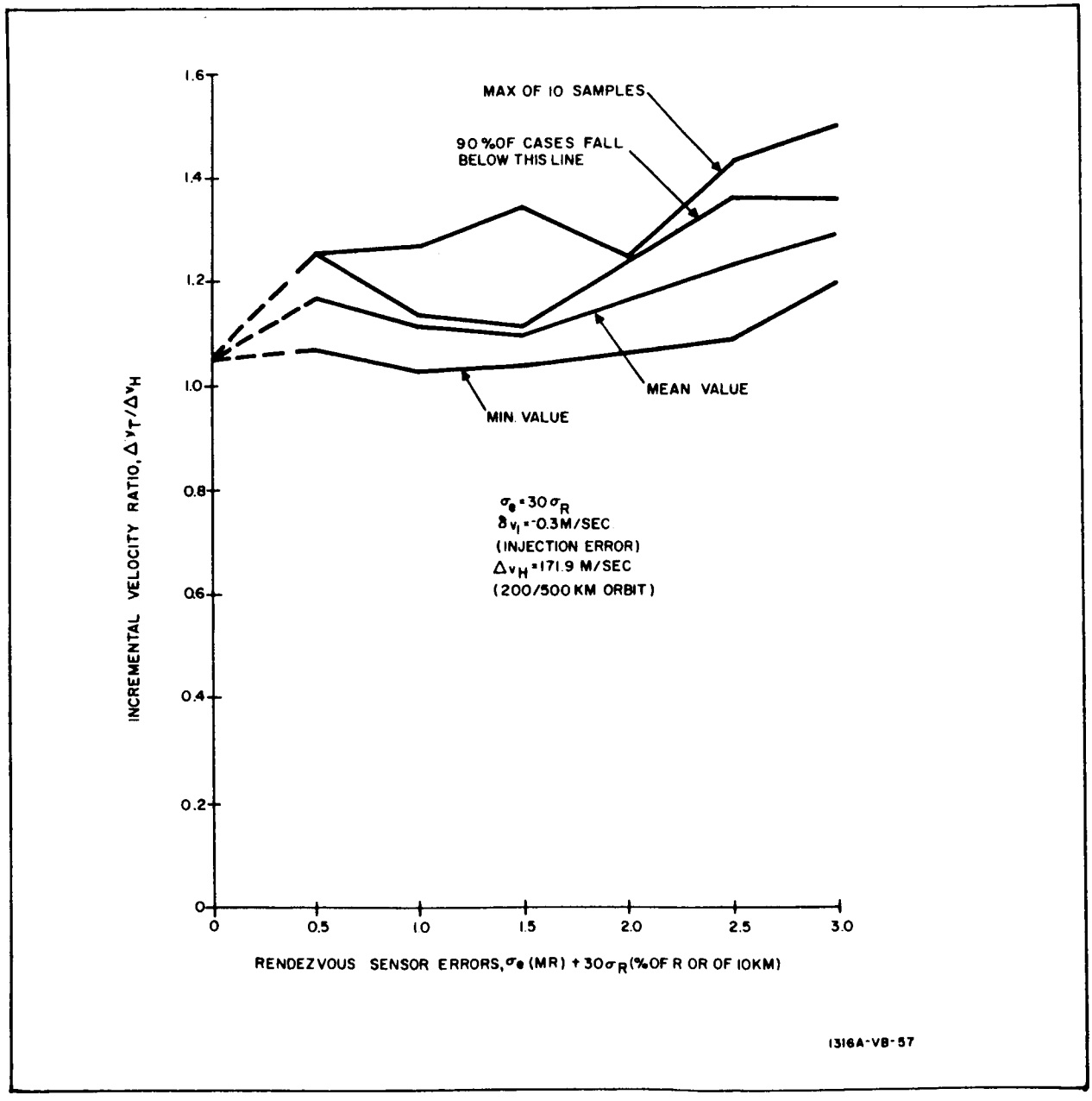

Figure 7-6. Effect of Rendezvous Sensor Errors on Propellant Consumption

function of noise level on the sensor measurements. The rendezvous sensor requirements are based on an interpretation of these results. It is arbitrarily specified that the point where the 100-percent line (maximum of the 10 samples) uses a velocity ratio $\frac{\Delta V}{\Delta V_H}$ of 1.5 constitutes a reasonable level of accuracy. Using this criterion, the results compared with a state of the art rendezvous radar system are as shown in table 7-4.

TABLE 7-4
COMPARISON OF ACCURACIES

Quantity	Sensor Accuracy (3σ)	State of the Art Accuracy (3σ)
Range*	0.3% of R or 30 m	0.1% of R or 10 m
Angle	9 mr	3 mr

* The required range accuracy is a percent of range or a fixed range whichever is larger.

7.4.3 Dynamic Range Requirements for Rendezvous Sensors

Figures 7-7 and 7-8 show the range rate and LOS angular rate for nominal Hohmann transfers to various target altitudes. At ranges below 75 km, the magnitude of the range rate is seen to vary between approximately 50 and 225 m/sec. The magnitude of LOS angular rate is seen to vary between 0 and 0.4 mr/sec over the same ranges. Larger values of LOS rate will very likely result as the chaser deviates from the nominal trajectory because of errors and perturbations. Allowing for such errors, the dynamic ranges given in table 7-5 are postulated.

TABLE 7-5
RENDEZVOUS SENSOR DYNAMIC RANGE REQUIREMENTS

Quantity Measured	Dynamic Range	
	Min.	Max.
Range	0 0	25 km (for 18.5-km acquisition range) 80 km (for 75-km acquisition range)
Range Rate	-350 m/sec (closing)	100 m/sec (opening)
LOS Rate	-2 mr/sec	+2 mr/sec
Gimbal Angles, Elevation and Azimuth (nominal values)	-20 deg	+20 deg

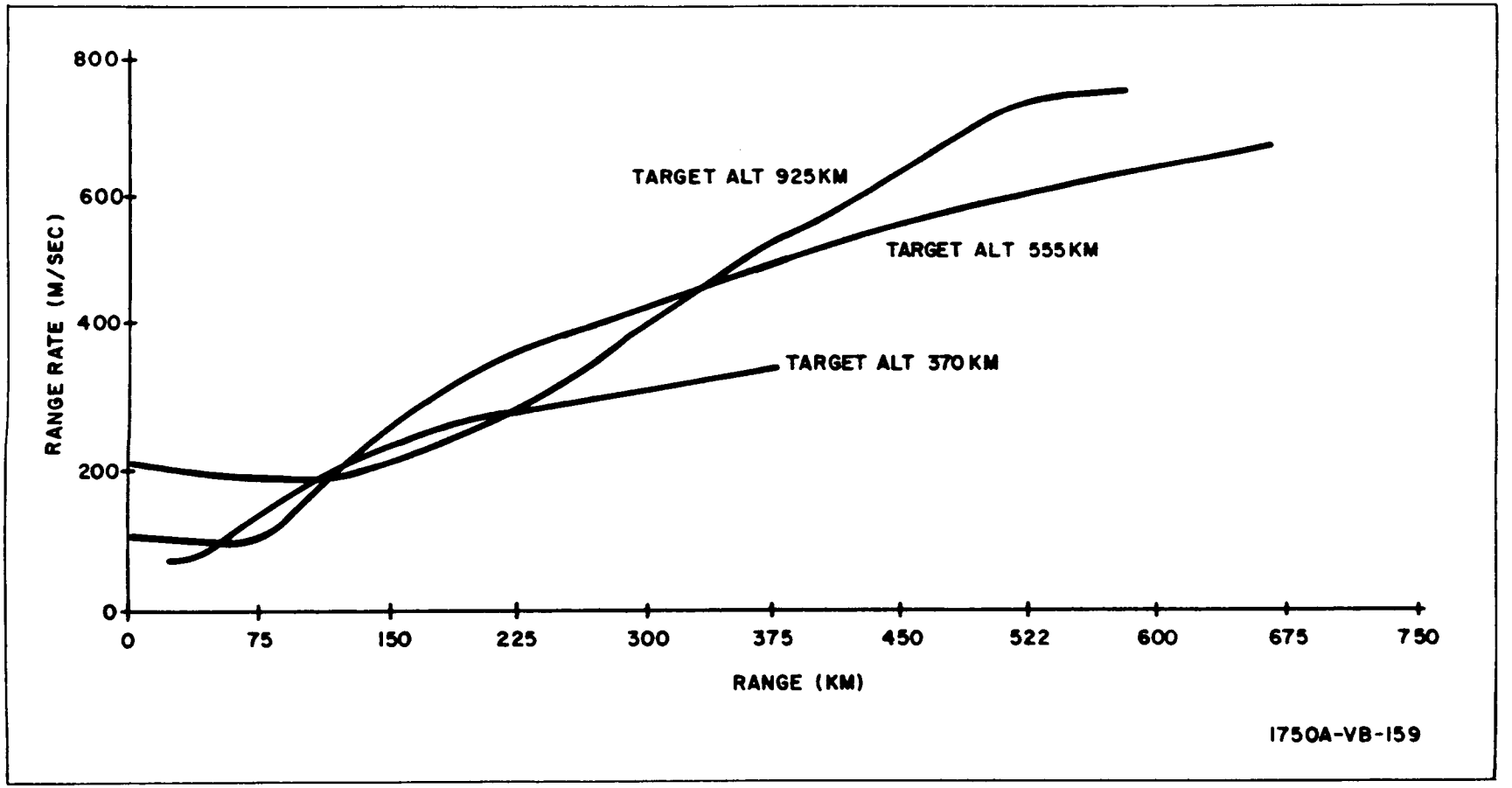

Figure 7-7. Range Rate Versus Range for an Ideal Hohmann Transfer (Chaser Initially in 185-km Coplanar Parking Orbit)

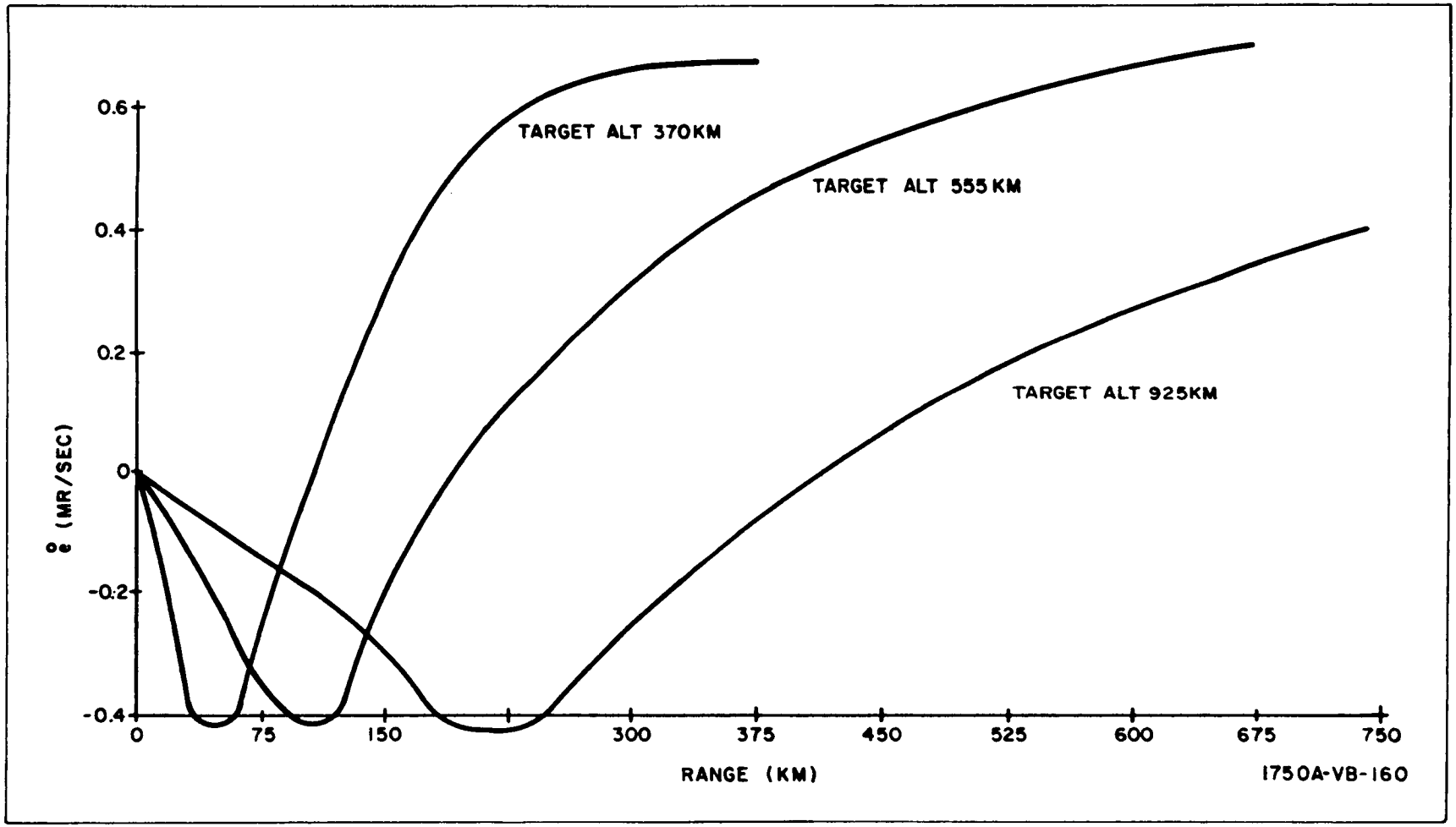

Figure 7-8. LOS Rate Versus Range for an Ideal Hohmann Transfer
(Chaser Initially in 185-km Coplanar Parking Orbit)

7.4.4 Results of Midcourse Analysis

As would be expected, the more observables measured the greater is the reduction in the uncertainties of the state variables. Of the six combinations studied, the matrix utilizing range, range rate, and angle provided the best results. Of the matrixes using two observables, the matrix using range and range rate gave the best results. These matrixes are given in table 7-6.

TABLE 7-6
CORRECTION MATRIXES

$$\left[C\left(R,\ \dot{R}\right]\right.$$

$$\begin{bmatrix} \left(\frac{Y}{R}\right)^2 & -\frac{XY}{R^2} & 0 & 0 \\ \frac{XY}{R^2} & \left(\frac{X}{R}\right)^2 & 0 & 0 \\ \frac{Y}{R^3}\left[\dot{R}_Y - R_{\dot{Y}} - 3x\,R\,\dot{\theta}\right] & \frac{1}{R^3}\left[Y\left(R\dot{X} - R\dot{X}\right) + \left(X^2 - 2Y^2\right)R\dot{\theta}\right]\left(\frac{Y}{R}\right)^2 & -\frac{XY}{R^2} & \\ \frac{1}{R^3}\left[X(R_{\dot{Y}} - \dot{R}_Y) - (Y^2 - 2x^2)R\dot{\theta}\right] & \frac{X}{R^3}\left[\dot{R}X - R\dot{X} + 3Y\,R\,\dot{\theta}\right] & \frac{-XY}{R^2} & \left(\frac{X}{R}\right)^2 \end{bmatrix}$$

$$\left[C\left(R,\ \dot{R},\ \theta\right)\right]$$

$$\begin{bmatrix} 0 & 0 & 0 & 0 \\ 0 & 0 & 0 & 0 \\ \frac{-Y}{R^2}\left[\dot{Y} + 2\dot{\theta}\,x\right] & \frac{Y}{R^2}\left[\dot{X} - 2\,\dot{\theta}Y\right] & \left(\frac{Y}{R}\right)^2 & -\frac{XY}{R^2} \\ \frac{X}{R^2}\left[\dot{Y} + 2\,\dot{\theta}x\right] & \frac{X}{R^2}\left[\dot{X} - 2\,\dot{\theta}Y\right] & -\frac{XY}{R^2} & \left(\frac{X}{R}\right)^2 \end{bmatrix}$$

The position uncertainties at rendezvous, obtained using the matrixes, are presented in figures 7-9 and 7-10. Position uncertainties are plotted along the ordinate and $\omega_T T_1$ at the time of correction is plotted along the

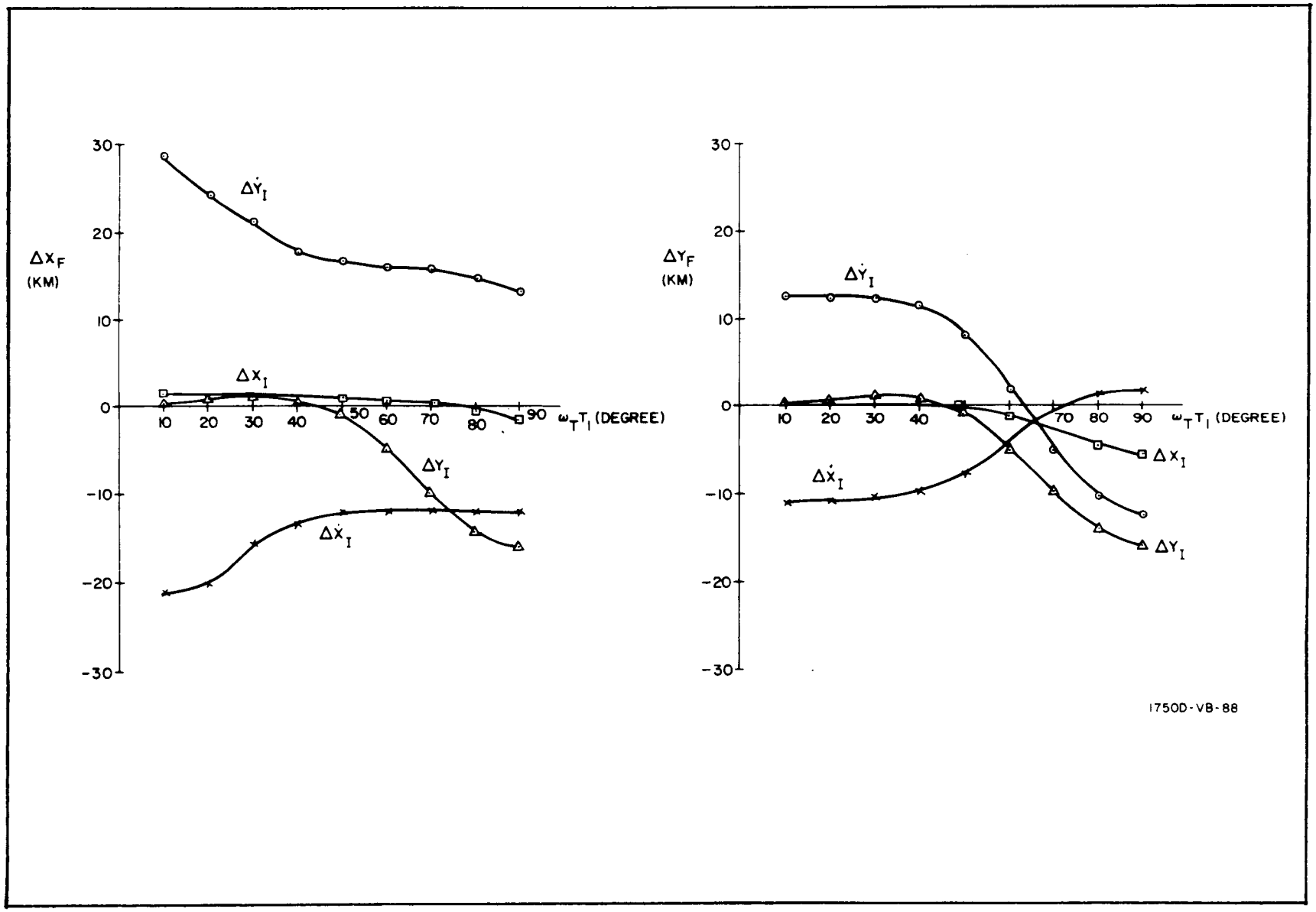

Figure 7-9. Uncertainties in Estimated Position vs Point of Measurement When Range Rate, Angle Correction Matrix is Used

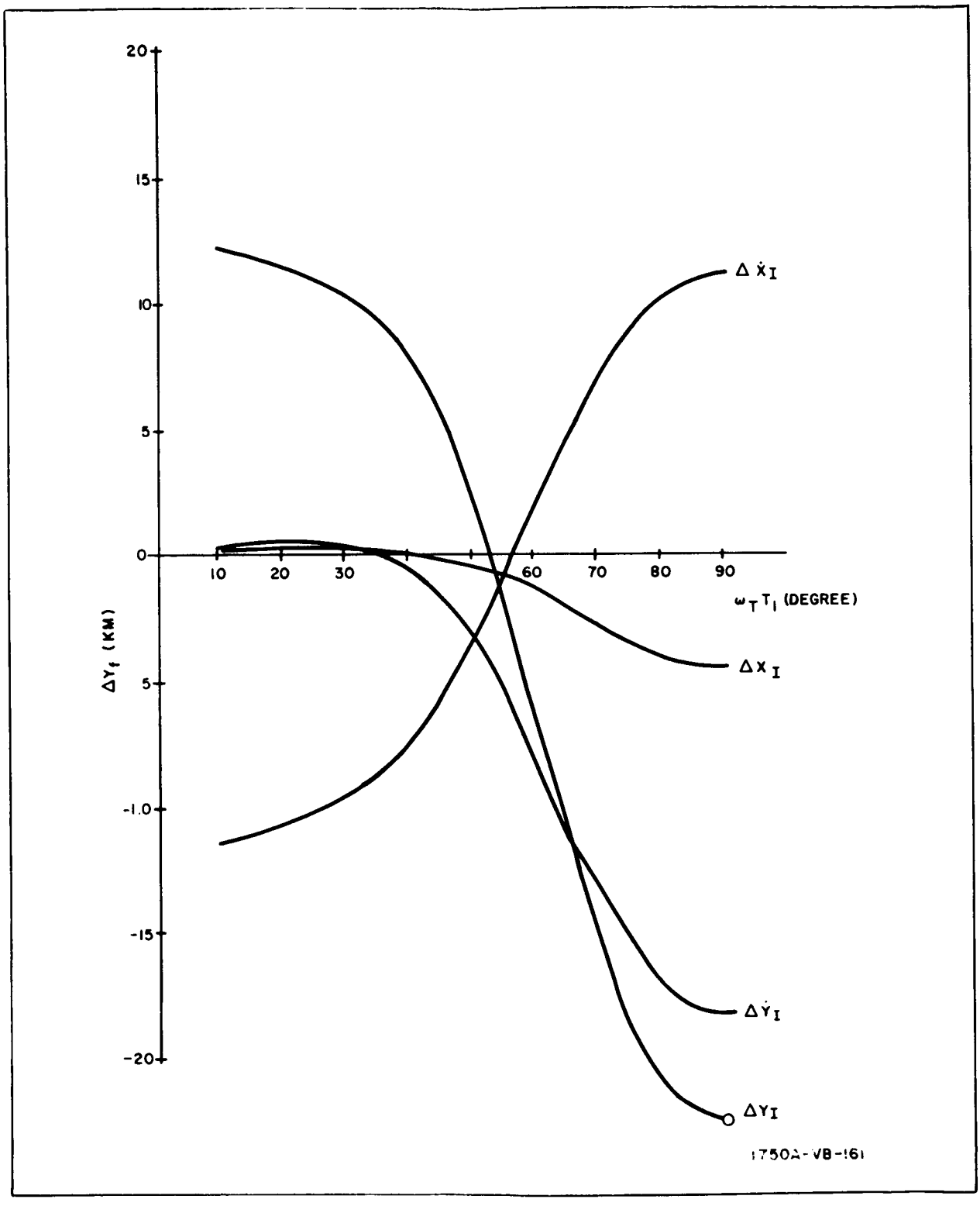

Figure 7-10. Uncertainties in Estimated Final Position Versus Point of Measurement when Range Range Rate Angle Correction Matrix is Used (No Data Available for ΔX, vs $\omega_T T_1$)

abscissa. A curve is included for each injection error: ΔX_I, ΔY_I, $\Delta \dot{X}_I$, $\Delta \dot{Y}_I$. For comparison, the injection errors and the resulting uncorrected position uncertainties at rendezvous are presented in table 7-7.

TABLE 7-7
INJECTION ERRORS AND RESULTING UNCORRECTED POSITION UNCERTAINTIES AT RENDEZVOUS

Position Uncertainties	Injection Error			
	ΔX_I = 1.85 km	ΔY_I = 1.85 km	$\Delta \dot{X}_I$ = 3.05 m/sec	$\Delta \dot{Y}_I$=3.05m/sec
ΔX_f	1.85 km	30 km	-23.4	11.5
ΔY_f	0	13 km	-11.3	5.55

7.5 CONCLUSIONS

It appears from the analyses performed that state of the art sensor capabilities are sufficient to perform a rendezvous. However, as mechanization and dynamic errors are introduced, sensor requirements become more stringent.

Qualitative results obtained from an analog simulation of pilot controlled rendezvous indicate that measurement and data processing requirements need not be as rigid when a human is in the control loop. This is due primarily to the ability of the pilot to smooth the data presented to him.

There is a direct relationship between sensor inaccuracies and the propellant consumed during rendezvous. Therefore, increased sensor accuracy will result in lower fuel requirements.

By taking one or more measurements during the midcourse portion of the transfer orbit, the true state variables at active rendezvous are known with a greater degree of precision, thereby allowing more accurate correction maneuvers. However, it appears that the injection and active rendezvous phases can be performed with sufficient accuracy to preclude the need of midcourse correction. Furthermore, should a provision be made for a midcourse correction procedure, a more sophisticated method would be to take measurements at a number of successive points and smooth the resulting data, thereby making greater use of equipment and information at hand.

8. REFERENCES

2-1 Kalman, R.E., A New Approach to Linear Filtering and Prediction Problems, Trans. ASME, Series D, Journal of Basic Engineering, Vol. 82, No. 1, March 1960, pp. 35-45.

2-2 Smith, G.L., S.F. Schmidt and L.A. McGee, Application of Statistical Filter Theory to the Optimal Estimation of Position and Velocity on Board a Circumlunar Vehicle, NASA TR R-135, 1962.

2-3 Smith, G.L., Secondary Errors and Off-Design Conditions in Optimal Estimation of Space Vehicle Trajectories, NASA Ames Research Center, NASA TN D-2128, January 1964.

2-4 Smith, G.L., and E.V. Harper, Midcourse Guidance Using Radar Tracking and Onboard Observation Data, NASA Ames, NASA TN D-2238, April 1964.

3-1 Kalman, R.E., A New Approach to Linear Filtering and Prediction Problems, Trans ASME, Series D, Journal of Basic Engineering, Vol. 82, No. 1, March 1960, pp. 35-45.

3-2 Smith, G.L., S.F Schmidt, and L.A. McGee, Application of Statistical Filter Theory to the Optimal Estimation of Position and Velocity on Board a Circumlunar Vehicle, NASA TR R-135, 1962.

3-3 McLean, J.D., S.F. Schmidt, and L.A. McGee, Optimal Filtering and Linear Prediction Applied to a Midcourse Navigation System for the Circumlunar Mission, NASA TN D-1208, 1961.

3-4 Battin, R.H., A Statistical Optimizing Navigation Procedure for Space Flight, ARSJ Vol. 32, No. 11, November 1962, pp. 1681-1691.

3-5 Pines, S., H. Wolf, D. Woolston, and R. Squires, Goddard Minimum Variance Orbit Determination Program, Goddard Space Flight Center Report No., X-640-62-191.

3-6 Levine, G.M., Application of Midcourse Guidance Technique to Orbit Determination, IAS Paper No. 63-16; IAS 31st Annual Meeting, January 21-23, 1963, New York.

3-7 Smith, G.L., and L.A. McGee, Midcourse Navigation Scheme, NASA Intercenter Technical Conference on Control, Guidance, and Navigation Research for Manned Lunar Missions, July 24-25, 1962.

3-8 Gunckel, T.L., Orbit Determination Using Kalman's Method, Journal of the Institute of Navigation, Vol. 10, No. 3, Autumn, 1963

3-9 Tunnell, P.J., and H.C. Lessing, Guidance Techniques for Lunar Approach and Letdown of the Apollo Spacecraft, Intercenter Technical Conference on Control, Guidance, and Navigation Research for Manned Lunar Missions, Ames Research Center, July 24 and 25, 1962, pp. 320-331.

3-10 Bowditch, N., American Practical Navigator, U.S. Hydrographic Office, Washington, 1962, p. 1149.

3-11 Schlegel, L.B., Covariance Matrix Approximation, AIAA Journal Vol. 1, No. 11, November 1963, p. 2672.

REFERENCED BIBLIOGRAPHY

Reference	Volume	Ref. No.	Page
Baker Jr., R. M. L. and G. W. Westrom, Analysis and Standardization of Astrodynamic Constants, AAS Preprint 61-27, 1961	III	2-12	2-56
Battin, R. H., A Statistical Optimizing Navigation Procedure for Space Flight, ARSJ, Vol. 32, No. 11, November 1962, pp. 1681-1696.	I	3-4	3-1, 3-18
	II	4-5	4-9, 4-13, 4-14
		5-3	5-8, 5-9, 5-10
	III	2-2	2-8, 2-18, 2-35, 2-39, 2-40, 2-41, 2-51
		3-4	3-1, 3-22, 3-46
	V	8	A-21, A-25
		5	B-21
Bellman, R. E., Introduction to Matrix Analysis, McGraw-Hill Book Company, Inc., New York, 1960	I	(Unref.)	
	III	2-5	2-15
	V	1	B-5
Bowditch, N., American Practical Navigator, U.S. Hydrographic Office, Washington, 1962, p. 1149	I	3-10	3-3, 3-16
	III	3-8	3-9, 3-45
Browner, D. and G. M. Clemence, Moments of Inertia of the Moon, A Review of Space Research, National Academy of Sciences, National Research Council Publication 1079, Iowa State University, June-August 1962, pp. 3-9, 3-10	I	(Unref.)	
	V	5	C-12
Bryson, A. E. and W. F. Denham, A Steepest Ascent Method for Solving Optimum Programming Problems, Journal of Applied Mechanics, June 1962, pp. 247-257	I	(Unref.)	
	III	4-1	4-4, 4-46
	V	1	D-3

Reference	Volume	Ref. No.	Page
Bryson, A. E., K. Mikami, and C. T. Battle, Optimum Lateral Turns for a Reentry Glider, Aerospace Engineering, Vol. 21, No. 3, March 1963, p. 21.	I V	(Unref.) 2	C-9
Burley, R. R. and R. J. Weber, Lunar Takeoff, ARS Journal, Vol. 32, No. 8, August 1962, p. 1296.	II III	7-2 5-3	7-5 5-11
Cicolani, L. S., Trajectory Control in Rendezvous Problems Using Proportional Navigation, NASA TN D-772, April 1961	IV	1	B-1
Cohen, C. J. and E. C. Hubbard, A Non-singular Set of Orbit Elements, NWL Report No. 1756	I V	(Unref.) 1	A-14
Cohessy, W. H., R. S. Wiltshire, Terminal Guidance System for Satellite Rendezvous, IAS Paper No. 59-93, June 1959	IV	1-1	1-8, 2-11, 2-54, 2-57
Davenport, P. B., Coordinate Systems and Transformation for Earth Satellite Prediction, Westinghouse Electric Corp., Report No. AA-2547-61, December 1961	V	1	F-11
Denham, W. A. and J. L. Speyer, Optimum Measurement and Velocity Correction Programs for Midcourse Guidance, AIAA Journal, Vol. 2, No. 5, May 1964	I III	(Unref.) 2-8	2-35
Duke, N. M., E. A. Goldberg, and I. Pfeffer, Error Analysis Considerations for a Satellite Rendezvous, ARS Journal, Vol. 31, No. 4, April 1961, pp. 505-513	V	3	E-14, E-19
Gapcynski, J. H. and R. H. Tolson, Analysis of the Lunar Return Mission, NASA Langley Research Center, NASA TN D-1939, August 1963	I III	(Unref.) 2-4	2-13, 2-18, 2-59
Gille, J-C., M. J. Pelegrin, and P. Decaulne, Feedback Control Systems, McGraw-Hill Book Company, Inc., New York, 1959	I III	(Unref.) 4-3	4-22
Goldstein, Classical Mechanics, London Addison-Wesley 1950, p. 105	I V	(Unref.) 3	A-14

Reference	Volume	Ref. No.	Page
Green, W. G., Logarithmic Navigation for Precise Guidance of Space Vehicles, IRE Transactions on Aerospace and Navigation Electronics, June 1961, pp. 59-113	IV	3	B-1
Gretz, R. W., Error Sensitivities in Satellite Ascent and Orbital Transfer, ARS Journal, Vol. 32, No. 12, December 1962, pp. 1860-1866	III V	5-5 2	5-24 E-13
Gunckel, T. L., Orbit Determination Using Kalman's Method, Journal of the Institute of Navigation, Vol. 10, No. 3, Autumn, 1963	I III V	3-8 3-6 6	3-1, 3-17 3-1, 3-7, 3-45 A-21
Hamilton, T. W. et al., The Ranger 4 Flight Path and its Determination From Tracking Data, Jet Propulsion Laboratory Tech. Dept. 32-345, September 15, 1962	I II	(Unref.) 3-1 4-11	 3-3, 3-4 4-14
Hearings Before the Committee on Aeronautical and Space Sciences, United States Senate, Eighty Seventh Congress, Second Session on H. R. 11737, NASA Authorization for Fiscal Year 1963, U. S. Government Printing Office, Washington, 1962	II	2-1	2-1
Heiskanen, W. A., and F. A. Vening Meinesz, The Earth and Its Gravity Field, McGraw-Hill Book Co., Inc., Chapter 5, 1958	III	5-7	5-26
Irish, L. A., A Basic Control Equation for Rendezvous Terminal Guidance, IRE Transactions on Aerospace and Navigation Electronics, September 1961, pp. 106-113	IV	2	B-1
Jensen, J., Lock, D. Kraft and G. Townsend, Design Guide to Orbital Flight 1, McGraw-Hill Book Company, 1962	IV V	(Unref.) 4	 E-14
Kalman, R. E., A New Approach to Linear Filtering and Prediction Problems, Trans. ASME, Series D, Journal of Basic Engineering, Vol. 82, No. 1, March 1960, pp. 35-45	I II III V	2-1 3-1 4-9 2-6 3-1 5 2	2-1 3-1 4-11 2-17, 2-18 3-1 A-20 B-7, B-11

Reference	Volume	Ref. No.	Page
Kriegsman, B.A., and M.H. Reiss, Terminal Guidance and Control Techniques for Soft Lunar Landing, ARS Journal, Vol. 32, March 1962, pp. 401-413	I II III V	(Unref.) 6-3 4-4 2	 6-8 4-51, 4-55 D-50
Laning, J.H., And R.H. Battin, Random Processes in Automatic Control, New York, McGraw-Hill Book Company, 1956	I IV V	(Unref.) 1 11 5	 D-4 A-37 D-55
Leitmann, G., Optimizing Techniques with Application to Aerospace Systems, New York, Academic Press, 1962, p. 218	V	10	A-30
Levine, G.M., Application of Midcourse Guidance Technique to Orbit Determination, IAS Paper No. 63-16, IAS 31st Annual Meeting, January 21-23, 1963 New York	I III	3-6 3-10	3-1 3-17
Mackay, J.S., Approximate Solution for Rocket Flight With Linear-Tangent Thrust Attitude Control, ARS Journal, Vol. 30, No. 11, November 1960, pp. 1091-1093	II III	7-1 5-2	7-5 5-11
Magness, T.A., and J.B. McGuire, Comparison of Least Squares and Minimum Variance Estimates of Regression Parameters, Ann. Math. Stat., Vol. 33, June 1962, p. 462	I V	(Unref.) 4	 A-19
Marshall SFC, Earth Orbital Operations, Tracking Mode (U), MTP-CP-62-1, Vol. 1 (Confidential)	I II	(Unref.) 4-2	 4-4
McLean, J.D., S.F. Schmidt, and L.A. McGee, Optimal Filtering and Linear Prediction Applied to a Midcourse Navigation System for the Circumlunar Mission, NASA TN D-1208, 1961	I	3-3	3-1, 3-17, 3-18
	II	4-8	4-11, 4-13 4-15
		5-4	5-8, 5-9, 5-10
	III	2-9	2-40, 2-50
		3-3	3-1, 3-6, 3-12, 3-39, 3-41, 3-42, 3-45, 3-46
	V	7	A-21, A-26, A-28
		4 4	B-19 C-11

Reference	Volume	Ref. No.	Page
Moulton, F.R., An Introduction to Celestial Mechanics, The MacMillan Co., 1959	I III	(Unref.) 2-3	 2-9
NASA MTP M-63-1, Lunar Logistic System, Vol. I, Summary, March 15, 1963, (Confidential)	II	1-2	1-5, 1-6
Nelson, W.C., and E.E. Loft, Space Mechanics, Prentice-Hall, Inc., 1962, pp. 66 and 160	III	5-6	5-25
Noton, A.R., E. Cutting, F.L. Barnes, Analysis of Radio-Command Midcourse Guidance, Jet Propulsion Laboratory Report No. 32-28, September 8, 1960	I II	(Unref.) 3-2 4-7 5-1	 3-3, 3-4 4-11, 4-14 5-7
Pfeiffer, C.G., Guidance of Unmanned Lunar and Interplanetary Spacecraft, AIAA Astrodynamics Conference Paper No. 63-399, Yale University, New Haven, Conn., August 1963	I II	(Unref.) 4-10 5-5	 4-11, 4-12 5-9, 5-10
Pines, S., H. Wolf, D. Woolston, and R. Squires, Goddard Minimum Variance Orbit Determination Program, Goddard Space Flight Center Report No. X-640-62-191	I III V 	3-5 3-9 2 1	3-1 3-13, 3-14, 3-18 A-4, A-8, A-19, A-25 C-1
Pitman, G.R., (Editor), Inertial Guidance, John Wiley and Sons, Inc., 1962	III V	5-4 1	5-23 E-1
Schlegel, L.B., Covariance Matrix Approximation, AIAA Journal, Vol. I, No. 11, November 1963, p. 2672	I III	3-11 3-11	3-17 3-45
Skolnik, M.I., Introduction to Radar Systems, New York, McGraw-Hill Book Company, Inc., 1962	I V	(Unref.) 7	 B-47
Smith, G.L., Secondary Errors and Off Design Conditions in Optimal Estimation of Space Vehicle Trajectories, NASA Ames Research Center, NASA TN D-2128, January 1964	I III V	2-3 2-7 6	2-13 2-20, 2-55, 2-56, 2-57 2-58 B-41
Smith, G.L., and E.V. Harper, Midcourse Guidance Using Radar Tracking and Onboard Observation Data, NASA Ames, NASA TN D-2238, April 1964	I II III	2-4 4-13 2-1	2-16 4-16 2-7, 2-65, 2-66, 2-68

Reference	Volume	Ref. No.	Page
Smith, G. L., and L. A. McGee, Mid-course Navigation Scheme, NASA Inter-center Technical Conference on Control, Guidance, and Navigation Research for Manned Lunar Missions, July 24-25, 1962	I	3-7	3-1, 3-17
	III	3-5	3-1, 3-7,
Smith, G. L., S. F. Schmidt, and L. A. McGee, Application of Statistical Filter Theory to the Optimal Estimation of Position and Velocity Onboard a Circum-lunar Vehicle, NASA TR R-135, 1962	I	2-2	2-1
		3-2	3-1, 3-18
	II	4-6	4-11, 4-14, 4-15
		5-2	5-7, 5-8, 5-9, 5-10
	III	3-2	3-1, 3-46
	V	9	A-25
		3	B-7
		3	C-11
Sterns, E. V. B., Navigation and Guidance in Space, Prentice-Hall Inc., Chapter 2, 1963.	III	5-1	5-9
Thatcher, J. W., Operational Status of the Deep Space Instrumentation Facility as of July 1, 1962, Jet Propulsion Laboratory Tech. Report No. 32-319, August 13, 1962	I	(Unref.)	
	II	3-3	3-3, 3-4
		4-12	4-14
Tolson, R. H., Effects of Some Typical Geometrical Constraints on Lunar Trajec-tories, NASA Langley, NASA TN D-938	I	(Unref.)	
	II	4-4	4-4
Tunnell, P. J., and H. C. Lessing, Guidance Techniques for Lunar Approach and Letdown of the Apollo Spacecraft, Intercenter Technical Conference on Control, Guidance, and Navigation Re-search for Manned Lunar Missions, Ames Research Center, July 24-25, 1962, pp. 320-331	I	3-9	3-1
	II	6-1	6-7, 6-8
	III	3-7	3-4
		4-2	4-19, 4-20, 4-22
U.S. Naval Research Laboratory Memo-randum Report No. 1275, Methodology for Generating Advanced Weapons Systems Applied to an Air-to-Surface Missile Limited War System (U), February 1962, Washington, D. C. (Secret)	II	1-1	1-2

Reference	Volume	Ref. No.	Page
Weber, R.J., W.M. Pauson, R.R. Burley, Lunar Trajectories, NASA Lewis, NASA TN D-866, August 1961	I II	(Unref.) 4-1	4-3
Woolston, D.S., Declination, Radial Distance, and Phases of the Moon for the Years 1961 to 1971 for Use in Trajectory Considerations, NASA Langley, NASA TN D-911, August 1961	I II	(Unref.) 4-3	4-4
Wylie, C.R., Advanced Engineering Mathematics, New York, McGraw-Hill Book Company, Inc., 1956, p. 782	I V	(Unref.) 4	D-54
Zadeh, L.A., On the Extended Definition of Linearity, Proceedings of the IRE, Vol. 50, No. 2, February 1962, p. 200	II	6-2	6-8

UNREFERENCED BIBLIOGRAPHY

	Vol.	Sect.
Bonelle, G.J., Radar Design for Manned Space Vehicles, Missile and Space Division, Raytheon Company, Bedford, Mass.	I	4
Bryson, A.E., Statistically Optimizing Multivariable Terminal Control, Raytheon Internal Note, November 12, 1962	IV	
Buchan, J.S., Apollo Rendezvous Simulator Study (U), Chance Vought Corp., Summary Report No. 324.3, July 12, 1962. (Confidential)	I	4
Citron, S.J., S.E. Duning, and H.F. Meissinger, A Self-Contained Terminal Guidance Technique for Lunar Landing, presented at APS annual meeting, Los Angeles, California, November 1962	I	4
Cramer, H., Mathematical Methods of Statistics, Princeton University Press, 1946.	IV	
Dodgen, J.A., W.D. Mace, et.al , Instrumentation, Communications, Life Support, and Auxiliary Power, NASA L36F413, April 16, 1962.	I	4
Erissenden, R.F., B.B. Burton, E.C. Foudriat, and J.B. Whitten, Analog Simulation of a Pilot-Controlled Rendezvous, NASA TN D-747, 1961.	IV	
Gates, C.R., J.R. Scull, and K.S. Watkins, Space Guidance, Astronautics Magazine, Vol. 6, No. 11, November 1961.	I	4
Heidbreder, G.R., Stelatrac - A Modular Spaceborne Terminal Guidance Radar, PG SET Record, National Symposium on Space Electronics and Telemetry, October 1962.	I	4
Hildebrand, F.B., Methods of Applied Mathematics, Prentice Hall, Chapter 1, 1952.	IV	
Hollister, W.M., The Design of a Control System for the Terminal Phase of a Satellite Rendezvous, MIT, June 1959.	IV	

MIT Report No. RM-373 (Rev. A), Guidance and Navigation System for Lunar Excursion Module, August 1962.	I	4
Makenison, M.W., R.M.L. Baker Jr., and G.W. Weston, Analysis and Standardization of Astrodynamic Constants, AAS Preprint 61-27, 1961.	I	2
Queijo, D.M. and G.K. Miller Jr., Analysis of Two Thrusting Techniques for Soft Lunar Landings Starting From a 50-Mile Altitude Circular Orbit, NASA TN D-1230, March 1962.	I	4
Raytheon Company, Missile and Space Division, Guidance and Control for Manned Lunar Flight, Control Engineering, June 1962	I	4
Raytheon Report, BR-1259A, Space Vehicle Navigation Systems Study, July 31, 1961	IV	
Sears, N.E., P.G. Fellman, Terminal Guidance for a Satellite Rendezvous, presented at the ARS Controllable Satellite Conference, MIT, April and May 1959	IV	
Sperry Rand Corporation Report, Navigation, Guidance, and Rendezvous, Pub. No. AB-1210-0004-3, Vol. III, January 1962	I	4
Steffan, K.F., A Satellite Rendezvous Terminal Guidance System, presented at the ARS 15th Annual Meeting, Shoreham Hotel, Washington, D.C., December 5-8, 1960; 1494-60	IV	